The Drivers of Community Assembly for Canopy Trees in the Brazilian Amazon

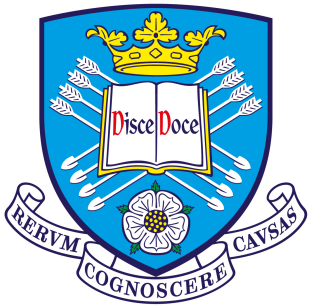

The University Of Sheffield.

A thesis submitted to the University of Sheffield for the degree of Doctor of Philosophy

Mike R. Massam

Department of Animal and Plant Sciences

May 2020

This thesis is dedicated to my parents,

Kathy & Kevin Massam

for their unending support and encouragement. Truly, I would be nothing without them.

Preface

This thesis is submitted in an approved alternative format to ease the process of rewriting and reformatting for publication. I am the primary contributor for all chapters, each has been written solely by me and my thesis remains a coherent body of work with all further explanatory text and statistical data that is required of a PhD. thesis is provided in the appendices.

The co-authors for resulting publications (specifically: Chapter 2, Chapter 3 and Chapter 4) will be my two supervisors, Prof. David Edwards[1] and Prof. Carlos Peres[2], who have provided guidance, support and the datasets implemented.

In Chapter 5, I discuss preliminary results for future studies. Again, I will be the primary contributor to any resulting publications but Ileana Acosta [3], Joeseph Haywood[4], Thomas Pearson[5] and Thiago Mouzinho[6] will be included as further co-authors for any publications resulting from the field data for their substantial academic and field contributions.

[1]Department of Animal and Plant Sciences, University of Sheffield, UK. david.edwards@sheffield.ac.uk

[2]School of Environmental Sciences, University of East Anglia, UK. C.Peres@uea.ac.uk

[3]Department of Animal and Plant Sciences, University of Sheffield, UK. iarcea-costa1@sheffield.ac.uk

[4]Department of Animal and Plant Sciences, University of Sheffield, UK. josephrhaywood@gmail.com

[5]Department of Animal and Plant Sciences, University of Sheffield, UK. tom.wp6@gmail.com

[6]Instituto Nacional de Pesquisas da Amazôna, Brasil. thiagomouzinhobio@gmail.com

Acknowledgements

Firstly, I would like to express my deepest thanks to my supervisors, Prof. David Edwards and Prof. Carlos Peres, for giving me this opportunity and for being a constant source of inspiration, self-belief and unwavering support, for which I am eternally grateful.

I would like to thank everyone at AMATA S.A, not only for funding our accommodation and allowing me to conduct my research within their concession, but for the warmth and kindness that every staff member showed me during my field seasons.

I cannot express enough my thanks to my partner, Bertha Rohenkohl, for her unwavering love and support, and to my friends that have supported me throughout this journey. Despite my distance at stressful times they have continued to give me support and encouragement. Thank you to Azmat Rashid, Nadia Sheath, Alex Brown, Anthony Koumi, Fiona Deacon, Joshua Twining, Louise Archer, Camilla Foglietti, Thiago Mouzinho, Thomas Pearson, Renata Cunha, Angela Nature Chira and Antoine Koumi.

Enormous thanks go to Renata Cunha, Thiago Mouzinho, Joseph Haywood, Francis Bruin, Bianca Torres, Thomas Pearson, Callum Nixon, Valeria Scura del Hierro, Christina Derrick, Ieaun Lamb, Tati Macedo, Katie Cook, Jefferson Silva, Betania Alves, Tomas Godoy, Jorge Martins, Andre Caldas, Ileana Acosta and Alex Elias dos Santos for their immense efforts in the field, without which, our comprehensive field dataset would not have been possible.

Last, but certainly not least, I would like to thank my parents, Kathy and Kevin Massam. They have enabled me at every turn and supported me to get to where I am. Everything I have, I owe to them and, with only words, I cannot thank them enough.

Abstract

The Amazon rainforest is hyperdiverse, supporting as many as 16,000 tree species. However, the processes governing the spatial structure of plant community composition is poorly understood. This is especially true of large canopy trees which have proven difficult to study owing to the small spatial scales of the current network of forest plots. This is a key knowledge gap given that canopy trees are the primary seed dispersers, competitors and carbon storers. In this thesis I use landscape scale, contiguous forest inventories from the logging sector to address this. I first assess the capacity of neutral models to adequately reconstruct the observed patterns of beta-diversity. I demonstrate that stochastic dispersal and environmental filtering processes superimpose to drive compositional turnover. While dispersal processes explain the majority of compositional turnover, environmental filtering can operate at small spatial scales to dictate community composition. I then assess compositional turnover under the lens of niche conservatism. Phylogenetic diversity metrics revealed that environmental variables play a greater role in driving community composition of canopy trees than was previously detectable and that environmental factors can operate at scales as low as 1 ha to influence community composition. Lastly I examined the key drivers of species aggregation patterns and asked whether species functional traits could explain the degree of aggregation. Surprisingly, canopy trees exhibited similar aggregation patterns to those of juveniles with respect to environmental associations and dispersal limitation. Further, I found that species dispersal syndrome and seed mass controlled aggregation patterns. Put together, my findings show that both environmental variables and dispersal limitation are key drivers of the spatial structure of large tropical canopy tree community composition and that species identity and functional traits play an important role. As we enter the Anthropocene, tropical forests face increasing threats of logging and land-use change. My results reveal key community assembly processes which should be taken into consideration when planning sustainable forest management and conservation measures.

Contents

List of Figures

List of Tables

Chapter 1

Introduction

At the very core of community ecology, is the goal to understand the processes responsible for driving the composition of species within communities. The key questions in community ecology are disarmingly simple, yet, despite enormous research efforts, definitive answers to many key questions remain elusive.

A particularly heavily debated topic surrounds the fundamental question of how large numbers of plant species are able to coexist at small spatial scales. The pervasive hurdle in tackling the question has rested in resolving the competitive exclusion principle (Hardin, 1960) which posits that two species competing for the same resource cannot coexist if one has the slightest of competitive advantages. In the long-term, the dominant species will always out-compete the other to extinction.

The response offered by classical ecology is niche theory (Gause, 1934), which asserts that coexistence between competing species relies on the occupancy of different niches. Although niche theory is easily observable in communities with trophic levels, and thereby different resource requirements and availability, this concept falls apart for plant communities. Plants require a similar set of resources, competing for light, water, CO_2 and soil nutrients, and have limited mechanisms of acquiring them. This is best demonstrated by the fact that for all extant seed plants, only three pathways for carbon acquisition exist whereas over 30,000 defensive compounds have evolved (Harborne, 1993). Clearly, there are strong constraints on the evolutionary capacity for nutrient acquisition mechanisms. So the question persists, how can competing plant species coexist despite the absence of niche differences demanded by classical niche theory?

Over 100 hypotheses have been proposed to overcome this challenge by delaying or preventing competitive exclusion (Palmer, 1994), each of which attempt to demonstrate that the premises of the competitive exclusion principle are violated under given conditions (Wright, 2002). However, the contexts in which, and the

degree to which, competing theories act in maintaining high levels of plant species richness remains undetermined.

Resolving these competing theories is of particular relevance to tropical forest ecosystems which are capable of supporting extraordinary levels of plant species diversity. Global terrestrial biodiversity is centred on the tropics (Fig. 1.1), where a single hectare of rainforest can support over 280 tree species (De Oliveira and Mori, 1999, Valencia et al., 1994) $\geq$ 10 cm diameter at breast height (DBH). How such high levels of plant species diversity are maintained at small spatial scales in, typically, nutrient-poor environments remains a continually debated subject with both deterministic environmental and stochastic processes being implicated (Wright, 2002).

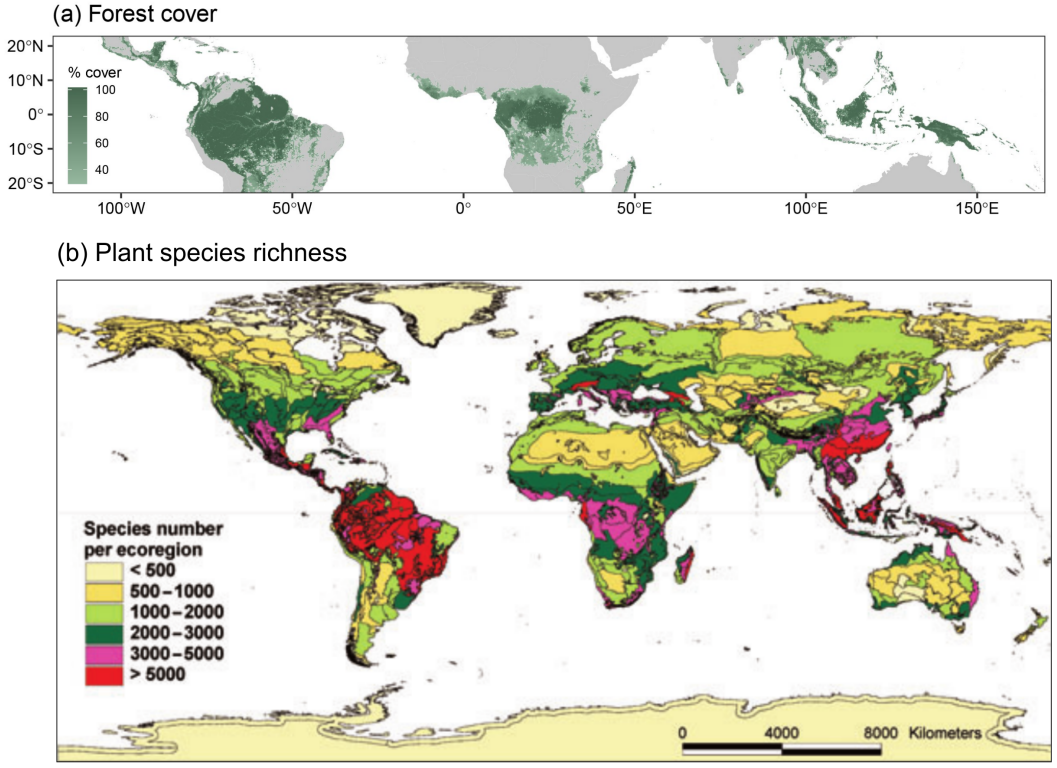

Figure 1.1: Map of global rainforests (a; Figure from Edwards et al. (2019)) and global plant species richness (b; Figure from Kier et al. (2005))

1.1 Coexistence mechanisms

The mechanisms of species coexistence proposed to overcome the competitive exclusion principle in explaining how such high levels of plant diversity can persist in the tropics can be broadly categorised into two camps: those that assert a meaningful role in the differences of ecological strategies between coexisting species, and

those that propose that stochastic dispersal, mortality and recruitment are sufficient to explain given diversity, the latter coined 'neutral theory'.

1.1.1 Neutral Theory

Neutral theory is, perhaps, the most controversial mechanism proposed to explain species coexistence. Hubbell (2001) proposed that species on the same tropic-level are functionally equivalent – they are demographically equivalent with respect to their per capita mortality, recruitment, dispersal and speciation rates, regardless of any underlying environmental factors. Under classic neutral theory, species coexistence is maintained by a balance between local extinction and speciation/immigration (Fig. 1.2).

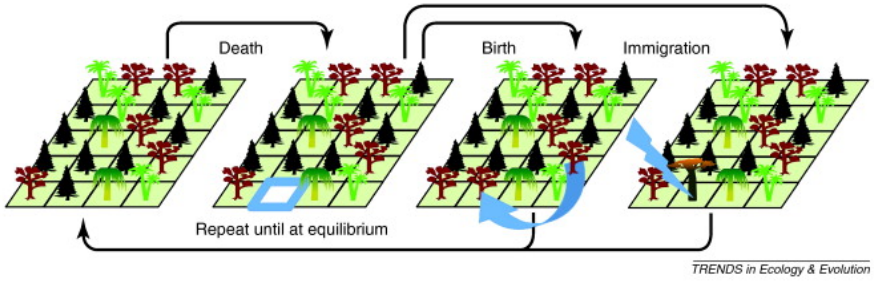

Figure 1.2: Species coexistence under classic neutral theory. Figure from Rosindell et al. (2011)

At first glance, neutral theory contradicts our intuition of what we see in the field and of what we understand about plant environmental tolerances. However, under neutral theory, functional equivalence is not meant to imply that species-specific characteristics do not exist in the real world. Instead, neutral theory approaches the subject of species coexistence from the simplest possible hypothesis, i.e. functional equivalence, and adds complexity to the system as required to reproduce observed patterns of species coexistence and community composition . To this end the question then becomes, what is the maximum complexity necessary to adequately reproduce patterns of community composition? (Hubbell, 2005)

Neutral models have, indeed, been successful in demonstrating how species may coexist without needing to address the competitive exclusion principle. Further, more complex neutral models which incorporate species abundances, spatially explicit models and varying seed-dispersal kernels have been able to reproduce a variety of observed community composition metrics such as relative species abundance curves (Volkov et al., 2003), species-area relationships (Rosindell and Cornell, 2009), species aggregation and β-diversity patterns (May et al., 2015). However, the underlying assumption of species functional equivalence is incompatible with the

countless studies demonstrating species-habitat correlations, ecological succession and species functional trait-based competition (Purves and Turnbull, 2010). As such, neutral theory has proven to be a valuable tool as a null model against which to study the importance of deterministic ecological processes.

1.1.2 Deterministic coexistence mechanisms

In contrast to neutral theory, deterministic mechanisms of species coexistence accept that species are functionally different. These proposed mechanisms of coexistence aim to demonstrate that one or more of the conditions necessary for competitive exclusion are violated. Two of the six key premises of the competitive exclusion principle (see Wright (2002)) state that interspecific competition will result in the exclusion of all but one species when:

(1) Rare species are not favoured demographically
(2) The environment is spatially and temporally homogeneous

Evidence whereby species coexistence is promoted via the violation of both of these conditions has been documented in the tropics:

(1) Negative density dependence

Diminished performance in the present of high densities of conspecifics is known as negative density dependence and manifests as increased mortality, decreased recruitment or slower growth. Both pest facilitation and intraspecific competition can contribute to negative density dependence, allowing rare species to be favoured demographically, thereby promoting species coexistence. The Janzen-Connell hypothesis (Connell, 1971, Janzen, 1970) argues that an abundance of host-specific pests near conspecific adult species can impair seedling recruitment, opening space for other species to occupy. A meta-analysis by Comita et al. (2014) revealed widespread support for Janzen-Connell processes, especially within the tropics. Further, intraspecific competition for the same set of resources has repeatedly been found to impair performance of abundant species in the tropics (Alvarez-Buylla, 1994, Condit et al., 1994, Gilbert et al., 1994, Martinez-Ramos, Silva Matos et al., 1999).

(2) Environmental niche theory

Environmental niche theory asserts that species coexistence can occur when different species occupy different niche spaces or utilise resources in different ways.

Numerous studies have demonstrated that spatial environmental heterogeneity influences plant community composition in the tropics (Clark et al., 1998, John et al.,

2007a, Kraft et al., 2008, Silvertown et al., 1999, Svenning, 1999, Whittaker, 1967). The physiological tolerances of plants differ between species with varying degrees of tolerance to drought, shade and soil composition (McKane et al., 2002, Sairam and Tyagi, 2004, Valladares and Niinemets, 2008, Yordanov et al., 2000). As such, spatial variation in climatic, edaphic and hydrological factors can influence species distributions via environmental filtering and habitat associations, thereby promoting species coexistence. For example Harms et al. (2001a) demonstrated that 64% of species at Barro Colorado Island exhibited significant habitat associations.

Environmental filtering influences the competitive interactions between species, whereby species that are well-adapted to a given habitat will outcompete poorly-adapted species (Anderse et al., 2014, Baltzer et al., 2005, Russo et al., 2008). Ultimately, environmental filtering drives community composition (Werner and Homeier, 2015), a concept that is universally accepted within community ecology.

1.2 Community composition and beta-diversity

Our understanding of β-diversity also remains a poorly subject within community ecology. β-diversity defines the processes governing the turnover of species composition across space. β-diversity is the link dictating the relationship between local (alpha) and regional (gamma) diversity (Whittaker, 1960). Research in this area can shed light on core theoretical research. In particular, it can aid explanation of how huge numbers of species are able to coexist within hyperdiverse systems, especially tropical forests (Valencia et al., 1994). Environmental factors are well known to be responsible for the turnover of species across environmental gradients, for example, the substantial turnover of species that occurs with elevation from lowlands to mountain tops. However, the magnitude of the role of environmental gradients on β-diversity, the key environmental factors at play, and the spatial scales at which they operate to produce community turnover remain poorly understood in the tropics.

As we enter the Anthropocene, severe land-use change, over-hunting, climate change and other anthropogenic-driven disturbances are causing a mass extinction event. Understanding the processes that maintain diversity over space can play a crucial role in quantifying these impacts and, in turn, developing conservation strategies to minimise biodiversity loss (Socolar et al., 2016).

1.3 Reconciling niche and neutral theory: The niche-strength continuum

Although niche theory is supported by a swathe of evidence, deterministic models based on niche differentiation fail to account for the full degree of diversity observed in tropical forests (Silvertown, 2004). Equally, the premise of species-equivalence under neutral theory is often violated, and while neutral models have successfully managed to reconstruct observed patterns of β-diversity at small scales (May et al., 2015), they have failed to replicate β-diversity patterns across large scales (Condit et al., 2002).

Although it is clear that neutral theory alone cannot fully account for community composition, recent thinking has driven research on the notion that both deterministic environmental and stochastic processes can superimpose, playing dual roles in the spatial structure of community composition (Adler et al., 2007). Multiple studies have demonstrated that stochastic dispersal and environmental variability both contribute to observed patterns of compositional turnover (Chang et al., 2013, Legendre et al., 2009, Lin et al., 2011, Liu et al., 2016, Pinto and MacDougall, 2010, Qiao et al., 2015). The question then turns to the degree in which tropical tree communities are structured along a 'niche-strength continuum', ranging from purely neutral to strongly niche-structured (Purves and Turnbull, 2010).

However, the challenge in disentangling the precise drivers lies in the fact that whilst community composition is spatially autocorrelated, so too is the underlying environment. Chisholm and Pacala (2010) demonstrated that both niche and neutral models can give rise to the same patterns of species abundance distributions. Patterns of β-diversity could, therefore, be explained by environmental filtering due to the underlying spatially autocorrelated environment, but equally by stochastic dispersal limitation.

1.4 Spatial scales of species patterns

At the frontier of current research is the consideration of the degree at which different processes act across different spatial scales (Hart et al., 2017). The difficulty in disentangling the relative roles of deterministic environmental filtering and stochastic processes across large scales stems from the lack of large-scale contiguous forest inventory data.

Large networks of permanent forest plots such as BCI (Hubbell et al., 2005), RAINFOR (Peacock et al., 2007), ATDN (ter Steege) and CTFS (Anderson-Teixeira et al., 2015) have provided invaluable insights into spatial ecological dynamics (Duque

et al., 2017, May et al., 2015, Phillips et al., 2004, ter Steege et al., 2006). However, individual plots are limited to 50 ha, a scale over which biodiversity patterns of large canopy trees cannot be fully assessed (Marvin et al., 2014). Even summed together, these plots represent only $\sim$ 2,000 ha, with plots often separated by large distances.

This represents a significant current limitation given that canopy trees are the primary competitors (Wright, 2002), seed dispersers (Thomson et al., 2011) and carbon storers (Pan et al., 2011). If deterministic and stochastic processes operate to shape spatial biodiversity patterns at different scales, this may explain why neutral models have successfully reproduced intra-plot β-diversity patterns (May et al., 2015) but failed at the inter-plot level (Condit et al., 2000a).

Recent advances in airborne imaging spectrometry have sought to bridge this scale-gap and have proven key to revealing β-diversity patterns at the landscape scale. Draper et al. (2019) demonstrated that patterns of β-diversity vary between forest-types, suggesting that deterministic niche processes play a key role across large spatial scales. Bongalov et al. (2019) further demonstrated that stochastic dispersal processes can account for compositional turnover within, but not *across* forest-types, suggesting that environmental filtering and neutral processes act at different scales. Alternatively, Draper et al. (2019) finds that stochastic processes cannot replicate observed β-diversity. As such, the use of 'spectral species' requires validation using spatially explicit forest inventory field data.

1.5 Study region and data

This thesis investigates the drivers of community assembly for canopy trees in the Amazon Basin. The Amazon rainforest spans an area of $\sim$6 million km^2 (Fig. 1.3), representing half of the planets remaining tropical forests and is highly diverse, supporting as many as 16,000 tree species (Ter Steege et al., 2013). The topography of the Amazon Basin is relatively flat with the large majority of this vast region sitting below 400 meters above sea level (m.a.s.l). It is subject to heavy rainfall between 2000 and 11,000 mm annually, with average temperatures ranging from 22 and 24°C.

In 2006, Brazil, which owns 60% of the Amazon, passed legislation to allow sustainable selective logging concessions within certain National Forests in attempt to curb deforestation (Azevedo-Ramos et al., 2015). The legislation demands that logging actions are planned in a sustainable manner such that commercially valuable species are not overexploited. Thus, trees are spatially mapped prior to planning and species identification is heavily monitored by the Brazilian Forestry service (SFB). This has led to an emergence of spatially explicit forest inventories of large canopy trees, identified to species-level.

Figure 1.3: Map of the Amazon Basin

Here I use such datasets, obtained from seven companies in the forestry sector to investigate the roles of deterministic environmental filtering and stochastic processes in driving the spatial structure of community composition for (1) large canopy trees (2) identified to the species-level, (3) across large spatial scales (4) of contiguous forest. This combination of dataset features have previously been unavailable, thus, have allowed me to address key questions that have previously been impossible to resolve.

1.6 Thesis aims and rationale

The main aims of this thesis are to determine how stochastic and deterministic processes operate to drive: (1) community composition, (2) compositional turnover, and (3) patterns of species aggregation for tropical canopy trees in the Amazon. I begin by comparing neutral simulations to observed patterns of β-diversity to disentangle the relative roles of environmental filtering and stochastic dispersal processes in dictating compositional turnover. I then compare phylogenetic β-diversity (PBD) metrics against, traditional, taxonomic β-diversity (TBD) metrics to assess whether niche conservatism can elucidate the role of environmental variables within spatially autocorrelated environment. Finally, I use spatial point pattern modelling in concert with five landscape-scale forest inventories spanning the Amazon Basin to identify aggregation patterns and determine their habitat associations and degree of dispersal limitation. Further, I assess how species functional traits determine species aggregation patterns. In the general discussion, I synthesise all results, giving an overall summary of my findings and their significance within community ecology. I then discuss the implications of these findings in the context of selective logging and provide some preliminary results for future studies. The specific objectives of each chapter is briefly outlined below:

Chapter 2. Fine-scale variation in environmental factors shape β-diversity in tropical canopy tree communities

Understanding of the relative importance of deterministic and stochastic processes in driving community composition remains elusive within community ecology. Neutral processes have often failed to replicate observed patterns of β-diversity. One explanation is that both processes act together to determine compositional turnover. Such patterns could be explained by environmental filtering due to the underlying spatially autocorrelated environment, but equally by stochastic dispersal limitation. This chapter uses spatially explicit floristic data from a complete forest census of canopy trees covering 5,100 ha of tropical forest in the Amazonian basin to: (1) Assess the scale and degree of spatial autocorrelation of community composition' (2) quantify the role of geographical distance, environmental factors and spatially autocorrelated environment in determining β-diversity; and (3) determine whether stochastic dispersal processes can fully account for β-diversity patterns within a single forest type.

Chapter 3. Phylogenetic beta-diversity informs the factors driving compositional turnover in tropical canopy tree communities

Recent ecological theory has explored the notion that stochastic and deterministic processes act jointly to explain compositional turnover. β-diversity studies in this vein have been widespread, but have typically focussed on taxonomic dissimilarities between assemblages. The implementation of PBD to unpick the components of β-diversity have recently become more prevalent, but has previously not been possible for large tropical canopy trees given the current network of tropical forest plots being limited to 50 ha or smaller in size. Here, I use spatially explicit floristic data from a complete forest census of canopy trees covering 5,100 ha of tropical forest in the Amazonian basin to address the following objectives: (1) Assess extent of spatial autocorrelation of taxonomic and phylogenetic community similarity to determine how lineages turnover across space; (2) quantify the contribution of spatial and environmental variables driving TBD and PBD; and (3) investigate the scales at which environmental and spatial variables operate to influence TBD and PBD.

Chapter 4. Do functional traits explain aggregation patterns of tropical canopy trees?

The spatial clustering of conspecific trees in tropical forests is observed across the full range of life-stages and at multiple spatial scales. However, aggregation can be explained by both environmental filtering and seed dispersal limitation. Coupling spatial point pattern analyses with functional traits provides the opportunity to distinguish the underlying mechanisms governing plant distributions. I investigate how environmental filtering, dispersal limitation and species functional traits interact to form aggregated intraspecific patterns in emergent tropical trees at a regional scale within spatially contiguous forests to: (1) categorise species aggregation patterns by their habitat associations and dispersal limitations; (2) assess how the strength of habitat associations and dispersal limitation varies across sites and within species; (3) test whether the strength of clustering and habitat associations can be described by species functional traits related to resource use and/or dispersal limitation; and (4) assess phylogenetic signal in aggregation and habitat association parameters.

Chapter 5. General introduction and future directions

I summarise the main findings of the thesis and put them in the wider context of how understanding the drivers of species distribution can inform improved sustainable forest management. In doing so, I first present some preliminary results that demonstrate how logging may impact β-diversity patterns. I then identify po-

tential questions related to recruitment-growth-mortality dynamics across a range of logging intensities and plant life-stages that can be answered utilising field data collected that I collected throughout the duration of my PhD.

Chapter 2

Fine-scale variation in environmental factors shape β-diversity in tropical canopy tree communities

2.1 Introduction

The relative importance of deterministic and stochastic processes in driving community composition remains a continually debated subject within community ecology. The question of how such high levels of plant species diversity are maintained in tropical forests (Wilson et al., 2012) is of particular interest, where competition for resources is strong and environments are typically nutrient-poor. In particular, explaining how species composition varies across space, i.e. β-diversity, continues to present a key question. The answer holds far-reaching implications for conservation (Liang et al., 2016, Socolar et al., 2016).

Correlation between environmental variables and plant community composition has long been observed (Clark et al., 1998, John et al., 2007a, Kraft et al., 2008, Svenning, 1999). Topographic features have a strong influence on variation in microclimate, hydrology and soil properties (Chadwick and Asner, 2016, Tiessen et al., 1994, Xia et al., 2016), promoting environmental filtering. Environmental filtering influences competitive interactions and, (Anderse et al., 2014, Baltzer et al., 2005, Russo et al., 2008) ultimately, drives community composition (Werner and Homeier, 2015). However, deterministic models based on niche differentiation have failed to account for the degree of diversity observed in tropical forests (Silvertown, 2004).

Conversely, neutral theory (Hubbell, 2001) proposes that stochastic processes

of mortality, dispersal and recruitment are sufficient to maintain the high levels of species diversity in tropical forests. Neutral models have successfully replicated spatial biodiversity patterns such as species-area relationships and species abundance distributions (Hubbell, 2001, May et al., 2015). However, the premise of species-equivalence under neutral theory has been proven invalid (Purves and Turnbull, 2010). Whilst neutral models have been able to match β-diversity patterns at local scales, they have been unable to so over large scales (Condit et al., 2002). Furthermore, neutral simulations have been unable to simultaneously replicate species-area relationships and β-diversity patterns under the same parameters (May et al., 2015).

One proposed explanation for the failure of either deterministic and stochastic (neutral) processes to replicate observed β-diversity patterns is that both processes act together to determine compositional turnover (Adler et al., 2007). However, the complication in demonstrating this lies in the fact that whilst community composition is spatially autocorrelated, so too is the underlying environment. Chisholm and Pacala (2010) demonstrated that both niche and neutral models can give rise to the same patterns of species abundance distributions. Patterns of β-diversity could, therefore, be explained by environmental filtering due to the underlying spatially autocorrelated environment, but equally by stochastic dispersal limitation.

The difficulty in disentangling the relative roles of deterministic environmental filtering and stochastic dispersal processes arises from the lack of large-scale continuous forest inventory data. Whilst large networks of permanent forest plots (e.g. BCI, RAINFOR, ATDN, CTFS) have provided key insights into spatial ecological dynamics (Duque et al., 2017, May et al., 2015, Phillips et al., 2004, ter Steege et al., 2006), individual plots are limited to 50 ha, a scale over which biodiversity patterns of canopy trees cannot be fully assessed (Marvin et al., 2014). This presents a key knowledge gap given that canopy trees are the primary competitors (Wright, 2002) and seed dispersers. Further, if deterministic and stochastic processes operate to shape spatial biodiversity patterns at different scales, this may explain why neutral models have successfully reproduced intra-plot β-diversity patterns (May et al., 2015) but failed at the inter-plot level (Condit et al., 2000a).

Recent advances in airborne imaging spectrometry have bridged the scale-gap, accurately estimating β-diversity patterns at the landscape scale (Bongalov et al., 2019, Draper et al., 2019). Such studies have demonstrated that patterns of β-diversity vary between forest-types, corroborating the notion that deterministic niche processes play a key role in shaping community composition at a large scale. Bongalov et al. (2019) further demonstrate that stochastic dispersal processes can account for compositional turnover within, but not *across* forest-types, corroborating the notion that β-diversity patterns can be explained by spatially autocorrelated envi-

ronmental filtering and stochastic dispersal processes operating at different scales. Conversely, Draper et al. (2019) finds that stochastic processes cannot replicate observed β-diversity. However, their use of the Poisson cluster process does not consider dispersal limitation or differences in forest type. As such, the question remains whether fine niche structuring can drive patterns of β-diversity i.e. within a single forest type.

While advances in technology that allow aerial mapping of biological diversity provide a powerful technique for studying biodiversity patterns over large spatial scales, spectral reflectance data is not yet capable of identifying plants to the species level. The emergence of landscape-scale forest inventory data within the logging sector therefore affords the unique opportunity to link both approaches. Here, we use spatially explicit floristic data from a complete forest census of canopy trees covering 5,100 ha of tropical forest in the Amazonian basin to:

(1) Assess the scale and degree of spatial autocorrelation of community composition

(2) Quantify the role of geographical distance, environmental factors and spatially autocorrelated environment in determining β-diversity

(3) Determine whether stochastic dispersal processes can fully account for β-diversity patterns within a single forest type.

2.2 Materials and Methods

2.2.1 Study site

The study site (1°13'12"S 52°33'36"W) is located within the wet tropical lowland forest of the Amazon Basin, in the region of Vale do Jari, Pará, Brazil (Fig. 2.1). The dominant soil type is ferrasol, (Dijkshoorn et al., 2005) characterised by high clay content and low nutrient availability, and climate is typical of equatorial regions with a mean annual precipitation of 2055 mm and temperature of 25°C. The site is under concession for sustainable forest management by the logging company Orsa Florestal, in accordance with environmental legislation imposed by the Brazilian Institute of Environment and Renewable Natural Resources (IBAMA). A complete, spatially mapped, forest inventory was conducted between 2002–2003 for all stems $\geq$ 35 cm diameter at breast height (DBH) over 5100 ha of undisturbed forest. Mapping was conducted manually, operating within 12.5 m width bands and species were identified to species level where possible. Geolocation and species identification has previously been verified for key species (Ferreira, 2009). The census, comprises

283,954 stems of 377 species, 196 genera and 56 families (see Table A.1 for species list and abundances). Species nomenclature was standardised to adhere to The Plant List database (TPL, 2013).

2.2.2 Quantifying β-diversity

To quantify β-diversity across the landscape, we divided the floristic data into cells of 3 ha (173 m $\times$ 173 m) in size, which provides an optimal trade-off between variance in species richness / stem density and stability of alpha diversity (Fig. A.1). After overlaying a 3 ha mesh across the landscape, we manually placed further cells within the sampling area since the set of tessellated cells that fit fully within the sampling area resulted in under-representation of some local regions, a product of the irregularly shaped network of sampling 'islands' (Fig. 2.1a). The resulting cell configuration gave 1036 cells with a mean stem density of 150 (ranging from 48–280). We removed the 8% of stems that were not identified to species level. While this may result in reduced cell dissimilarity, β-diversity is highly robust to such levels of species exclusions (Pos et al., 2014). We calculated β-diversity using the Bray-Curtis dissimilarity index (d_{BC}), an abundance weighted extension of the Sørensen index (Legendre and Legendre, 2012);

$$d_{BC_{jk}} = \frac{\sum_i |x_{ij} - x_{ik}|}{\sum_i x_{ij} + x_{ik}} \tag{2.1}$$

where $d_{BC_{jk}}$ is a value bounded by [0, 1], describing dissimilarity between cells j and k with high values representing strong dissimilarity, and x_{ij} and x_{ik} represent species abundance of species i for cells j and k, respectively. The resulting distance matrix comprised 536,130 pairwise comparisons.

2.2.3 Environmental variables

To identify the contribution of environmental factors to compositional differences, we calculated five topographical variables known to influence community composition: elevation, slope, Topographic Position Index (TPI), Topographic Wetness Index (TWI) and Terrain Ruggedness Index (TRI). Elevational gradients are associated with ambient humidity, precipitation, wind velocity and soil composition gradients (Jucker et al., 2018, Sundqvist et al., 2013). Hill slope is responsible for the distribution of soil nutrients (Chadwick and Asner, 2016, Xia et al., 2016). TPI refers to cell position with respect to hilltops and valleys and has been linked to evapotranspiration rates, solar radiation and species associations (Clark et al., 1999a, Dyer, 2009). TWI gives a measure of water availability, but has further been linked with soil depth, soil pH and nutrient availability (Moore et al., 1993). TRI gives a measure

of the variance in topography is thus linked with many of the aforementioned associations. Furthermore, many of these metrics are likely be implicated in dispersal limitation, particularly for autochorous and anemochorous species.

All variables were derived from the terrain-corrected ALOS PALSAR Digital Elevation Model (DEM) (JAXA/METI, 2011) at a resolution of 12.5 m. Elevation was taken as the mean elevation within the cell (range 6–115 m.a.s.l). Slope was calculated as the mean slope of the four planes formed by considering 3 cell corners at a time. TPI compares the elevation of a pixel against the mean elevation within a 50 m radius, with positive values representing ridges and negative values representing valleys (Guisan et al., 1999). TWI was calculated per Böhner and Selige (2006) via SAGA (Conrad et al., 2015) which improves upon the standard TWI by correcting erratic flow patterns on flat areas and deep valleys, and averaged across each cell. Finally, TRI was calculated as $\sqrt{\frac{\sum_{n=1}^{8}(p_i - p_n)^2}{8}}$, where p_i is the focal pixel and p_n is one of the 8 surrounding pixels, averaged across the cell. Variable correlation and spread is displayed in Figure A.2.

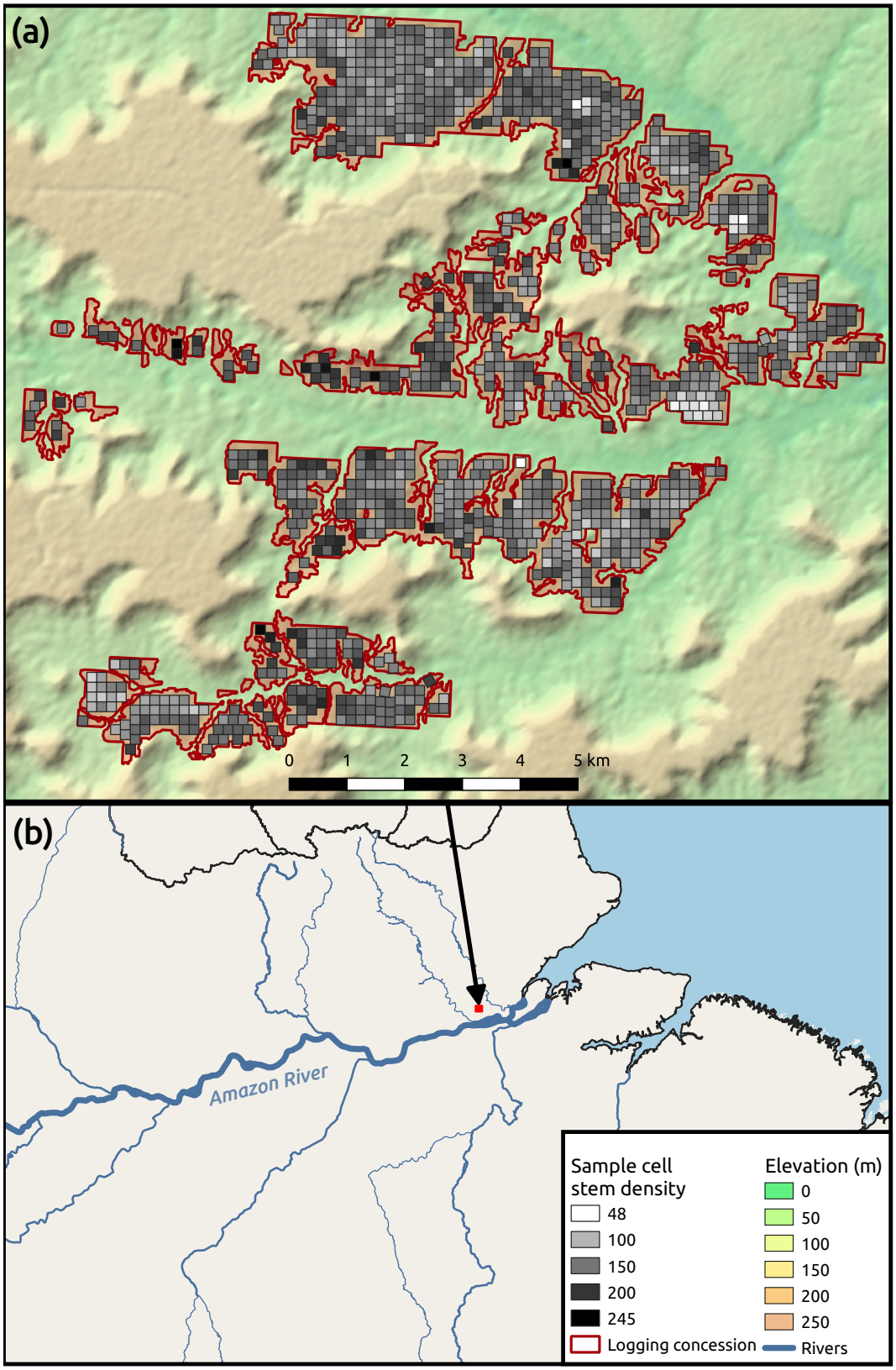

Figure 2.1: The forest inventory in Vale do Jari, Pará, Brazil (b) spans a heterogeneous environment. Floristic data was separated into 1036 3 ha cells of varying density (a).

2.2.4 Statistical methods

Assessing spatial autocorrelation of community composition

We determined the degree of spatial autocorrelation across the whole study area via a Mantel correlogram. Here, we created a geographical distance matrix corresponding to our community dissimilarity matrix. The Mantel correlogram assesses autocorrelation over geographical space by assigning distance classes and performing the Mantel test (Mantel, 1967), which tests for correlation between distance matrices, for each distance class. Significance is tested by randomly shuffling the values of the community dissimilarity matrix for 999 permutations. Positive Mantel r values demonstrate greater compositional similarity than expected by chance and negative values demonstrate dissimilarity. We used Sturges' rule (Sturges, 2012) to determine the number of distances classes to use. Further, since the number of comparable cell pairs decreases as the geographical separation approaches the two most distant cells, we set a distance class limit such that no cell is discounted for any given distance class. (Legendre and Legendre, 2012)

Quantifying environmental and geographical effects

To determine the relative roles of environmental and geographical distance, both individually and jointly , we implemented Generalised Dissimilarity Modelling (GDM) (Ferrier et al., 2007) to partition β-diversity variance into its environmental (E), distance (D) and co-variance components. Here, the co-variance component (D$\times$E) refers to the variance described by spatially autocorrelated environment.

GDM is an extension of matrix regression that accommodates non-linearity between β-diversity and each environmental and geographical component. This is achieved by fitting non-linear functions directly to each variable in the form of flexible I-splines (Ramsay and Others, 1988), giving the best relationship between cell environmental/geographical distance and compositional turnover. The combination of these I-splines provides a linear-predictor coined as the 'predicted ecological distance', enabling the curvilinear relationship between inter-cell ecological distance and β-diversity to be estimated. The salient feature of this method is that the maximum height of each I-spline represents the total amount of compositional turnover associated with the given variable while holding all other variables constant, thereby indicating its relative importance.

The slope of the I-spline also indicates the rate of species turnover along the variable in question (Ferrier et al., 2007). This allowed us to address our second question regarding the relative importance of geographical and environmental distance in predicting compositional dissimilarity. We used the default of three I-spline func-

tions per predictor and determined variable significance and importance by randomising the positions of each variable in the dissimilarity matrix in turn, over 50 permutations, and noting the loss of explanatory power. Backwards stepwise selection was used to obtain the final model in which all variables were significant. GDM was conducted using the `gdm` package (Manion et al., 2018) in `R` (R Core Team, 2019).

Neutral simulations

In determining the role of stochastic dispersal processes in the formation of compositional dissimilarity gradients, we produced a set of spatially-explicit neutral simulations with which to compare against observed patterns, using a similar approach to Bongalov et al. (2019). We implemented a backwards-time coalescence approach (Rosindell et al., 2008), which replicates the results of forwards-simulated neutral models with several orders of magnitude in reduced computational cost.

Spatially explicit neutral simulations generally function on the following principles:

- An arena composed of n individuals of m species is established
- A random individual is chosen to die and a replacement individual occupies its space
- The species identity of the replacement is determined by either:
  (a) a speciation event, of probability v (the per capita speciation rate); or
  (b) dispersal from an existing individual with probability $1 - v$ where species identity is determined by a dispersal kernel such that the replacement is more likely to an offspring of nearby individuals
- The process is repeated over many time-steps to produce a final community

We established an arena surrounding the study site composed of 3 ha cells (Fig. A.3a). We used an arena 100 times the area of the study site extent (Fig. A.3b), providing a more realistic scenario of how migration into the study site may occur in the Amazon Basin. Stem density of each cell was matched to that of the observed forest inventory, while all cells falling outside the study site were assumed to have the median observed density. We used a two parameter, fat-tailed dispersal kernel since it replicates a more biologically realistic kernel than the typical Gaussian Probability Density Function (PDF) (Clark et al., 1999b). Specifically, we implemented a dispersal kernel, equivalent to that in Rosindell and Cornell (2009), with rescaled parameters where σ roughly corresponds to the peak and τ dictates to the fatness

of the tail (Fig. 2.2). Note that decreasing values of τ produce fatter tails and as $\tau \to \infty$, the kernel becomes equivalent to the Gaussian PDF. We simulated 350 neutral communities using `pycoalescence` (v1.2.7a available at https://pypi.org/project/pycoalescence/) with 50 combinations of dispersal kernel parameters, selected by Latin hypercube sampling, with $\sigma \in [0.1, 2]$ and $\tau \in [0.1, 20]$, for seven speciation rates $v \in \{1\text{e}{-7}, 5\text{e}{-6}, 1\text{e}{-6}, 5\text{e}{-5}, 1\text{e}{-5}, 5\text{e}{-4}, 1\text{e}{-4}\}$.

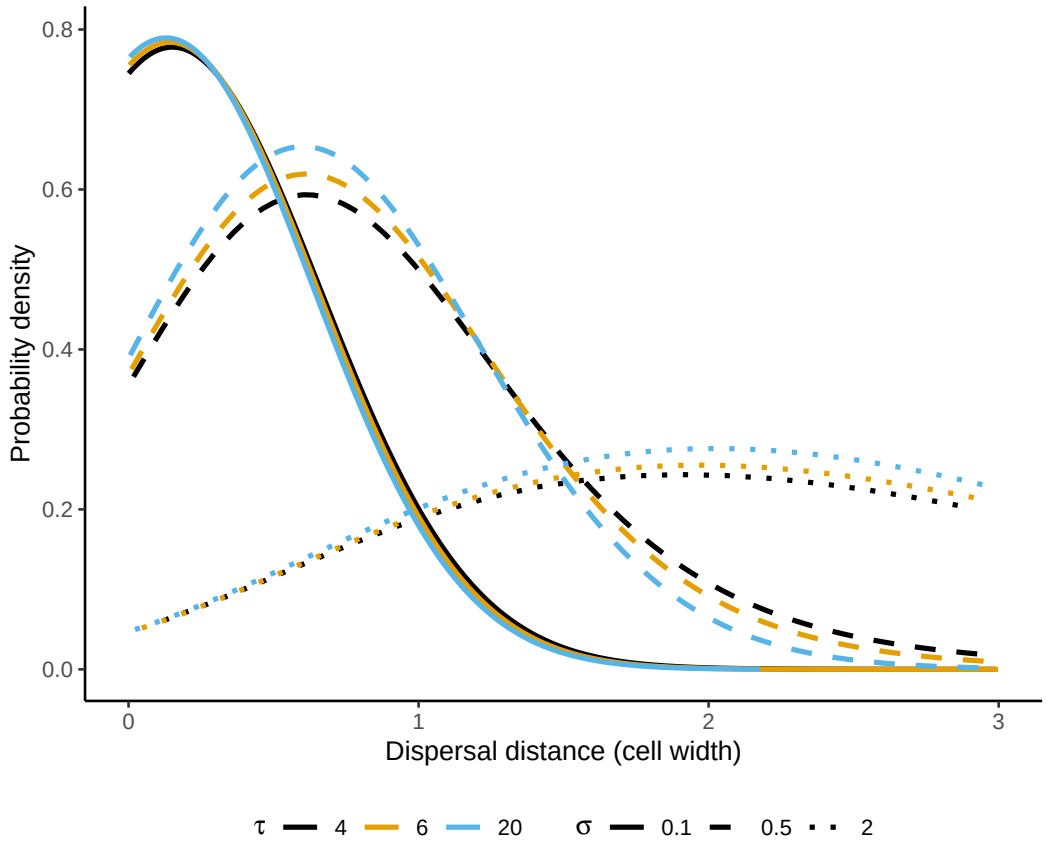

Figure 2.2: The dispersal kernel implemented in our neutral simulations is controlled by two parameters: σ which dictates the peak; and τ which dictates the fatness of the tail.

Assessing the contribution of stochastic processes to β-diversity patterns

Given that any spatial autocorrelation within our simulated neutral communities is inherently a product of geographical distance, we should expect that there exists a parameter set that can replicate the observed pattern of compositional turnover attributed to geographical distance only (D) at our study site i.e independent of environmental factors (E) and spatially autocorrelated environment (D$\times$E). Further, given that stochastic dispersal processes act independently of environmental filtering, we should also expect that a parameter set can replicate observed composi-

tional turnover attributed to spatial autocorrelation (D + D$\times$E) i.e. geographical distance only (D) and spatially autocorrelated environment (D$\times$E). It then follows that, if a single parameter set is able to reconstruct the observed pattern of spatial autocorrelation explained by geographical distance only (D) and geographical distance and spatially autocorrelated environment (D + D$\times$E) concurrently, that stochastic dispersal processes are the primary driver of spatial autocorrelation in community composition. Conversely, if distinct simulation parameters are necessary to match observed patterns, environmental filtering plays a key role in spatial autocorrelation of communities.

To test this, it was first necessary to align each neutral community with the sample cells used in the observed community since some cells were manually placed as mentioned in section 2.2.2. To achieve this, the stationary Poisson process was used to randomly distribute individuals to points within each neutral cell. Communities were subsequently resampled across the sample cell configuration used for the observed dataset (Fig. A.3c). GDM analyses were subsequently run for each simulated census with geographical distance as the only predictor variable since environmental variables are not relevant under a neutral framework. The resulting I-splines from each model were then compared to I-splines of the observed community representing: (a) the geographical component only (D) and (b) the full extent of spatial autocorrelation (D + D$\times$E).

Determining matches between simulated and observed patterns

To decide whether a given I-spline was an adequate match to I-splines of the observed data, it was necessary to define a rejection threshold pertaining to the deviation between observed and simulated communities. To this end, we defined a baseline level of uncertainty for each I-spline that reflects the underlying variation in the observed data (May et al., 2015). Observed pairwise cell comparisons were randomly divided into five 'samples' such that no cell-pair was shared between samples, yet cells were roughly equally represented across samples. This prevented biases that might arise from cells with environmental, geographical or compositional identities at the extremes being overrepresented within a sample (Fig. A.4). I-splines for each sample were extracted and the average I-spline across all samples was calculated (Fig. 2.3). Subsequently, the mean relative deviation (mRD) between each sample, s, and the average I-spline was calculated as;

$$mRD_{i,s} = \frac{1}{n_i} \sum_{x=1}^{n_i} \left| \frac{S_{samp}(i,x,s) - \bar{S}(i,x)}{\bar{S}(i,x)} \right| \tag{2.2}$$

where $\bar{S}(i,x)$ is the average I-spline, i, derived from the five samples at geo-

graphic distance, x.

The baseline uncertainties, ϵ_i, then, were defined as the *greatest* observed $mRD_{i,p}$, giving rejection thresholds of 0.0744 and 0.0846 for D and D$\times$E respectively. This definition of baseline uncertainty is similar to that of May et al. (2015), who used the stricter, *mean* $mRD_{i,p}$. However, note that β-diversity specifically, could only be matched to their neutral simulations by adjusting the species diversity of their, non-spatial, meta-community beyond the bounds congruent to other spatial summary statistics without relaxing rejection thresholds. Our definition of baseline uncertainty thereby stands as a coherent and valid method of rejection.

We divided each neutral simulation in the same way, with each sample composed of equivalent cell-pairs and, again, took the average I-spline across the samples. A given parameter set, p, was defined as a match when the mRD between the average simulated and average observed I-splines was less than the rejection threshold, under the slightly modified definition:

$$mRD_{i,p} = \frac{1}{n_i} \sum_{x=1}^{n_i} \left| \frac{\overline{S_{sim}}(p,x) - \overline{S_{obs}}(i,x)}{\overline{S_{obs}}(i,x)} \right| \tag{2.3}$$

where, $\overline{S_{obs}}(i,x)$ is the average I-spline, i, and $\overline{S_{sim}}(p,x)$ is the average I-spline for parameter set p at geographical distance x. Note, $\overline{S_{sim}}(p,x)$ has no i component since simulated GDMs contain no environmental variables.

In short, a given parameter set was deemed to replicate the observed pattern of compositional turnover when it deviated from the observed pattern less than the highest underlying variability exhibited at the study site. This enabled us to answer our third question of whether stochastic dispersal processes can explain the pattern of spatial autocorrelation at the study site or whether environmental filtering plays a key role.

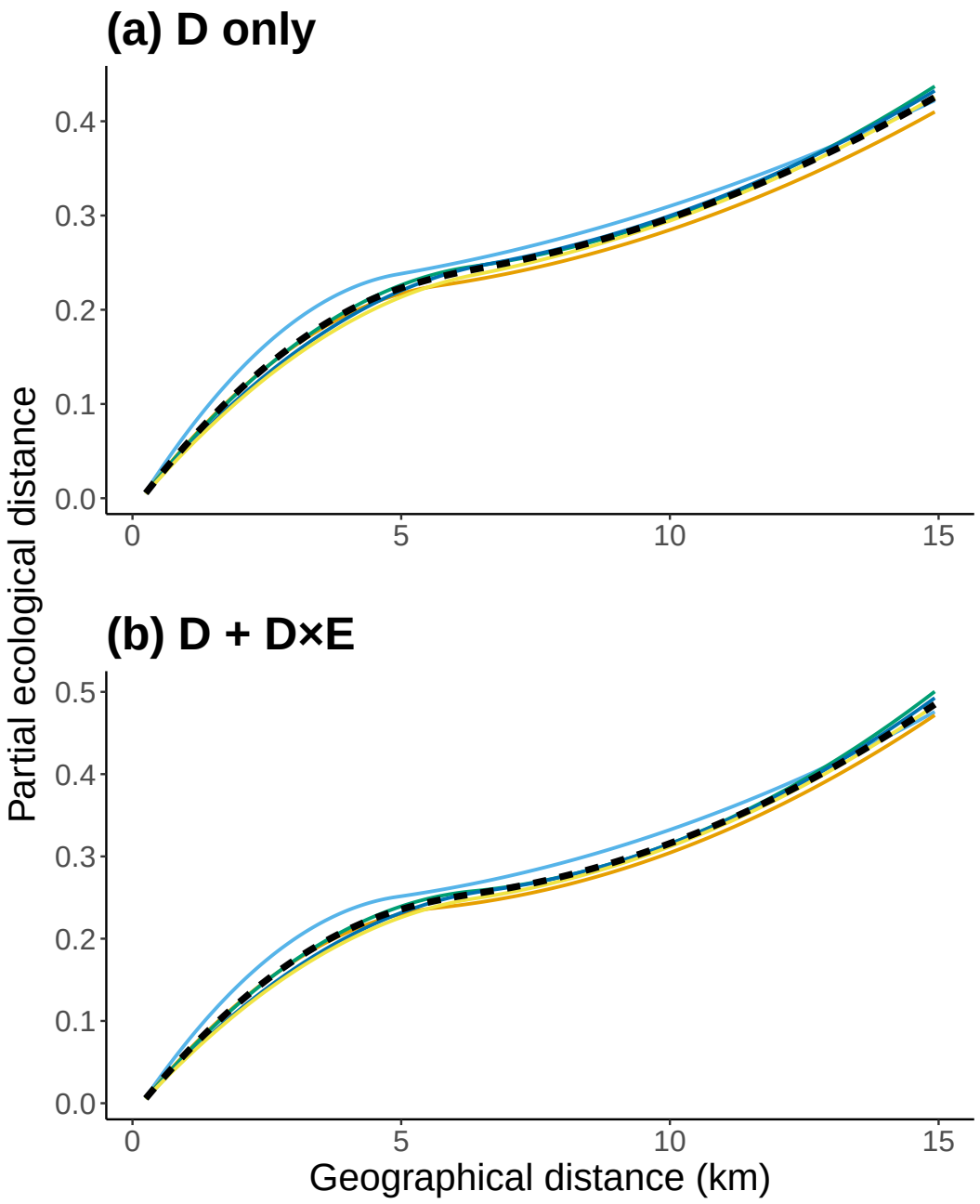

Figure 2.3: I-splines, representing contribution to observed dissimilarity of distance (a) and spatial autocorrelation (b) were extracted for five samples of the forest inventory to determine rejection thresholds, ϵ_i, for simulated communities. Rejection thresholds were defined as the mean relative deviation between the sample that deviated the most from the I-spline averaged across all samples (dashed black line). Thin coloured lines represent I-splines for individual samples, here the sample represented by the blue I-splines exhibited the greatest mRD, giving rejection thresholds, ϵ, of 0.074 and 0.085 for D and D$\times$E respectively

2.3 Results

2.3.1 Spatial autocorrelation of community composition

Community similarity between cells was significantly correlated with geographical separation up to the 8.5 km limit of our analysis (Fig. 2.4) Canopy tree communities were more similar than expected by chance up to distances of 4.2 km. Positive correlation ceased at cell separations of roughly 4.9 km, but beyond this distance, plots were increasingly more dissimilar than expected by chance.

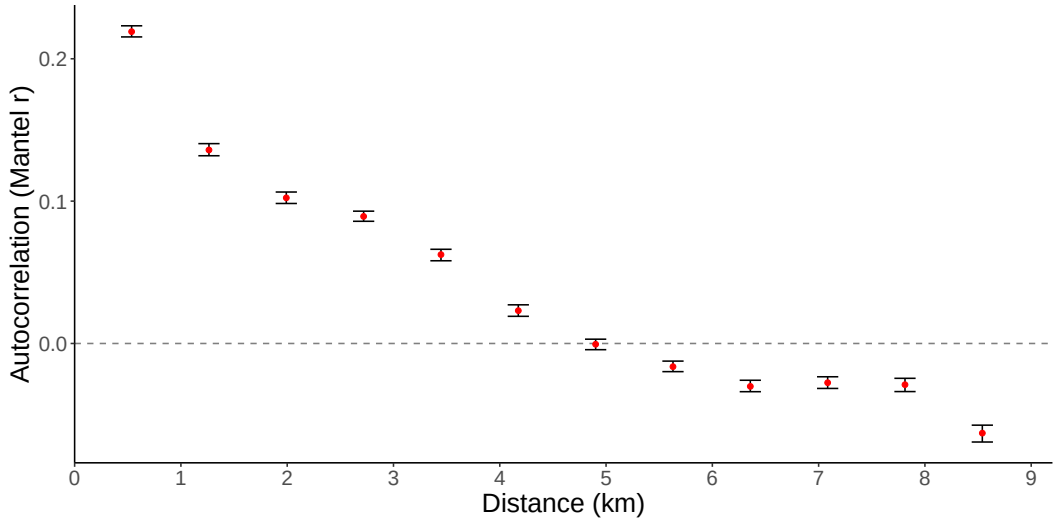

Figure 2.4: Canopy tree community composition exhibits spatial autocorrelation at scales of up to 8.5 km at Vale do Jari. Positive values of Mantel r signify that communities are more similar than expected by chance and vice versa. Confidence intervals are calculated from 500 bootstrap permutations.

2.3.2 The contribution of environmental and geographical distances to β-diversity

β-diversity was partitioned into three components using Generalised Dissimilarity Modelling (GDM); environmental (E), geographical distance (D) and spatially autocorrelated environment (D$\times$E), where D + D$\times$ E represents the full extent of spatial autocorrelation. Four of the six considered variables were significantly associated with β-diversity; geographical distance between cells and differences in Topographic Wetness Index (TWI), elevation and Topographic Position Index (TPI). All variables together explained 14.7% of community dissimilarity, with geographical separation representing the majority of explained variance (10.6%) while only 1.2% was significantly attributable to environmental variables.

The spatial structure of the underlying environment (D$\times$E) was not able to fully account for the spatial autocorrelation (D + D$\times$E) at the study site, explaining 2.8% of the variance, (Fig. 2.5a). Cell pair difference in TWI was the most important environmental variable, explaining 0.56% of the variance, followed by elevation and TPI, explaining 0.4 and 0.1% respectively. Slope and Terrain Ruggedness Index (TRI) were not significantly associated with β-diversity and were removed from the final model via backwards stepwise selection (Table 2.1).

TWI and TPI contributed to community dissimilarity only beyond a given threshold (Fig. 2.5c&e), such that cell-pairs with extreme differences in water availability and "ridge top vs valley bottom" cell-pairs were more dissimilar yet no dissimilarity was observed within dry and valley bottom cell-pairs. Conversely, separation in geographical distance and elevation resulted in community dissimilarity at small offsets along the full extent of their gradients (Fig. 2.5b&d).

The full model produced a curvilinear response across ecological distance, which represents cell-pair differences as a combination of all variables. The contribution of ecological distance to community dissimilarity decayed along its gradient, although this effect was minimal and the model fit was close to linear (Fig. 2.5f).

Table 2.1: Results from β-diversity variance partitioning of GDM Vale do Jari forest inventory data. Geographic distance, Topographic Wetness Index (TWI), elevation and Topographic Position Index (TPI) were significantly associated with β-diversity. Note, the full amount of variance explained by constituents of E could not be allocated due to co-variance with D.

Partition	**Variance explained (%)**	**Variable importance (%Δ(Deviance))**	p
D	10.60	71.96	0***
E	1.24	8.33	0***
D$\times$E	2.83	–	NA
Total	**14.67**	**–**	**0*** **
D + D$\times$E	13.44	–	NA
E + D$\times$E	4.07	–	NA
Constituents of E			
TWI	0.56	4.46	0***
Elevation	0.40	3.02	0***
TPI	0.10	0.85	0.02*
Co-variance	3.01	–	NA

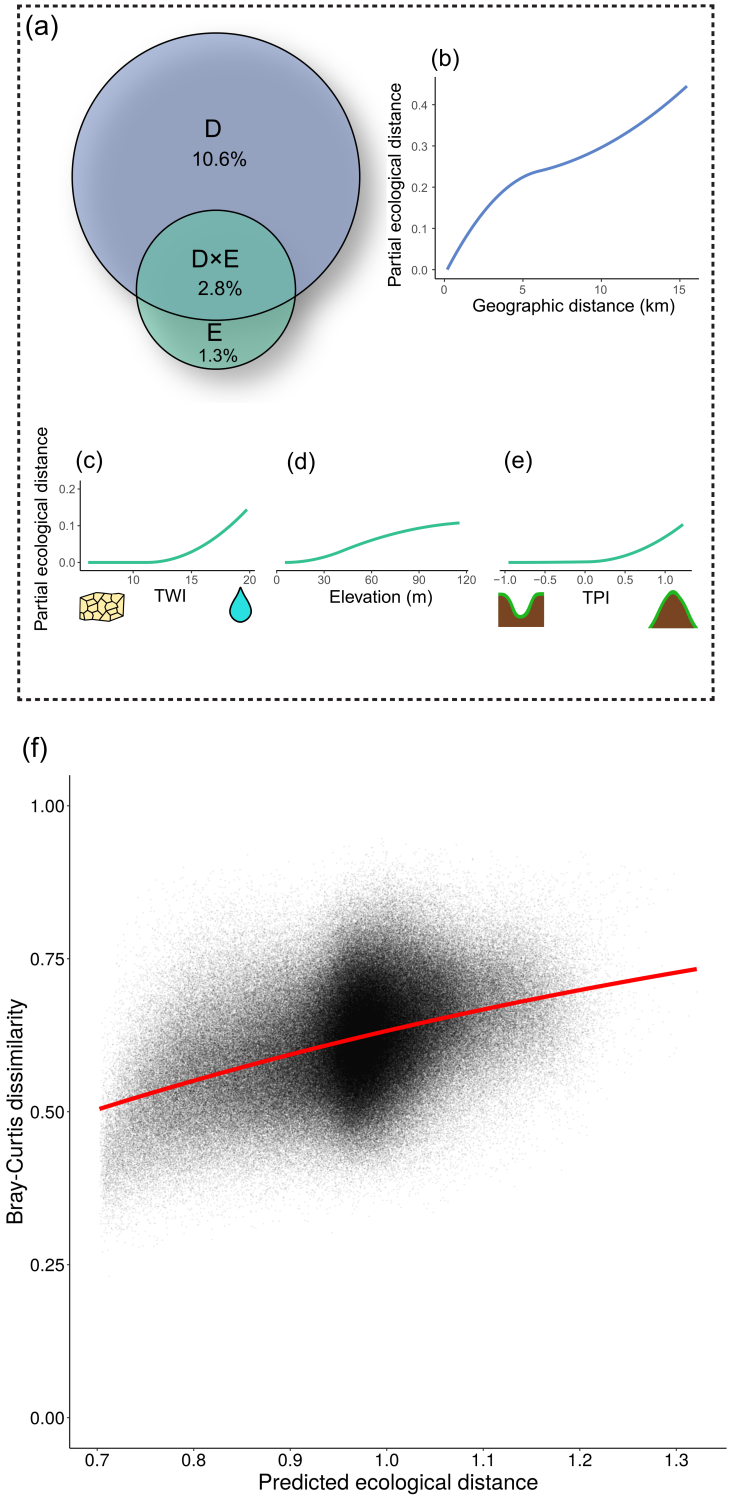

Figure 2.5: Variance in compositional turnover was partitioned into that explained by geographical separation (D), environmental differences (E) and spatially autocorrelated environment (D×E) (a). GDM produced I-splines (partial regression fits) for each variable significantly associated with β-diversity (b-e). The maximum height of each I-spline represents the total amount of compositional turnover associated with that variable and the shape indicates how the rate of turnover varies along the gradient. Compositional dissimilarity increased with predicted ecological distance, which represents cell-pair separation for all variables (f).

2.3.3 The role of stochastic dispersal processes

Under a neutral framework, stochastic dispersal processes act independently of the underlying environment. Therefore, we expect neutral models to be able to reconstruct the observed pattern of compositional turnover attributed to both geographical distance (D) and geographical distance plus spatially autocorrelated environment (D + D$\times$E). Further if spatial autocorrelation of community composition is primarily driven by dispersal and dispersal is truly stochastic we can expect that a single parameter set can replicate both D and D + D$\times$E jointly.

Of the 350 neutral communities simulated we found two parameter sets that matched the observed patterns of β-diversity attributed to geographic distance (D) and three for β-diversity attributed to spatial autocorrelation (D + D$\times$E) (Fig. 2.6). However, no parameter set was a match for both D and D + D$\times$E (Table 2.2) which is consistent with the notion that local environmental filtering is a key driver of β-diversity within spatially autocorrelated environments (D$\times$E).

Table 2.2: Parameter sets of matching neutral models. No parameter set was able to replicate the patterns of both D and D + D$\times$E simultaneously.

Speciation rate	σ	τ	$mRD_{D\ only}$	$mRD_{D+D\times E}$	Match$_{D\ only}$	Match$_{D+D\times E}$
1e^{-5}	1.69	6.55	0.068	0.122		✓
1e^{-5}	1.16	16.61	0.070	0.118		✓
1e^{-5}	1.35	10.52	0.118	0.082	✓	
5e^{-5}	1.06	9.12	0.076	0.067	✓	
5e^{-6}	0.51	5.64	0.096	0.084	✓	

$\epsilon_{D\ only}$ = 0.0744
$\epsilon_{D+D\times E}$ = 0.0846

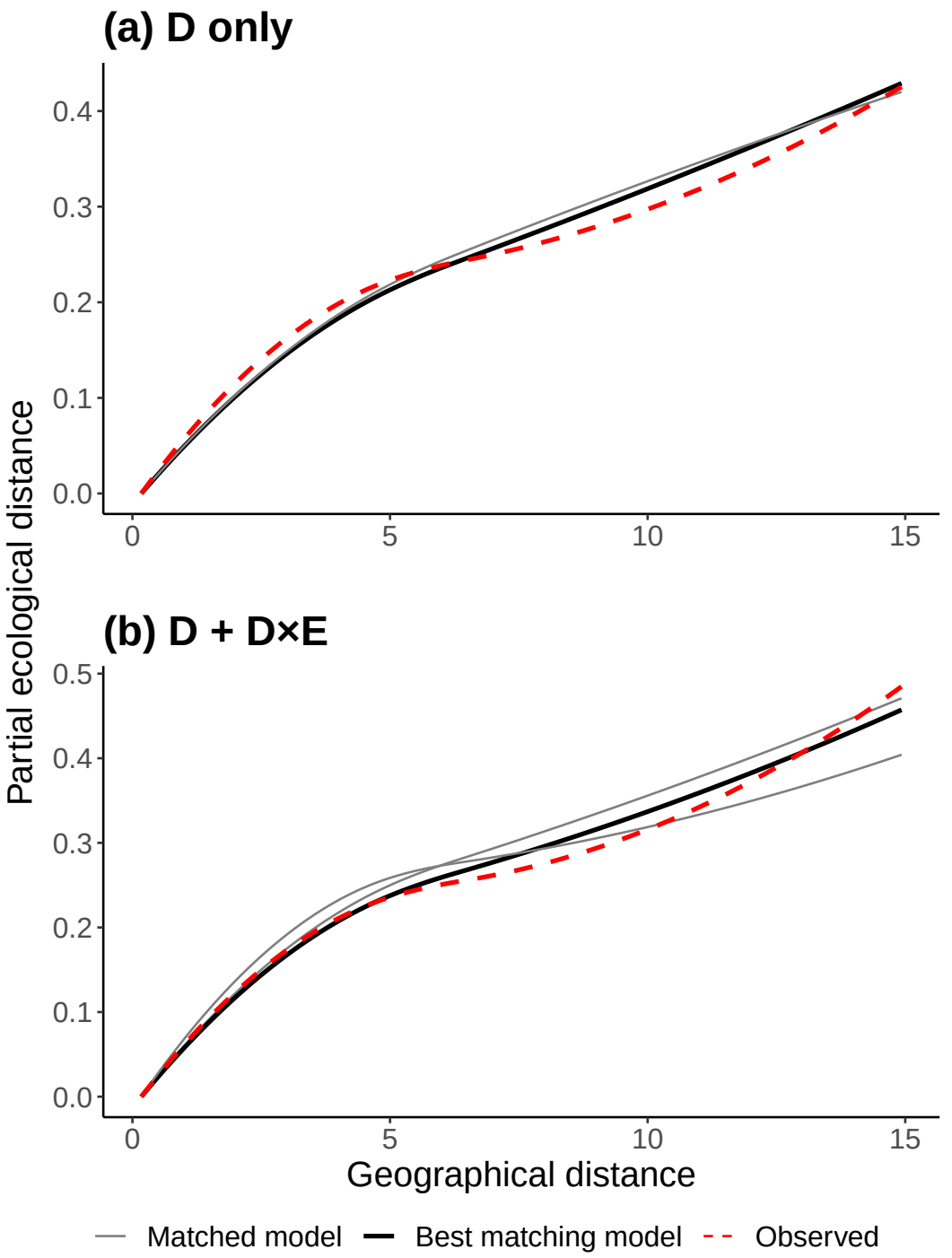

Figure 2.6: I-splines generated via GDM, representing the contribution to β-diversity observed in the forest inventory at Vale do Jari (red) and those modelled by matching neutral simulations (black). Two neutral simulations successfully matched the pattern of compositional turnover that does not covary with environmental structure (D only) (a). Three simulations matched the full pattern of spatial autocorrelation (D + D$\times$E) (b), but no parameter set was able to replicate the patterns of both D and D + D$\times$E. See Table 2.2 for simulation parameters.

2.4 Discussion

Our findings advance the our understanding of the role of deterministic and stochastic processes in driving β-diversity in tropical forests. The use of landscape scale forest inventory data afforded the opportunity to disentangle the underlying components driving compositional turnover of canopy trees species, addressing a critical knowledge gap given the key role that canopy tree communities play in dispersal, competition, ecosystem functioning and carbon storage. We demonstrate that spatial autocorrelation of community composition for canopy trees extends well beyond what was previously detectable under the existing network of tropical forest plots and that various environmental factors play a role in shaping community composition along niche gradients. Building upon recent philosophical, theoretical and empirical assertions that neutral and deterministic processes act together to construct patterns of community composition (Bongalov et al., 2019, May et al., 2015, Purves and Turnbull, 2010, Wennekes et al., 2012), we corroborate the dual roles of environmental and stochastic dispersal processes with landscape-scale field data. We further show that environmental structuring is not limited to distinct forest-type shifts. Stochastic dispersal processes are unable to fully reconstruct spatially autocorrelated patterns of community composition within a single forest type, indicative of environmental structuring at scales finer than previously demonstrated for canopy tree communities.

2.4.1 The scale of spatial autocorrelation

Spatial autocorrelation of community composition is widely observed in tropical forests, with our results showing a similar pattern to previous studies in the region revealing autocorrelation decay with distance between communities (Condit et al., 2002, Duque et al., 2009, Zhang et al., 2013). However, the majority of results are derived from small forest plots of up to 50 ha, a scale at which large canopy tree community assembly is undetectable. Further, inter-plot studies are often separated over large distances of non-contiguous forest, which presents difficulties in making assertions on fine scale spatial autocorrelation, as well as, suffering from under-representation of rare species.

Typically, spatial autocorrelation of community composition decays rapidly at short distances, exhibiting almost no further decay beyond 4 km (Condit et al., 2000a, 2002, Duque et al., 2009). Our results present a key finding that for large canopy trees, community autocorrelation is maintained over larger scales than was previously known, with community similarity persisting up to distances of 5 km and continuing to decline up to at least 8.5 km. Whilst novel, this finding should not be so

surprising. Firstly, seed dispersal is strongly correlated with tree height, allowing for greater dispersal distances amongst canopy tree communities (Thomson et al., 2011). Secondly, longer life cycles and survival rates associated with adult stature (Visser et al., 2016) may enable the maintenance of autocorrelation due to resistance to temporal environmental variance (Chisholm et al., 2014).

2.4.2 Environmental drivers of β-diversity

Environmental variance has long been observed as a key determinant of species distributions and biodiversity in tropical forests, across a range of scales (Draper et al., 2019, Harms et al., 2001b, Kahn, 1987, Lieberman et al., 1985, Tuomisto and Ruokolainen, 1994, Valencia et al., 2004). However the question of how environmental variation impacts canopy trees has remained elusive due to the spatial constraints of the current network of vegetation plots within tropical forests (Marvin et al., 2014). The large scale of the forest inventory analysed here enabled us to unpick the contributions of several environmental variables to compositional turnover.

Environmental variables (E only), explained only a small proportion of observed variance (1.3%), considerably less than has been observed for small woody stems at local scales (John et al., 2007b, Myers et al., 2013, Tuomisto et al., 2003). This suggests that at the seedling stage, environmental filtering occurs at much finer scales than is represented in our analysis. Habitat filtering occurs during the early life stages of trees (Baldeck et al., 2013), therefore, homogenising environmental variables at the scale of 3 ha reduces their explanatory power. Further, we considered only a handful of available topology-derived variables derived from DEMs, while soil composition is known to play a key role in environmental filtering (Anderse et al., 2014). Bongalov et al. (2019) were also able to attribute more variance to environmental variables through hyperspectral imaging of canopy trees. Their smaller cell size of 1 ha may help explain this, but more likely the greater degree of environmental heterogeneity within their sampling area is responsible for greater environmental constraints that generate increased impact on community composition.

Topographic Wetness Index (TWI) was the most important environmental variable at the 3 ha scale. Divergent water-use strategies are an important mechanism controlling environmental associations (Baltzer et al., 2005). Engelbrecht et al. (2007b) found that species drought sensitivity played a key role in shaping species distributions. Our results replicate these findings, influencing community dissimilarity only beyond a threshold of cell-value differences, suggesting that certain species fail to establish within drier environments.

Community dissimilarity responded to small changes in mean elevation. While elevation has been linked with differences in humidity and precipitation, the eleva-

tional gradient in the study sampling area is unlikely to be strong enough to impact such processes. Our result more likely reflects differences in soil chemistry, which covaries with elevational gradients (Chadwick and Asner, 2016, Xia et al., 2016), thereby impacting environmental filtering.

Lastly, we find Topographic Position Index (TPI) to have a small but statistically significant impact on community dissimilarity. Dissimilarity was only observed between valleys and ridges, i.e. not between cells with intermediate TPI values. Ridges are assumed to influence radiation load (Dyer, 2009) and dissimilarities may be driven by dominance of light demanding species.

Compositional turnover was present in the absence of any environmental variables (E + D$\times$E), with 10% of the variance in community composition attributable to geographic distance (D). This is highly consistent with the variance attributed in Bongalov et al. (2019), supporting our reasoning for the lower explained variance attributed to environmental variables. Overall, our results provide further proof that niche theory cannot fully account for community composition patterns.

2.4.3 Stochastic processes

Debate surrounding processes driving β-diversity have typically revolved around a niche vs neutral standpoint. More recently, the notion of stochastic dispersal and environmental processes superimposing to recreate the patterns of beta-diversity we observe has gained traction (Wennekes et al., 2012). Fully disentangling their relative roles has proven difficult since the component of β-diversity attributable to spatially autocorrelated environment (D$\times$E) can equally arise from niche or stochastic dispersal processes.

We show that environmental factors represent a key driver of β-diversity within spatially autocorrelated environments. Neutral simulations were able to reconstruct observed patterns of compositional turnover attributed to both geographical distance (D) and geographical distance, plus spatially autocorrelated environment (D + D$\times$E). However, no parameter set was capable of matching both patterns simultaneously. It follows that environmental variables must be an important component of the variance attributed to the spatially autocorrelated environment (D$\times$E) partition and cannot be attributed solely to stochastic dispersal. This finding gives further credence to the notion that stochastic and dispersal processes can act jointly to determine the patterns of compositional turnover.

This finding also suggests that strong environmental separation is not necessary for environmental variables to shape compositional turnover. Bongalov et al. (2019) demonstrate that neutral models could not match observed patterns of compositional turnover across forest-types and assert that species with similar competitive

strategies may interact in a neutral manner within forest types (where environmental variance is low) to drive compositional turnover. In contrast, we found that stark 'forest-type' differences are not necessary for environmental filtering to operate, environmental variables can act at finer scales *within* forest-types to affect compositional turnover.

This leaves us with two potential scenarios: (i) environmental filtering is a key driver at fine scales or (ii) dispersal is not truly stochastic. Scenario (ii) could manifest through the environment impacting dispersal limitation, such as anemochorous species having greater dispersal capacity at higher elevations; or via species specific dispersal kernels.

The processes driving β-diversity in tropical canopy tree communities are clearly more nuanced than strict niche vs neutral theories. Negative density dependence processes, for example, could further superimpose over compositional structuring. Future study should focus on reconciling the multitude of theories that have been proposed to explain community assembly (Wright, 2002). The opportunity to use landscape-scale forest inventories and hyperspectral imaging in concert presents a potentially fruitful way forward. Further, the study of phylogenetic and functional β-diversity could provide key insights into the role of environmental variance under niche conservatism.

2.4.4 Caveats

Our study has three key caveats. Firstly, although our sampling area allows for landscape-scale community patterns to be analysed, it is not fully contiguous. Forest inventory data was collected only in regions viable for selective logging; such 'sampling islands' are thus likely separated by areas with inherently different environmental conditions and probably tree communities (see Fig 2.1a). For example, elevation ranges from 0–240 m across the landscape but reaches a maximum of only 206 m within the sampling area, with mean cell elevation spanning only 6–115 m. This may provide a potential explanation for the large scale of spatial autocorrelation of community composition reported; if environmental factors play a key role in determining community composition, we would expect greater dissimilarity between communities within and outside the sampling area. High-fidelity hyperspectral imaging at the landscape scale (Bongalov et al., 2019, Draper et al., 2019) corroborates the notion that spatial autocorrelation plateaus at scales of roughly 4 km. However, Bongalov et al. (2019) found roughly similar scales of autocorrelation for communities that traverse forest-types. While hyperspectral imaging provides a powerful technique for analysing diversity patterns over large scales, 'spectral species' do not necessarily represent biologically distinct species, instead acting as a proxy for under-

lying biodiversity patterns. Combining hyperspectral imagining with the emerging landscape-scale forest inventories would help to resolve this issue.

Second, logging companies used trained para-botanists. However, whilst these are particularly expert at identifying commercially viable species, there is a danger that some rarer or harder to separate species were misidentified. Nevertheless, it is unlikely that mis-identification would have occurred within specific components of environmental gradients and not others.

Lastly, although this study presents a case for local scale environmental filtering in driving the community assembly, our dataset represents only a 'snapshot' of community composition in time. This precludes strong assertions regarding the *processes* governing community assembly to be made, since processes are inherently time-dependent. However, given the current data constraints and the long life spans of canopy trees, our results provide evidence to support the notion that environmental factors operate at local scales to shape canopy tree community composition.

Chapter 3

Phylogenetic beta-diversity informs the factors driving compositional turnover in tropical canopy tree communities

3.1 Introduction

Understanding processes governing the turnover of species composition – termed β-diversity – remains a key unresolved issue in community ecology, with core implications for applied and theoretical research. β-diversity is the link dictating the relationship between local (alpha) and regional (gamma) diversity (Whittaker, 1960). In a world facing increasing land-use change, over-hunting and other anthropogenic-driven disturbances, understanding the processes that maintain diversity over space can play a crucial role in conservation strategy (Socolar et al., 2016). Similarly, a key theoretical problem is to explain how large numbers of species are able to coexist within hyperdiverse systems, especially tropical forests (Valencia et al., 1994).

One heavily debated aspect of β-diversity surrounds the relative importance of stochastic processes and environmental factors in dictating compositional turnover. Debates have historically revolved around niche vs. neutral standpoints. Environmental filtering is well established as a key ecological process (Clark et al., 1998, John et al., 2007a, Kraft et al., 2008, Svenning, 1999) governing community composition, yet niche theory has long been recognised as being insufficient in explaining the high degree of species diversity in tropical forests (Grubb, 1977). However, more

than 100 mechanisms have been postulated to salvage niche theory (Wright, 2002).

Conversely, neutral theory (Hubbell, 2001) proposes that stochastic demographic, dispersal, mortality and recruitment processes can account for observed biodiversity. In reality, neutral theory is regularly violated, failing to: (1) explain multiple patterns of biodiversity concurrently (May et al., 2015); (2) account for negative density dependence mechanisms (Connell, 1971, Hubbell, 2001, Purves and Turnbull, 2010); and (3) replicate β-diversity patterns over large spatial scales (Condit et al., 2002).

Recent ecological theory has explored the notion that stochastic and deterministic processes act jointly to explain compositional turnover (Purves and Turnbull, 2010, Wennekes et al., 2012). Chisholm and Pacala (2010) demonstrated that spatial autocorrelation of community composition is generally accompanied by spatial autocorrelation of the underlying environment, meaning β-diversity patterns could equally arise from environmental filtering as from stochastic mortality-dispersal-recruitment mechanics. This has presented a major challenge for community ecologists.

Considerable efforts have been aimed at disentangling the ecological processes that drive β-diversity into their environmental and geographical components (Cáceres et al., 2012, Legendre et al., 2009, Myers et al., 2013). However, their relative importance varies with study design and spatial scale. Stochastic dispersal limitation has been implicated as dominating at local scales (Condit et al., 2002, Tuomisto et al., 2003), with environmental filtering operating at the landscape scale (Davidar et al., 2007, Hardy et al., 2012). The component attributed to spatially autocorrelated environment has, thus, proven difficult to unpick.

β-diversity studies in this vein have been widespread, but have typically focussed on taxonomic dissimilarities between assemblages. However, this approach considers all species as equivalent, not taking into account evolutionary dissimilarities. Analogous to taxonomic β-diversity (TBD), measures of phylogenetic β-diversity (PBD) represent differences in phylogenetic diversity between communities. PBD metrics come with the added dimensionality of evolutionary history and are, thus, more stringent measures of dissimilarity but comparisons with TBD provide key insights into the processes governing β-diversity (Graham and Fine, 2008, Jin et al., 2015). Jin et al. (2015) demonstrated that tracking phylogenetic β-diversity (PBD) along environmental gradients reveals niche responses of lineages, i.e., niche conservatism – a theory at odds with neutral theory. Under the premises of species equivalence and stochastic dispersal, inherent within neutral theory, PBD should not be expected to covary with environmental factors more than does TBD. Comparing patterns of taxonomic β-diversity (TBD) against phylogenetic β-diversity (PBD) thereby affords a valuable opportunity to unpick the relative roles of spatial and environmental factors

within spatially structured environments.

The implementation of PBD to unpick the components of β-diversity has recently become more prevalent, however, conflicting results (Hardy et al., 2012, Legendre et al., 2009, Liu et al., 2016, Qiao et al., 2015, Saito et al., 2015) have meant a clear pattern is yet to emerge. For large tropical canopy trees, the scale over which stochastic dispersal and environmental filtering act in driving β-diversity has been especially elusive. The current network of tropical forest plots (e.g. BCI, RAINFOR, ATDN, CTFS) are generally limited to 50 ha in size and are distantly separated, generating two key problems: (1) community dynamics of canopy tree communities operate at a far greater scale; and (2) the large spatial separation excludes the potential of quantifying the component of β-diversity attributed to spatially autocorrelated environment. This presents as a key knowledge gap given that canopy trees are the primary seed producers, competitors and carbon storers (Pan et al., 2011, Thomson et al., 2011, Wright, 2002).

Advances in airborne high-fidelity hyperspectral imaging technology have proven a powerful tool in bridging the gap in spatial scale (Bongalov et al., 2019, Draper et al., 2019, Jucker et al., 2018) and disentangling aspects of biodiversity patterns. However, the technology is not currently able to distinguish individual tree species and is therefore limited to assessing estimates of turnover of tree forms ('spectral species'). As such, phylogenetic β-diversity (PBD) patterns are not assessable via this route.

The recent emergence of landscape-scale forest inventory data from the forest sector, which identifies trees to species level, affords a fruitful opportunity to bridge this scale gap. However, the scale at which to divide floristic data into cells to capture both environmental and spatial variance remains an unknown for such datasets. A trade-off may occur whereby homogenisation of environmental variables over large scales reduces their explanatory power, yet become irrelevant at fine scales due to processes such as negative density dependence and stochastic demographic interactions dominating.

Here, we use spatially explicit floristic data from a complete forest census of canopy trees covering 5,100 ha of tropical forest in the Amazonian basin to address the following objectives:

(1) To assess and compare the extents of spatial autocorrelation of taxonomic and phylogenetic community similarity to determine how lineages turnover across space.

(2) To quantify the contribution of spatial and environmental variables driving taxonomic β-diversity (TBD) and phylogenetic β-diversity (PBD)

(3) To investigate the scales at which environmental and spatial variables operate to influence TBD and PBD

We expect that:

(1) Spatial autocorrelation of taxonomic community composition will be greater than phylogenetic community composition due to the added dimension in variance of evolutionary history, inherent in metrics of phylogenetic similarity measures.

(2) Environmental variables will explain a greater proportion of phylogenetic β-diversity (PBD) than taxonomic β-diversity (TBD) since environmental affinities are likely to shared across closely related species.

(3) Environmental variables will operate primarily across large scales as previously asserted but will further be significantly detectable at finer scales, especially for PBD.

3.2 Materials and Methods

3.2.1 Study site

The study site (1°13'12"S 52°33'36"W) is based in the region of Vale do Jari, Pará, Brazil, a wet tropical lowland forest of the Amazon Basin, (Fig. 3.1). The soil is characterised by high clay content and low nutrient availability (Dijkshoorn et al., 2005), with mean annual precipitation of 2055 mm and a mean temperature of 25°C. The site is under concession for sustainable forest management by the logging company Orsa Florestal, in accordance with environmental legislation imposed by the Brazilian Institute of Environment and Renewable Natural Resources (IBAMA).

Floristic data comprises 283,954 spatially mapped stems $\geq$ 35cm over $\sim$5100 ha of undisturbed forest from a forest inventory conducted between 2002–2003. Stems were mapped manually, operating within 12.5 m width bands and species were identified to species level where possible, with 377 species, 196 genera and 56 families recorded (see Table A.1 for species list). Geolocation and species identification were independently verified for key species (Ferreira, 2009).

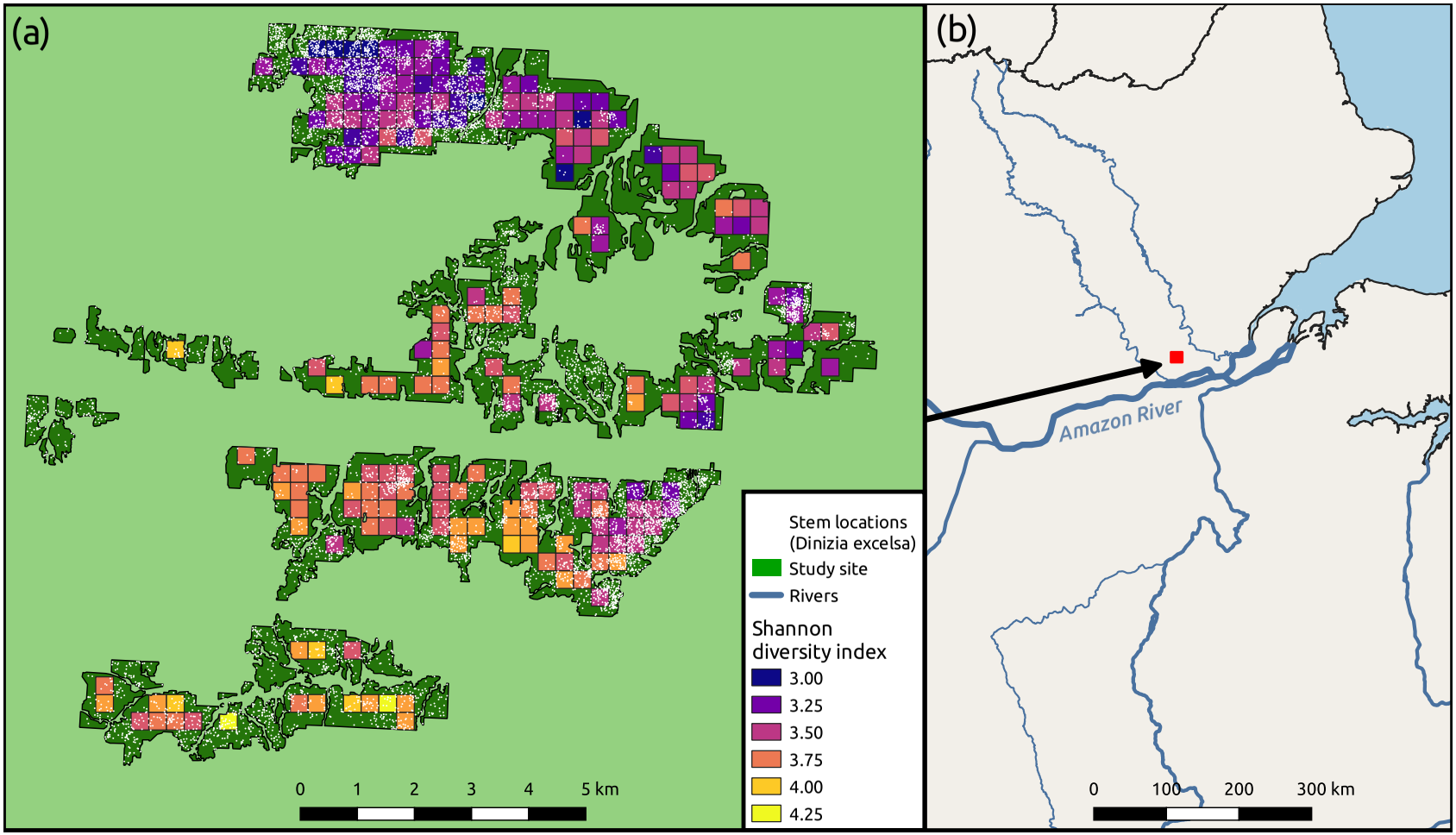

Figure 3.1: The study site is located in the Vale do Jari region of Pará, Brazil (b). The complete forest inventory comprises ~280,000 stems of 377 species $\geq$ 35cm diameter at breast height (DBH). Floristic data was divided into cell sizes of 1, 3, 5 and 10 ha. 10 ha cells and geolocations of *Dinizia excelsa*, represented as white dots, are provided as examples (a).

3.2.2 Environmental variables

In analysing the role of environmental factors dictating patterns of taxonomic β-diversity (TBD) and phylogenetic β-diversity (PBD), we considered five environmental factors known to influence habitat and community composition. Elevation, slope, Topographic Position Index (TPI), Topographic Wetness Index (TWI) and Terrain Ruggedness Index (TRI) were derived from a terrain-corrected Digital Elevation Model (DEM) (JAXA/METI, 2011) with resolution of 12.5 m.

Elevational gradients are associated with ambient humidity, precipitation, wind velocity and soil composition gradients (Jucker et al., 2018, Sundqvist et al., 2013). Hill slope is responsible for the distribution of soil nutrients (Chadwick and Asner, 2016, Xia et al., 2016) and was calculated as the mean slope of the four planes which are formed by connecting combinations of 3 cell corners. TPI refers to a pixel's position in the landscape with respect to hilltops and valleys and has been linked to evapotranspiration rates, solar radiation and species associations (Clark et al., 1999a, Dyer, 2009). TPI is calculated as the relative elevation compared to pixels within a 50 m radius. TWI gives a measure of water availability, but has also been linked with soil depth, soil pH and nutrient availability (Moore et al., 1993) and was calculated using the SAGA algorithm (Conrad et al., 2015) per Böhner and Selige (2006). TRI gives a measure of the variance in elevation and is, therefore, linked with many of the aforementioned associations. It was calculated as the elevational deviation from the 8 surrounding pixels. All environmental factors, with the exception of slope, were taken as the mean value of the pixels within a sampling cell. Variance inflation factors (VIFs) were checked for multicollinearity prior to all analyses but in no case did VIFs exceed 10 (Naimi, 2015).

3.2.3 Spatial variables

To investigate the scale at which spatial and environmental factors operate in driving β-diversity, four cell size scenarios were created by dividing the forest inventory data into 1 ha (100 m $\times$ 100 m), 3 ha (173 m $\times$ 173 m), 5 ha (224 m $\times$ 224 m) and 10 ha (316 m $\times$ 316 m) cells.

For each cell size scenario, we used distance-based Moran's eigenvector maps (dbMEMs) as spatial variables (Dray et al., 2006). DbMEM variables are an efficient way of modelling spatial structure at multiple scales. They are derived from an extension of principle coordinates of neighbourhood matrix (PCNM) analysis (Borcard and Legendre, 2002) in which the Euclidean geographic distances are decomposed into a set of eigenvectors that represent the spatial structure of the cell arrangement. The salient features of dbMEMs are that: (1) they are proportional to Moran's

l coefficient, enabling eigenvectors that model positive spatial correlation to be easily identified; and (2) they are ordered such that the first spatial eigenvectors show broad-scale spatial correlation increasing to finer scales (Fig. B.2). (Borcard et al., 2018)

Significant dbMEMs were selected on the detrended community matrices via forward selection using the Blanchet et al. (2008) double stopping criterion. Forward selection retained 47 of 1289, 44 of 324, 20 of 154, and 24 of 51 dbMEM variables for 1 ha, 3 ha, 5 ha and 10 ha cell size scenarios respectively (Fig. 3.2). R_a^2 for the reduced set of dbMEM variables was nearly equivalent to the full set for all cell size scenarios. Significant environmental variables were selected in the same manner but on the undetrended community matrices as per Borcard et al. (2018). Calculation and forward-selection of dbMEM variables were conducted using the `adespatial` package (Dray et al., 2019).

3.2.4 Quantifying taxonomic and phylogenetic β-diversity

An abundance of β-diversity metrics have been utilised in previous studies (Anderson et al., 2011, Tucker et al., 2017) resulting in some redundancy (Jin et al., 2015, Swenson, 2011). Therefore, a selection of metrics pertinent to unpicking the processes dictating community composition and turnover at both taxonomic (TBD) and phylogenetic (PBD) were considered:

(1) Taxonomic β-diversity (TBD) was quantified using the Bray-Curtis dissimilarity index (d_{BC}) (see Eqn. 2.1) as a means of comparison to phylogenetic β-diversity (PBD) metrics.

Then, in comparing patterns of TBD, we considered three metrics of PBD that differ in their sensitivity to the depth of phylogenetic differences between communities, allowing us to discern whether turnover is phylogenetically basal or terminal:

(2) Phylosor (β_{sor}) is a presence-absence index related to the Sørensen index (Legendre and Legendre, 2012), measuring the fraction of branch-length shared between two communities, defined as:

$$\beta_{sor_{ij}} = \frac{2 \times BL_{ij}}{BL_i + BL_j} \tag{3.1}$$

where BL_{ij} is the total length of the branches shared between communities i and j and BL_i and BL_j are the total branch lengths found in communities i and j, respectively.

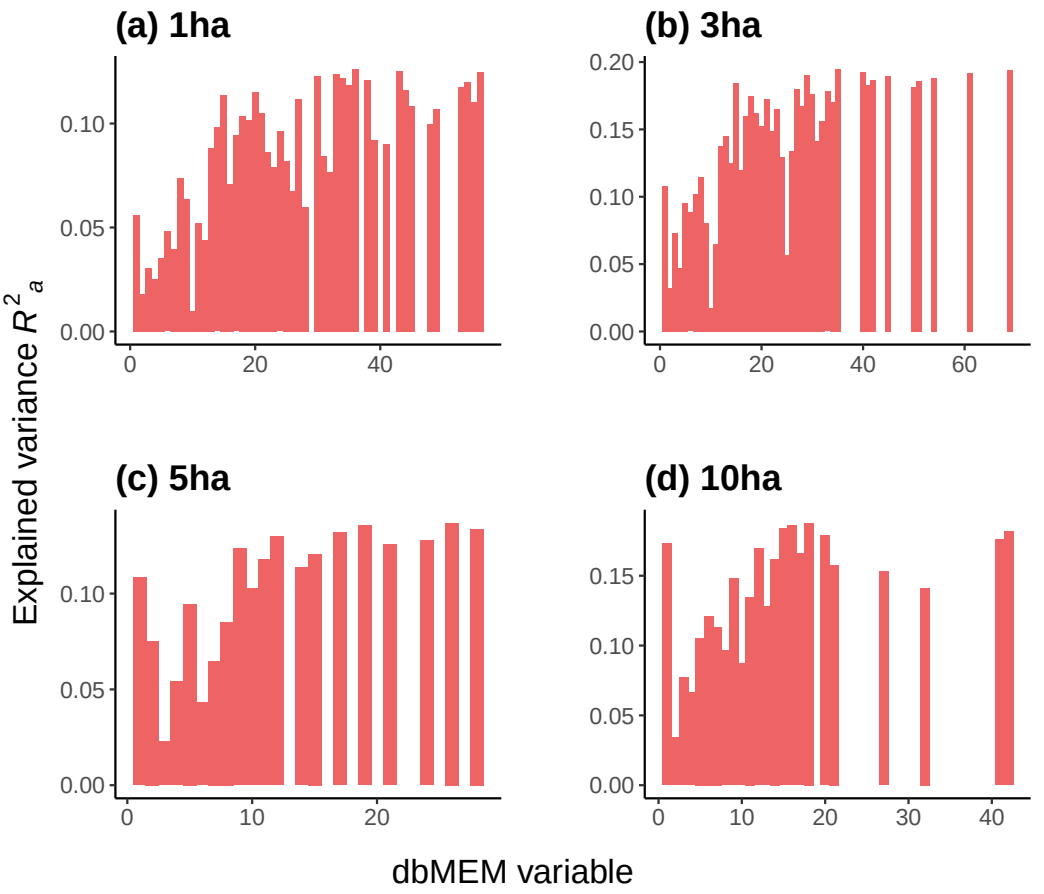

Figure 3.2: Adjusted R^2 values for the distance-based Moran's eigenvector map (dbMEM) variables used as spatial variables in distance-based redundancy analysis (dbRDA) analyses. Forward selection retained 47 (a), 44 (b), 20 (c) and 24 (d) dbMEM variables, sorted from broad- to fine-scaled variation along the x-axis. R^2_a values for dbMEMs are shown only for those retained in by forward selection. Note, plots have been truncated along the x-axis showing only the retained dbMEM variables. The global set of dbMEM variables consisted of 1289, 324, 154 and 51 dbMEMs, respectively.

β_{sor} is considered as a terminal-PBD metric, with most variability coming from variation in terminal branches of the phylogeny, except for cases where communities turnover almost entirely at basal levels, which is highly improbable within canopy tree communities (Swenson, 2011).

(3) D'_{nn} is an abundance-weighted metric based on mean nearest taxon distance (MNTD), originally described by Ricotta and Burrascano (2009):

$$D'_{nn} = \frac{\sum_{i=1}^{nk_1} f_i \min \delta_{ik_2} + \sum_{j=1}^{nk_2} f_j \min \delta_{jk_1}}{2} \tag{3.2}$$

where min δ_{ik_2} is the minimum phylogenetic distance between species i and all species in community k_1 and all species in community k_2, min δ_{ik_1} is the minimum phylogenetic distance between species j in community k_2 and all species in community k_1, f_i and f_j are the relative abundance of species i and j and n is the species richness of the respective communities (Swenson, 2011).

D'_{nn} describes *how* closely related the closest relative in one community is to the other, while accounting for species abundance. It, therefore, acts as a robust measure of terminal-PBD.

(4) D'_{pw} is an abundance weighted metric based on mean pairwise distance (MPD):

$$D'_{pw} = \frac{\sum_{i=1}^{nk_1} f_i \overline{\delta_{ik_2}} + \sum_{j=1}^{nk_2} f_j \overline{\delta_{jk_1}}}{2} \tag{3.3}$$

where $\overline{\delta_{ik_2}}$ is the mean pairwise phylogenetic distance between species i in community k_2, $\overline{\delta_{jk_2}}$ is the mean pairwise phylogenetic distance between species j in community k_1, f_i and f_j are the relative abundance of species i and j and n is the species richness of the respective communities (Swenson, 2011).

D'_{pw} gives a measure of the overall phylogenetic dissimilarity between communities and detects changes occurring deeper in the phylogeny, while accounting for species abundance. It is sensitive to phylogenetic restructuring at basal levels and provides a metric of basal-PBD.

The phylogenetic tree implemented in the calculation of PBD metrics was reconstructed with the `V.PhyloMaker` package (Jin and Qian, 2019) which implements the current, largest, dated plant phylogeny, derived from a combination of the Smith and Brown (2018) and Zanne et al. (2014) mega-phylogenies (Figs. 3.3 & B.1). Genera and species were added to their families or genera following the same approach implemented in Phylomatic and BLADJ (Qian and Jin, 2016, Webb and Donoghue, 2005). Of the 377 species present at Vale do Jari, 52% were fully resolved, 44% resolved to the genus level and 4% to the family level only. While this results in some loss of explanatory power, PBD metrics derived from synthesis phylogenies correlate strongly with purpose built phylogenies (Li et al., 2019). Species nomenclature was standardised to adhere to The Plant List database (TPL, 2013).

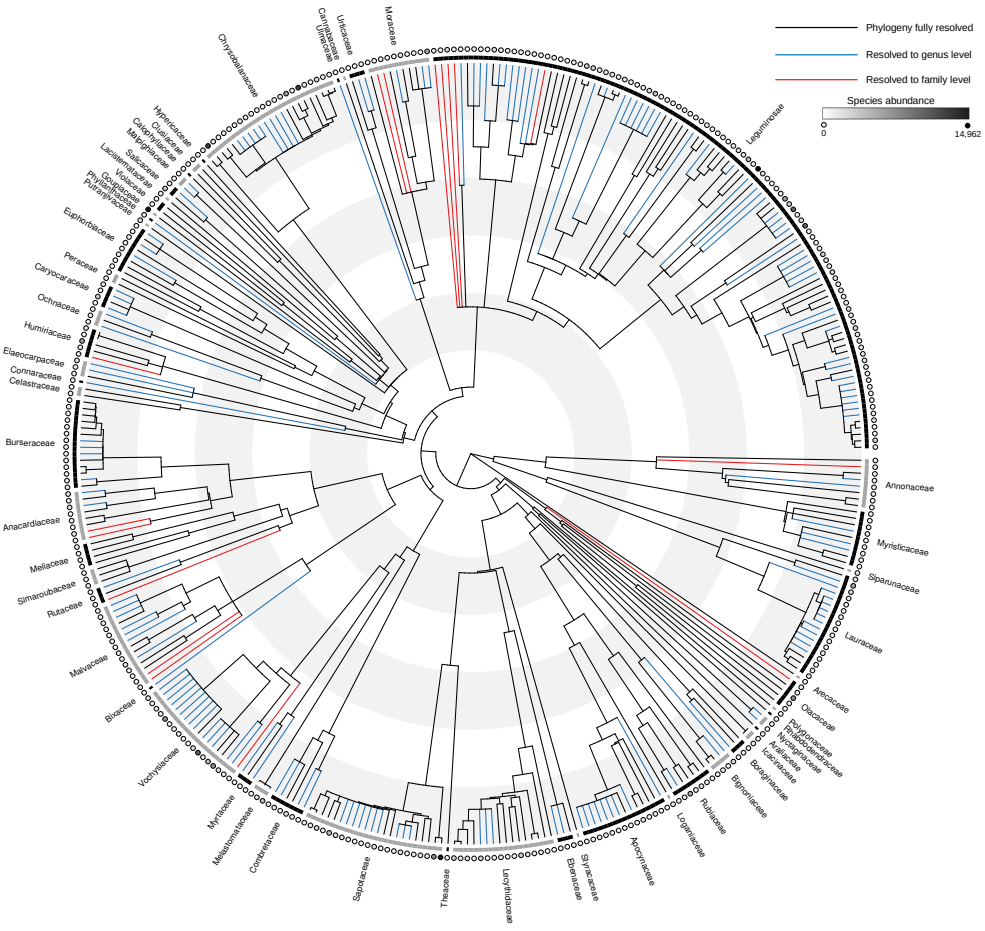

Figure 3.3: The phylogenetic tree used to derive metrics of phylogenetic β-diversity (PBD) was reconstructed from Zanne et al. (2014) & Smith and Brown (2018) mega-phylogenies. Shading of the points represent species abundance across the study site. Alternating black and grey bars at the tips separate plant families as a visual aid only. See Fig. B.1 for the phylogeny with species names provided.

3.2.5 Statistical methods

Assessing taxonomic and phylogenetic spatial autocorrelation

The scale of spatial autocorrelation of taxonomic and phylogenetic community composition, in conjunction with the influence of cell size, was assessed via Mantel correlograms (Legendre and Legendre, 2012). Forest inventory data were divided into 1 ha, 3 ha, 5ha and 10 ha cells and community dissimilarity matrices were paired with the corresponding geographical distance matrices for each index. The Mantel correlogram assesses autocorrelation over geographical space by assigning distance classes and performing Mantel tests (Mantel, 1967), which test for correlation between distance matrices at each distance class. Significance is tested by randomly shuffling the values of the community dissimilarity matrix for 999 permutations.

Positive Mantel r values demonstrate greater compositional/phylogenetic similarity than expected by chance and negative values demonstrate dissimilarity. The rate of change thereby indicates the rate of turnover across space. As a more stringent measure of dissimilarity, phylogenetic β-diversity (PBD) will always be lower than taxonomic β-diversity (TBD), however, the relative differences in extent of autocorrelation and rate of turnover allows the processes driving β-diversity to be unpicked (Graham and Fine, 2008).

We used Sturges' rule (Sturges, 2012) to determine the number of distance classes to use. Further, since the number of comparable cell pairs decreases as the geographical separation approaches the two most distant cells, we set a distance class threshold such that no cell is discounted for any given distance class.

Disentangling the drivers of TBD and PBD

Neutral-based theories of community assembly assume species equivalence. Under this assumption, we should not expect that the components of phylogenetic β-diversity (PBD) metrics attributed to environmental variables (E + D$\times$E) should differ from those of taxonomic β-diversity (TBD).

To test this, variance attributed to environmental variables only (E only), spatial variables only (D only) and spatially autocorrelated environment (D$\times$E) in driving TBD and PBD was partitioned over distance-based redundancy analysis (dbRDA) for each index and cell size scenario (Legendre and Anderson, 1999) . The adjusted R^2 metric (R^2_a) represents the relative contribution of each component. Further, the importance of each environmental variable was assessed via partial dbRDA to understand the key ecological drivers. Significance was tested via 999 permutation tests (Anderson, 2017).

Determining the scale at which environmental factors operate

To further understand the scale over at which environmental factors act to influence taxonomic β-diversity (TBD) and phylogenetic β-diversity (PBD), we further investigated patterns at the 3 ha cell size scenario. The 3 ha scenario was chosen, primarily because all environmental variables were retained following forward selection at this scale, suggesting that it represents the tipping point in the trade-off between homogenisation of environmental variables and relevancy at finer scales. Conveniently, this also grants comparability to the findings presented in Chapter 2.

The variance explained by each dbMEM variable was calculated via dbRDA and compared against the variance explained with environmental variables partialled out, enabling us to assess the scales at which environmental factors operate to shape TBD and PBD. To further elucidate this question, the 44 spatial dbMEM variables corresponding to the 3 ha cell size scenario were split into 'broad-scale', 'intermediate-scale' and 'fine-scale' fractions comprising 15, 15 and 14 dbMEMs, respectively. The variance was subsequently partitioned alongside the full set of environmental factors to inform how the variance explained by environmental factors (E + D$\times$E) act at broad- , intermediate- and fine-scales.

3.3 Results

3.3.1 Assessing taxonomic and phylogenetic spatial autocorrelation

Mantel correlograms allowed the extents of spatial autocorrelation to be compared between taxonomic β-diversity (TBD) and phylogenetic β-diversity (PBD) metrics and between cell size scenarios. All metrics of taxonomic and phylogenetic community composition exhibited a general trend of decreasing autocorrelation with geographical separation (spatial turnover) at 1 ha, 3 ha, 5 ha and 10 ha cell sizes. For each cell size the positive spatial autocorrelation was lost at $\sim$5 km with exception of D'_{pw} (a measure of basal-PBD), which was lost at $\sim$3 km.

As expected, TBD (d_{BC}) was higher than PBD, with spatial autocorrelation and turnover of nominal community composition being higher than turnover of evolutionary history for all cell size scenarios. Terminal-PBD (β_{sor}, D'_{nn}) was higher than basal-PBD (D'_{pw}), demonstrating that more phylogenetic turnover occurs at the tips of the phylogeny (within clades) than at basal nodes (across clades).

Although significant autocorrelation was detected at the 1ha scale, the strength and pattern of autocorrelation was increased with increasing cell size for all metrics which is consistent with compositional turnover of canopy trees operating at scales of at least 10 ha or greater. However, spatial autocorrelation of D'_{pw} became non-

significant at shorter distances with increasing cell size. (Fig. 3.4)

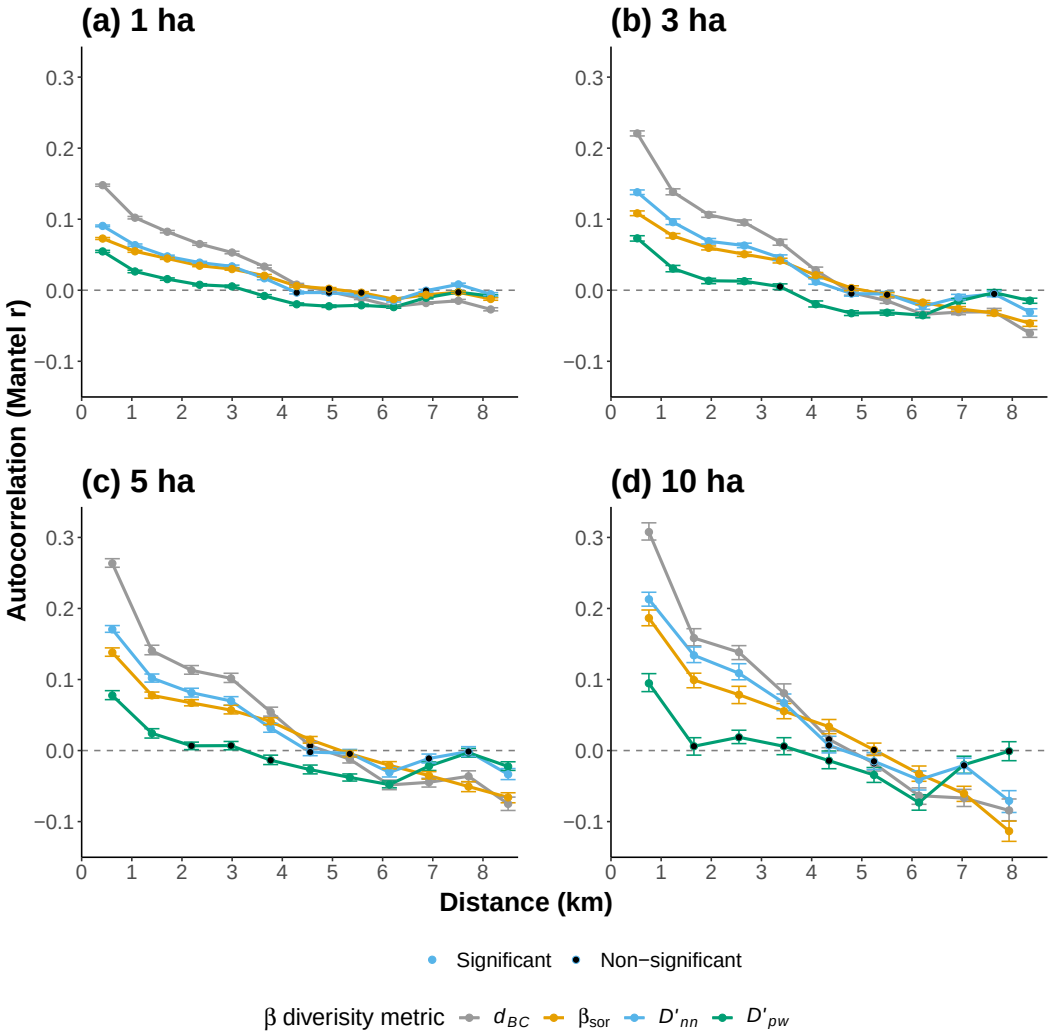

Figure 3.4: Taxonomic and phylogenetic community composition exhibited significant spatial autocorrelation. The degree of spatial autocorrelation increased for all metrics with increasing cell size (a–d). d_{BC}, β_{sor} and D'_{nn} all exhibit positive autocorrelation up to scale of ∼5 km, whereas D'_{pw} is positively autocorrelated up to ∼ 3 km. Positive values of Mantel r signify that community composition is more similar than expected by chance and vice versa. Confidence intervals are calculated from 500 bootstrap permutations.

3.3.2 Disentangling the drivers of TBD and PBD

Variance partitioning on dbRDAs enabled the roles of spatial and environmental variables to be disentangled. Spatial variables were the dominant drivers of both taxonomic β-diversity (TBD) and phylogenetic β-diversity (PBD). The total variance explained by all variables tended to increase with cell size, with the exception of

basal-PBD (D'_{pw}), which exhibited the opposite trend (Fig. 3.5a). Although, while significant, D'_{pw} (basal-PBD) explained a very small proportion of the variance, with R^2_a ranging from 0.015 to 0.026.

The total variance explained for D'_{nn} (terminal-PBD) was higher than for d_{BC} (TBD) for all cell sizes. Critically, variance attributed to both environment only (E) and spatially autocorrelated environment (D×E) was higher which is inconsistent with the premise of species equivalence under neutral theory (see Table B.1 for all R^2_a values). However, β_{sor}, another presence-based metric of terminal-PBD, did not show the same pattern.

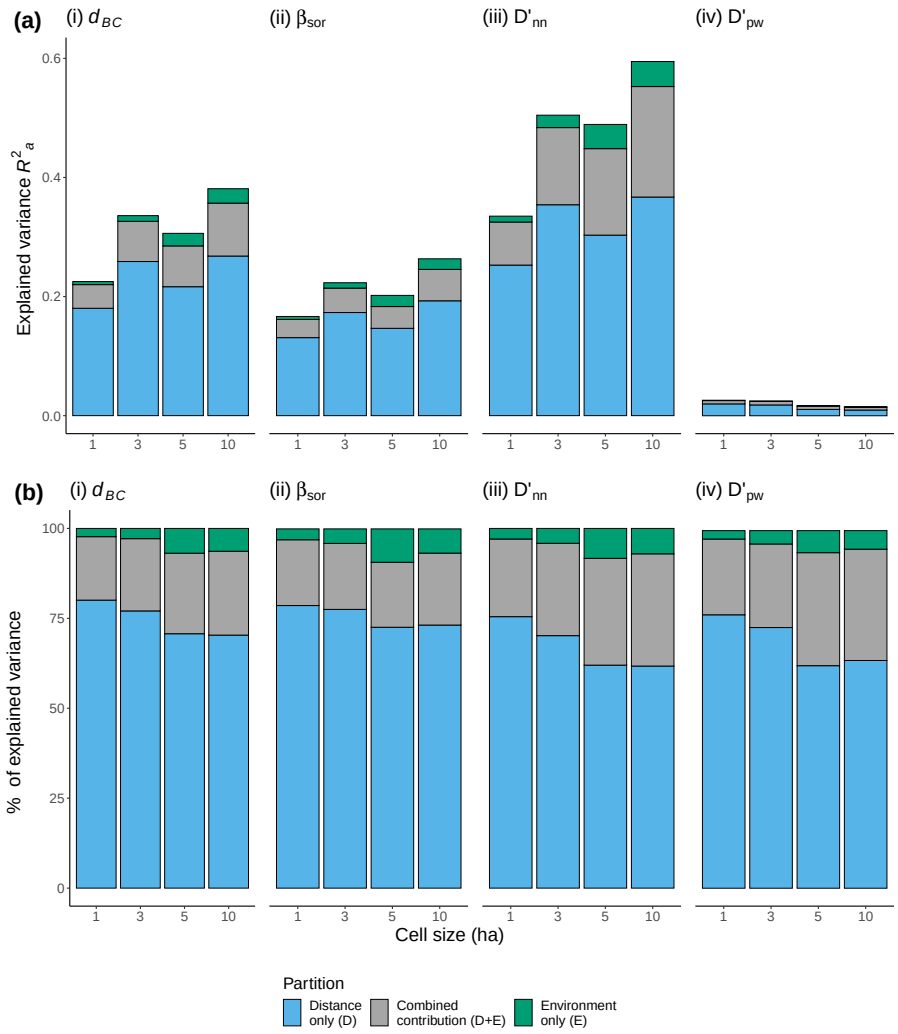

Figure 3.5: Variance was partitioned into spatial only (D), spatially autocorrelated environment (D×E) and environment only (E) over dbRDAs, measured as R^2_a (a), and displayed as the proportion of explained variance (b). All partitions were statistically significant (Table B.1)

The proportion of explained variance attributable purely to environment (E) was generally consistent across all metrics (within cell size scenarios) but slightly elevated for terminal-PBD metrics (β_{sor} & D'_{nn}). The proportion attributed to spatially autocorrelated environment was higher (D×E) for D'_{nn} and D'_{pw} than β_{sor} and d_{BC}.

Table 3.1: The percentage of explained variance attributed to spatial (D), spatially autocorrelated environment (D×E) and environmental (E) factors, derived from R^2_a values following variance partitioning on dbRDAs. Significance was calculated from 999 permutation tests, note, significance of spatially autocorrelated environment cannot be assessed due to covariance. Significance levels: $p^{***} \leq 0.001$, $p^{**} \leq 0.01$, $p^{*} \leq 0.05$, $p^{ns} > 0.05$

Cell size (ha)	n	D	D×E	E
d_{BC}				
1	3785	80.1***	17.6	2.3***
3	1048	77.1***	20.1	2.8***
5	541	70.7***	22.4	6.9***
10	215	70.3***	23.3	6.3***
β_{sor}				
1	3785	78.7***	18.3	3.0***
3	1048	77.6***	18.4	4.0***
5	541	72.6***	18.1	9.3***
10	215	73.2***	20.0	6.7***
D'_{nn}				
1	3785	75.5***	21.6	2.9***
3	1048	70.2***	25.7	4.1***
5	541	62.0***	29.7	8.3***
10	215	61.7***	31.2	7.1***
D'_{pw}				
1	3785	76.5***	21.2	2.4***
3	1048	72.9***	23.4	3.7***
5	541	62.2***	31.6	6.2***
10	215	63.7***	31.1	5.2*

Environmental variables retained via forward selection varied across cell size scenarios. At the 3 ha cell size, all environmental variables were retained, Topographic Position Index (TPI) was excluded for 1 ha, 5 ha and 10 ha cell sizes, and slope was also excluded at the 1 ha cell size. Topographic Wetness Index (TWI) and elevation were generally the most important environmental variables, especially for larger cell sizes, while Terrain Ruggedness Index (TRI) was more important at smaller cell sizes (Table 3.2).

3.3.3 Determining the scales at which environmental and spatial factors operate

Beyond comparative analyses across cell sizes, further investigation of each dbMEM variable via partial dbRDA at the 3 ha cell size allowed us to determine the scale at which environmental factors operate across a large range of spatial structuring.

Table 3.2: The amount of explained variance attributed to each constituent of environmental variation (R_a^2) following variance partitioning on partial dbRDAs. Empty variables are those that were not retained following forward selection for that cell size scenario. Significance was calculated from 9999 permutation tests. Significance levels: $p^{***} \leq 0.001$, $p^{**} \leq 0.01$, $p^{*} \leq 0.05$, $p^{ns} > 0.05$

Cell size (ha)	Elevation	TWI	TRI	TPI	Slope
d_{BC}					
1	0.146e–2***	0.153e–2***	0.199e–2***	–	–
3	0.151e–2***	0.195e–2***	0.288e–2***	0.034e–2*	0.070e–2***
5	0.495e–2***	0.982e–2***	0.403e–2***	–	0.035e–2^{ns}
10	0.779e–2***	1.055e–2***	0.349e–2**	–	0.156e–2^{ns}
β_{sor}					
1	0.111e–2***	0.207e–2***	0.219e–2***	–	–
3	0.139e–2***	0.231e–2***	0.319e–2***	0.043e–2^{ns}	0.041e–2^{ns}
5	0.401e–2***	0.660e–2***	0.363e–2***	–	0.044e–2^{ns}
10	0.859e–2***	0.740e–2***	0.026e–2^{ns}	–	0.000e–2^{ns}
D'_{nn}					
1	0.162e–2***	0.421e–2***	0.485e–2***	–	–
3	0.148e–2*	0.633e–2***	0.710e–2***	0.072e–2^{ns}	0.176e–2**
5	0.418e–2*	1.523e–2***	0.763e–2***	–	0.000e–2^{ns}
10	1.169e–2**	2.549e–2***	0.000e–2^{ns}	–	0.000e–2^{ns}
D'_{pw}					
1	0.010e–2***	0.017e–2***	0.024e–2***	–	–
3	0.006e–2*	0.014e–2***	0.041e–2***	0.006e–2*	0.019e–2***
5	0.025e–2**	0.051e–2***	0.028e–2***	–	0.001e–2^{ns}
10	0.012e–2^{ns}	0.038e–2*	0.015e–2^{ns}	–	0.000e–2^{ns}

The distribution of variation explained by individual dbMEM variables (D + D$\times$E) (ordered from broad- to fine-scaled spatial variables) was right-skewed for all indices except D'_{pw}, with broad-scaled dbMEM variables being the most important. However, this trend was irregular, for example dbMEM9, explained an unexpectedly large amount of turnover (Fig. 3.6). Visual analysis of the maps of dbMEM9 map scores (Fig. B.2) shows a strong North-South division which may account for this unexpected result which we address in the Discussion section.

Partialling out environmental factors from each dbMEM had varying impacts on individual dbMEM variables and somewhat influenced the distribution shape. However, the right-skewed distribution still prevailed. In fact, the importance of two most broad-scaled dbMEMs increased for all β-diversity indices. In contrast, beyond the first two dbMEMs the importance of dbMEMs generally reduced up to dbMEM19, beyond which, dbMEMs variable tended to increase again. The resulting distribution was, thus, further right-skewed at extreme broad scales but flattened across intermediate and fine scales. This pattern was most apparent for D'_{nn} (Fig. 3.6c). Equally noteworthy, is that the unexpectedly high variance attributed to dbMEM9 was explained by the spatially autocorrelated environment component (D$\times$E) across all metrics (Fig. 3.6).

Given the irregular distribution of variation explained by individual dbMEM variables, splitting the significant dbMEMs into broad-, intermediate- and fine-scaled fractions enabled us to evaluate the general scales at which spatially structured environment (D$\times$E) acts in driving β-diversity. For all metrics of β-diversity, spatially autocorrelated environment explained none of the variance at fine scales, acting more strongly at broad scales than intermediate scales. Echoing the right-skewed distribution of explained variance for spatial dbMEMs (Fig. 3.6), spatial variables only (D) explained increasingly less variation from broad- to fine-scale fractions (Fig. 3.7).

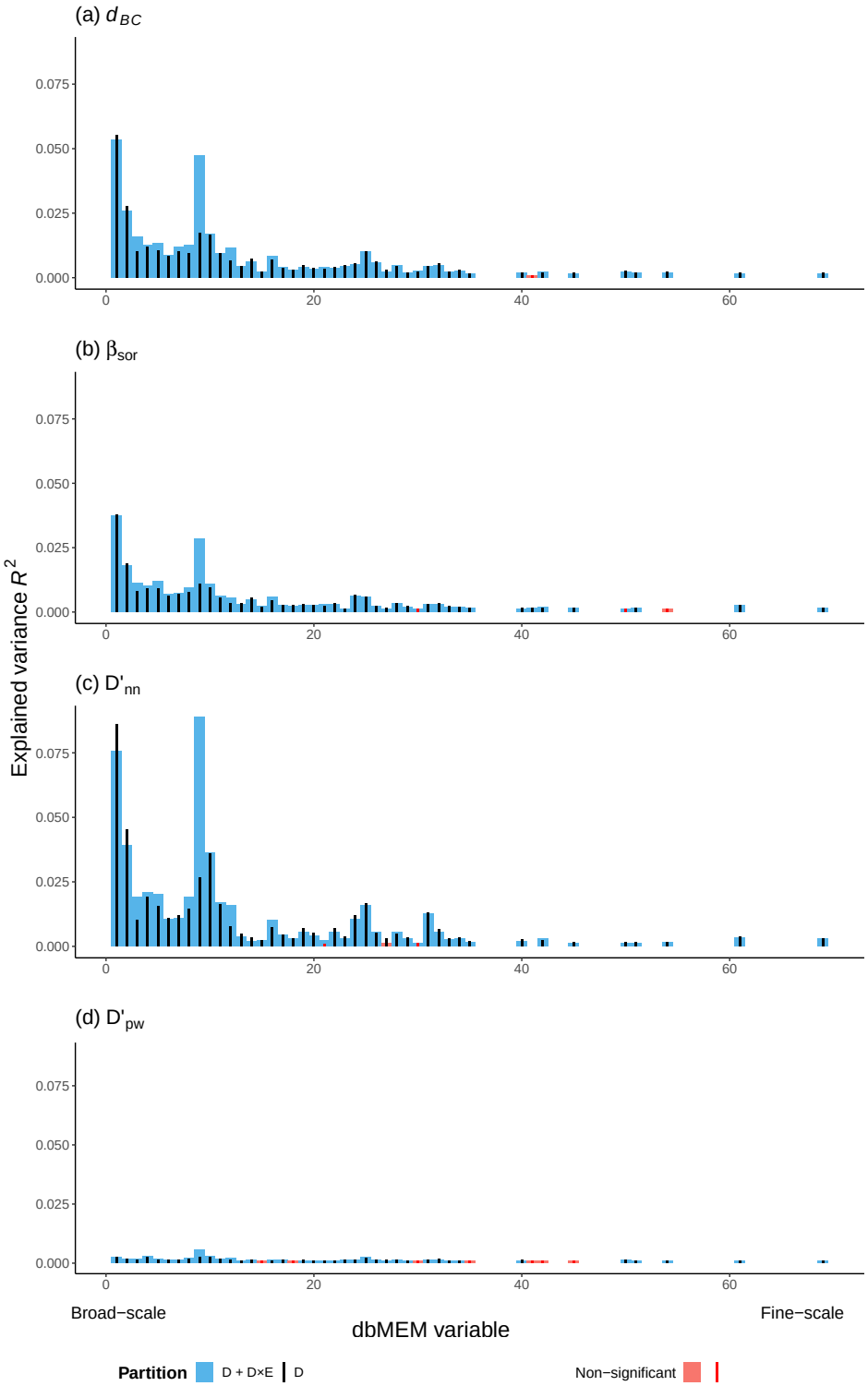

Figure 3.6: Variation in taxonomic (a) and phylogenetic (b–d) composition explained in partial distance-based redundancy analysis (dbRDA) by individual spatial distance-based Moran's eigenvector map (dbMEM) variables. Partialling out environmental variables had varying influence on the explained variance of individual spatial variables but broad-scaled spatial variables explained the majority of taxonomic β-diversity (TBD) and phylogenetic β-diversity (PBD). The dbMEM variables are sorted from broad to fine scaled along the x-axis (left to right). Thick bars represent the variance explained by each dbMEM (D + D$\times$E) and thin lines represent the variance with environmental factors partialled out (D). Red bars indicate non-significant variables.

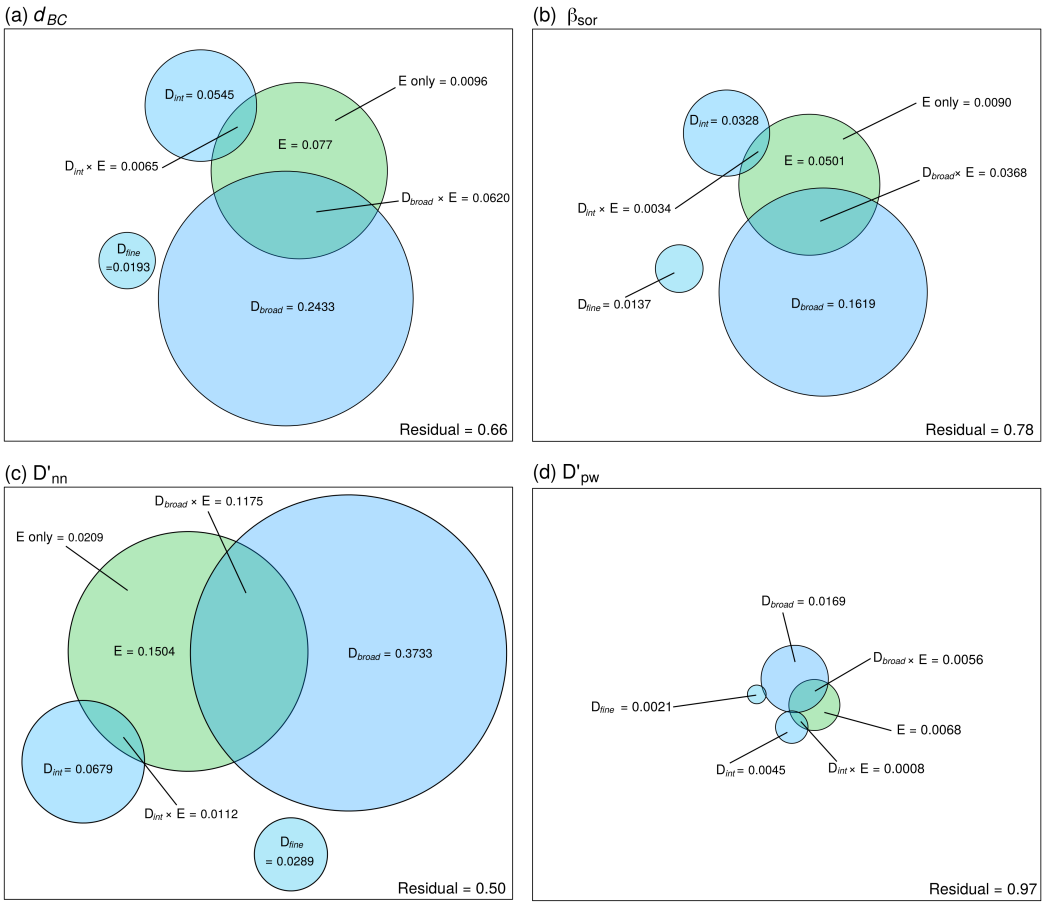

Figure 3.7: dbMEM variables were split into broad- (D_{broad}), intermediate- (D_{int}) and fine-scaled (D_{fine}) fractions and variance was partitioned across dbRDAs for d_{BC} (a), β_{sor} (b), D'_{nn} (c) and D'_{pw} (d). Spatially structured environment acted to shape β-diversity patterns most strongly at broad scales and did not act at fine scales. Note that the Venn diagrams are to scale with respect to the the proportion of explained variance, with bounding boxes representing total variance. All fractions were significant following 999 permutation tests.

3.4 Discussion

Our findings demonstrate the importance of considering evolutionary history of community composition in unpicking the relative roles of environmental and spatial factors in driving β-diversity patterns. The use of landscape scale forest inventory data, identified to the species level, afforded the opportunity to use phylogenetic β-diversity (PBD) analyses to assess the ecological drivers contributing to community assembly. To our knowledge, this is the first study to disentangle the roles of spatial and environmental factors driving β-diversity of large canopy trees via PBD analysis. Given the key role that canopy tree communities play in dispersal, competition, ecosystem functioning and carbon storage, we address a critical knowledge gap.

We demonstrate that species' names turnover more rapidly across space than their evolutionary relationships, specifically, species turnover occurs within closely related clades. We further demonstrate that spatial and environmental factors act jointly to construct patterns of community composition but we further show that PBD patterns track environmental gradients more closely than patterns of taxonomic β-diversity (TBD). This result is at odds with neutral theory, in which species are assumed to be equivalent. Our results also substantiate the notion that environmental factors shape β-diversity patterns most strongly at broad scales (Bongalov et al., 2019, Davidar et al., 2007, Hardy et al., 2012), however, environmental factors alone can act at scales as low as 1 ha in determining community composition, even within canopy tree communities.

Assessing taxonomic and phylogenetic spatial autocorrelation

Spatial autocorrelation of tropical tree community composition is widely observed but small-scale, large-separation, vegetation plot networks have limited our understanding of community turnover to juveniles at the fine-scale (Condit et al., 2002, Duque et al., 2009) or adults at the regional-scale (Qiao et al., 2015) for canopy trees. Further, the phylogenetic relationships between communities over across space has only recently begun to receive attention (Graham and Fine, 2008, Jin et al., 2015, Pashirzad et al., 2018), with only a handful of studies focussed tropical forests (Baldeck et al., 2016, Yang et al., 2015, Zhang et al., 2013)

We find that taxonomic community composition exhibited greater spatial autocorrelation and turnover across space than all measures of phylogenetic community composition, i.e., taxonomic β-diversity (TBD) was higher than phylogenetic β-diversity (PBD). This is an expected result since the added complexity of evolutionary history contained within PBD metrics determines that higher PBD than TBD should be expected (Graham and Fine, 2008). The interesting findings instead

came from comparing the spatial extents of community similarity for between TBD, terminal-PBD and basal-PBD.

Our results demonstrated that spatial autocorrelation of large canopy trees extend beyond distances previously reported for small forest stems(Condit et al., 2000a, 2002, Duque et al., 2009) and that extent of spatial autocorrelation of terminal-PBD metrics (β_{sor} & D'_{nn}) closely matched that of TBD (d_{BC}). Conversely, basal-PBD was weaker than terminal-PBD and basal phylogenetic similarity between communities persisted over shorter distances. Together, these findings demonstrate that the pattern of nominal turnover (TBD) exhibited in large tropical canopy trees is driven primarily by turnover at the terminal branches of the phylogeny at the landscape scale. Previous studies have attributed phylogenetic varying to different degrees of basal and terminal turnover depending on study design, vegetation type and biogeographical region (Jin et al., 2015, Liu et al., 2016, Pashirzad et al., 2018, Zhang et al., 2013). Our findings, thus, highlight the value of contiguous forest inventories in assessing phylogenetic turnover across spatial scale.

Disentangling the drivers of taxonomic β-diversity (TBD) and phylogenetic β-diversity (PBD)

While spatial patterns of TBD and PBD provide important insights into how community evolutionary history changes across space, only through variation partitioning were we able to unpick the key drivers of β-diversity.

PBD has emerged as a valuable tool in disentangling the relative roles of stochastic and deterministic processes driving β-diversity. Where the traditional ecophylogenetic framework proposed by Webb et al. (2002) has proven insufficient in asserting specific assembly processes (Losos, 2008, Mayfield and Levine, 2010), PBD can discern between processes tracked along environmental gradients. Under neutral theory, species are assumed to be equivalent. Equally, TBD is blind to species evolutionary history, thereby, comparing environmental partitions of TBD against PBD enabled us to further disentangle the role of environmental factors.

We find that environmental factors were capable of explaining greater variance of PBD than TBD. Specifically, both environmental factors alone (E) and spatially autocorrelated environment (D$\times$E) explained greater variance in D'_{nn}, a measure of terminal-PBD, than d_{BC} (TBD) (Fig. 3.5a). Further, the proportion of explained variance increased for environmental factors (E + D$\times$E), with reduced relative explanatory power of spatial variables. These results were not echoed by β_{sor}, an absence-presence index for terminal-PBD, however, dismissing species abundance precludes key information of ecological processes. The abundance of a given species can relate to the strength of environmental associations as well as the degree of competition

exclusion, both of which can impact terminal phylogenetic diversity.

Although the proportion of explained variance attributed to each partition for basal-PBD ($D'pw$) closely matched that of terminal-PBD, only a small proportion of absolute variance was explained. This finding matches previous studies PBD in tropical forests (Liu et al., 2016, Zhang et al., 2013) and suggests that environmental affinities are not maintained deep into evolutionary history. Instead, terminal-PBD patterns are indicative of strong selective pressures promoting recent species divergence (Jin et al., 2015).

Spatial variables remained the strongest drivers of PBD but this should not be surprising in this study. Firstly, studies that have found environmental factors to play the strongest role in community assembly typically traverse strong environmental gradients (Hardy et al., 2012, Jin et al., 2015, Liu et al., 2016) whereas the environment is comparatively homogenous at Vale do Jari. Secondly, we consider only a handful of topographical variables; Chang et al. (2013) demonstrated that including soil composition alongside topographical variables can reverse the prevalent driver in favour of deterministic niche processes. Indeed, spatial variables can only be fully attributed to dispersal processes when all environmental variables are taken into account, therefore, we likely underestimate the importance of environmental filtering here.

Thus, our findings demonstrate that environmental filtering plays a larger role in driving community composition of canopy trees than was previously detectable with TBD (Chapter 2) yet supports the notion that stochastic dispersal and deterministic niche processes superimpose to control β-diversity (Bongalov et al., 2019, Chisholm et al., 2014, Wennekes et al., 2012).

Determining the scales at which environmental and spatial factors operate

In determining the scale at which environmental factors operate in shaping patterns of β-diversity, we explored two lines of investigation. Firstly, we divided the forest inventory data into cells of 1 ha, 3 ha, 5 ha and 10 ha in area, enabling us to assess which, and to what degree, environmental factors influence β-diversity at various scales. Secondly, we investigated how the component of spatially autocorrelated environment varies along scales of spatial structure.

Cell size scenarios

We find that the strength of spatial autocorrelation for taxonomic (taxonomic β-diversity (TBD)) and terminal phylogenetic (terminal-phylogenetic β-diversity (PBD)) community composition decreased with decreasing cell size. This is consistent with

increasing variability in community composition at finer scales. Such variability could arise from: (1) negative density dependence (Hammond et al., 1998); (2) stochastic demographic processes which can occur when environmental gradients are weak (Purves and Turnbull, 2010); and/or (3) fine-scale environmental filtering. Although unpicking the precise roles of each process is beyond the capacity of our analysis, variation partitioning at each cell size enabled us to examine evidence for such processes:

(1) Negative density dependence, can be generated via resource competition or natural enemies (Connell, 1971, Janzen, 1970) acting at the fine-scale seedling-stage. Studies have demonstrated that close phylogenetic relatedness can drive negative density dependence (Ness et al., 2011, Paine et al., 2012). However, we find that across all cell sizes, communities were more similar than expected at terminal branches (D'_{nn}) than at basal nodes (D'_{pw}). Further, their relative differences did not change between cell sizes (Fig. 3.4), suggesting that negative density dependence does not play major role in driving community assembly of canopy trees at scales detectable in this study.

(2) In homogenous environments, species can interact in apparently neutral ways, essentially randomising community composition. Our finding that the proportion of variance attributed to spatially autocorrelated environment (D$\times$E) reduced with decreasing cell size supports this notion (Fig. 3.5 & Tables 3.1 & B.1). The reduced explanatory power of spatially structured environment with decreasing cell size in concert with increasing residual variance indicates that communities do not respond to weak environmental gradients over small scales.

(3) Given the near consistent result across all metrics that environmental variables alone (E) explained decreasing amounts of variance with decreasing cell size suggests that fine-scale environmental filtering has a limited impact in driving community composition of large canopy trees. It is worth noting that the variance explained at the 5 ha scale was marginally higher than at the 10 ha scale, however, larger cell sizes would need to be considered to determine a pattern.

Alternatively, the individual environmental factors found to significantly impact community composition varied with cell size. Further, the variance explained by each factor exhibits diverging patterns, with elevation and Topographic Wetness Index (TWI) explaining greater variance with greater cell size, Terrain Ruggedness Index (TRI) explaining the most variance at 5ha and slope explaining more variance at smaller cell sizes.

It is unsurprising that Topographic Position Index (TPI) is non-significant for larger cell sizes since it is related to valley-ridge effects which are highly localised and would be homogenised across large cells. Slope, too, operates at fine scales to control soil nutrient availability (Chadwick and Asner, 2016, Xia et al., 2016), yet neither were significant in the 1 ha cell size scenario. This is likely a reflection of the relatively homogenous environment at Vale do Jari but further demonstrates that stochastic demographic processes operate at fine scales. However, while spatial variables remain the dominant driver of β-diversity, we find that environmental variables can operate differentially and at scales as low as 1 ha in driving community composition.

In contrast to TBD and terminal-PBD, basal-PBD exhibited a different pattern. At cell sizes of 5 ha and 10 ha, significant spatial autocorrelation of basal phylogenetic composition (D'_{pw}) was lost at small distances. This suggests that turnover at basal nodes of the phylogeny occurs at smaller scales than can be captured within 5 ha (Fig. 3.4). Further, spatial variables explained increasingly more variance of basal-PBD with decreasing cell size whereas environmental variables remained unchanged (Table B.1. This suggests that dispersal limitation drives turnover at basal nodes of the phylogeny at very small scales, whereby, certain species are highly abundant and strongly aggregated.

Variance partitioning along scales of spatial structure

Our results from multi-scale analysis of dbMEM variables in the 3 ha cell size scenario show that broad-scale spatial structure is the dominant driver of compositional turnover for large canopy tropical trees and that environmental variables also act primarily at broad scales. The distribution of variation explained by dbMEM variables (D + D$\times$E), sorted from broad- to fine-scaled, was heavily right-skewed and somewhat irregular for all β-diversity metrics (Fig. 3.6).

Partialling out environmental variables resolved some irregular patterns but broad-scaled spatial variables remained the strongest driver. Environmental factors had varying impacts on individual dbMEM variables, suggesting that environmental variables can have differential impacts on different spatial structures, regardless of 'broadness'. In particular environmental variables explained the majority of the variance for dbMEM9 which was represented mostly by a single 'sampling island', located in a region of high Topographic Wetness Index (TWI).

Our results from variance partitioning over fractions of dbMEMs elucidated the irregular pattern exhibited from individual dbMEM analysis. Environmental variables alone (E) act to shape community composition at the 3 ha scale but describe

only a small amount of the total variance. However, structured environment (E + D×E) is capable of explaining a much greater amount of compositional turnover and acts over broad and intermediate scales. This pattern was observable across all metrics (Fig. 3.7)), yet spatially structured environment (E + D×E) explained twice the amount variance of phylogenetic β-diversity (PBD) than taxonomic β-diversity (TBD)

Our findings corroborate assertions in the literature that community assembly is driven primarily by spatial variables at fine scales and environmental variance over large scales (Bongalov et al., 2019, Davidar et al., 2007, Hardy et al., 2012). However, considering the relative environmental homogeneity at Vale do Jari combined with the role of phylogenetic associations, environmental variables have a greater influence in driving compositional turnover of large canopy trees than was previously detectable.

Limitations

Despite our key findings, several limitations of this study preclude us from making definitive assertions on relative roles of environmental and spatial drivers of β-diversity.

Primarily, the forest inventory at Vale do Jari is comprised of 'sampling islands' where connectivity between cells is limited. In the calculation of dbMEM variables, geographic distance matrices are truncated according the threshold distance that enables all cell sites to remain connected. For example, in the 3 ha cell size scenario, this threshold was $\sim$2.5 km, thereby constraining dbMEM variables as representing spatial structures spanning a minimum of 2.5km. Thus, our ability to truly unpick the drivers of fine-scale β-diversity patterns is limited in comparison to regular sampling designs (Chang et al., 2013, Legendre et al., 2009, Qiao et al., 2015) and could explain why such little variance was explained for D'_{pw} which exhibited positive spatial autocorrelation up to $\sim$3 km. The use of dbMEM variables also has implications for interpretation with irregular (Munoz, 2009) or separated samples (Borcard et al., 2018) which likely explains the irregular distribution of dbMEM variables. Further investigation may provide clearer insights into fine-scale contributions by taking a regularly spaced subset of the cells or by redefining the associated connectivity matrix.

Secondly, our analyses considered only a handful of topographically derived environmental variables. In reality, many more environmental factors may be capable of influencing community composition. For example, Chang et al. (2013) demonstrated that topographical factors explained only a small proportion of variance, yet, with topographical and soil variables considered, spatial variables became consid-

erably important. Our analyses have most likely underestimated the true power of environment in driving environmental variables.

Lastly, our assertions that phylogenetic diversity associations with environmental factors are driven by environmental factors rest on the notion that closely related species are functionally similar since, ultimately, species' functional traits respond to environmental conditions. Although phylogenetic diversity has been shown to capture functional diversity (Srivastava et al., 2012), closely related species can have divergent traits. Indeed, whilst functional and phylogenetic β-diversity patterns have been demonstrated to concur (Wang et al., 2015, Yang et al., 2015), Asefa et al. (2019) found contrasting results.

Conclusion

Our results demonstrate the value of emerging landscape scale forestry sector inventories in disentangling the drivers compositional turnover for large tropical canopy trees which have previously remained an unknown. Further, the use of phylogenetic β-diversity (PBD) metrics can elucidate the role of environmental factors in driving community assembly currently not possible using airborne hyperspectral imaging technology.

The improvement of megaphylogenies and plant functional trait databases could prove to be a key link in reconciling stochastic and deterministic processes. As more 100% forest inventories emerge, comparisons across the entire Amazon Basin may further disentangle the environmental and spatial drivers of β-diversity. With tropical forests at ever-increasing risks of anthropogenic change, our understanding of β-diversity is key to informing conservation efforts. Maximising taxonomic β-diversity is not always the appropriate conservation action (Socolar et al., 2016), hence, improving our understanding of how functional β-diversity operates remains a key knowledge gap with far-reaching implications for forest conservation.

Chapter 4

Do functional traits explain aggregation patterns of tropical canopy trees?

4.1 Introduction

The processes enabling the maintenance of high species diversity remains a fundamental problem in community ecology and is of special significance in tropical forests, where a single hectare can contain 280 tree species with diameter at breast height (DBH) $\geq$ 10 cm (Valencia et al., 1994). Well-observed evidence for environmental correlation (Clark et al., 1998, John et al., 2007a, Kraft et al., 2008, Svenning, 1999) and different environmental tolerances of species (Engelbrecht et al., 2007a, Poorter and Markesteijn, 2008) suggest that spatial heterogeneity is inherent to community assembly dynamics. However, models based on niche differentiation and limiting similarity fail to explain the level of observed diversity (Silvertown, 2004). A key question, therefore, is how so many species are able to co-exist given that they rely on the same set of resources. Many theories of coexistence, such as Neutral theory (Hubbell, 2001) and Janzen-Connell (Connell, 1971, Janzen, 1970), incorporate mechanisms whereby coexistence can occur independently of habitat, yet the relative roles of niche and non-niche based theories has remained elusive (Wright, 2002).

The spatial clustering of conspecific trees in tropical forests is observed across the full range of life-stages and at multiple spatial scales (Condit et al., 2000b, Réjou-Méchain et al., 2011). However, aggregation can be explained via both environmental filtering, (Cornwell and Ackerly, 2009, Harms et al., 2001a), in which species are excluded due to non-adaptation to local environmental factors, and/or seed dispersal

limitation (Hubbell, 2001, Seidler and Plotkin, 2006), in which species distributions are constrained by their capacity to disperse their seeds over long distances. For example, a highly specialised species may exhibit tight clustering due to spatially autocorrelated habitat and resource constraints or, equally, due to the inability to disperse over a larger distance. This can result in the drivers responsible for aggregation being confounded when not considered concurrently.

Advances in spatial point pattern analysis (Shen et al., 2009a, 2013, Waagepetersen and Guan, 2009) have allowed aggregation to be quantified independently of environmental covariates at fine spatial scales and empirical evidence of the dual roles of environmental filtering and dispersal limitation in the formation of species distributions have been demonstrated (Lin et al., 2011, Pinto and MacDougall, 2010). Given that plant functional traits influence both habitat associations (Engelbrecht et al., 2007a, Liu et al., 2014, Visser et al., 2016) and dispersal limitation (McFadden et al., 2019, Seidler and Plotkin, 2006), coupling spatial point pattern analyses with functional traits provides the opportunity to distinguish the underlying mechanisms governing plant distributions.

A critical knowledge gap is understanding intraspecific aggregation of canopy trees in climax communities. Whether spatial patterns driven by dispersal limitation persists beyond the juvenile stage is not well understood. This is a core problem in ecology given that canopy trees are the primary seed dispersers, that dispersal dynamics play a role in colonisation and diversity maintenance, and in turn, have important implications for succession, regeneration and conservation (Wang and Smith, 2002, Webb and Peart, 2001). Until recently, the majority of studies consider trees above 1 cm DBH and all are within plots not larger than 50 hectares (Lin et al., 2011, McFadden et al., 2019), a scale at which canopy tree aggregation cannot be assessed. This is due to the lack of spatially explicit forest inventory data of canopy trees at a large enough scale to make spatial point pattern analyses viable. So, whilst our understanding of the processes governing species aggregation at the juvenile stage and at the local-scale is developing rapidly, the key question of how, and if, these dynamics translate to the climax community remains a core knowledge gap in the 'seed dispersal loop' (Wang and Smith, 2002).

We investigate how environmental filtering, dispersal limitation and species functional traits interact to form aggregated intraspecific patterns in emergent tropical trees at a regional scale within spatially contiguous forests. We assess five sites across the Amazon Basin (Fig. 4.1), totalling $\sim$52,000 hectares and comprising $\sim$390,000 spatially mapped trees $\geq$ 40 cm DBH of 133 species. These data are derived from the advent of regulated reduced-impact logging over the last 8 years, in which trees are spatially mapped, offering a unique opportunity to work over massive spatial scales.

Using these data, we tackle the following specific objectives:

(1) To categorise whether each tree species exhibits habitat association and/or dispersal limitation via goodness-of-fit for a series of spatial point pattern models. We predict that given the reduced role of both dispersal limitation and environmental covariates in dictating aggregation patterns in larger species, as identified by McFadden et al. (2019), that dispersal limitation and habitat associations will play a limited role in the intraspecific aggregation of canopy trees;

(2) To assess how the strength of habitat associations and dispersal limitation varies across sites and within species. We predict that the strength of habitat associations will depend on the degree of environmental heterogeneity at each site and that dispersal limitation will be consistent for species that occur at multiple sites.

(3) To test whether the strength of clustering and habitat associations can be described by species functional traits related to resource use and/or dispersal limitation. We expect that anemochorous and autochorous species will be more dispersal limited than animal dispersed species (Seidler and Plotkin, 2006) and that species associated with drier topography will have more resource-conservative traits i.e. lower specific leaf area (SLA), lower leaf nitrogen content and higher dry seed mass; and

(4) To control for common ancestry among species by assessing phylogenetic signal in aggregation and habitat association parameters, predicting that phylogeny will explain a large proportion of variation in aggregation strength given that dispersal mode rarely varies within genus.

4.2 Materials and Methods

4.2.1 Study sites

The study sites are located across the wet lowland tropical forests of Brazil and Peru, spanning the Amazon Basin. Annual rainfall ranges from 2005 to 3324 mm across site locations (Hijmans et al., 2005) with elevation not exceeding 236 meters above sea level (m.a.s.l) (JAXA/METI, 2011). We obtained forest inventory data from seven logging companies in six areas of contiguous forest.

Inventory data are split across five sites, located in the Napo district, Peru (NP, Fig. 4.1b), Jamari and Jacundá National Forests (RO, Fig. 4.1c) Rondônia, Saracá-Taquera

National Forest (ST, Fig. 4.1d) Vale do Jarí (VJ, Fig. 4.1e) and Caxiuanã National Forest (CX, Fig. 4.1f), Pará, Brazil. We considered Jamari and Jacundá National Forests as a single site due to their proximity and matching soil types (Fischer et al., 2008). Although they are no longer directly spatially contiguous following some deforestation over the past 20 years, we would not expect this timescale to impact the canopy tree community.

Concessions are split into Annual Production Units (APUs) in which forest censuses are conducted in the year preceding harvest. Trees $\geq$ 40 cm diameter at breast height (DBH) are mapped, measured and identified to the species level where possible, for species of interest to the concessionaire (ranges from 61 to 351 species). For all subsequent analyses, we excluded riparian strips and non-operational areas, where inventories were not conducted, from the observation windows.

To account for potential mis-identification, we considered only commercial species, species protected by law and highly conspicuous species. At several concessions, independent botanical verifications have been conducted and strict monitoring of inventory and logging activities within Brazilian National Forests by the Brazilian Forestry Service (SFB) diminishes the possibility of systematic mis-identification. We further eliminated species where confusion with other species was a possibility.

Our analyses thereby considered 211 spatial point patterns of 133 species (NP: 35, RO: 31, ST: 35, VJ: 74, CX: 36) for which species identification was reliable, totalling $\sim$392,000 spatially mapped and identified trees across $\sim$60,000 ha. Nomenclature was standardised to adhere to The Plant List database (TPL, 2013).

4.2.2 Environmental data

To determine the impact of abiotic environmental factors on observed spatial patterns, we considered three local-habitat attributes (Fig. C.1). Elevation, at 12.5 m resolution (JAXA/METI, 2011), which was further used to calculate slope and the SAGA Wetness Index (TWI) (Böhner and Selige, 2006), which improves upon the standard Topographic Wetness Index (Beven and Kirkby, 1979). Environmental covariates were checked for multicollinearity via VIF assessment (Brown, 2015).

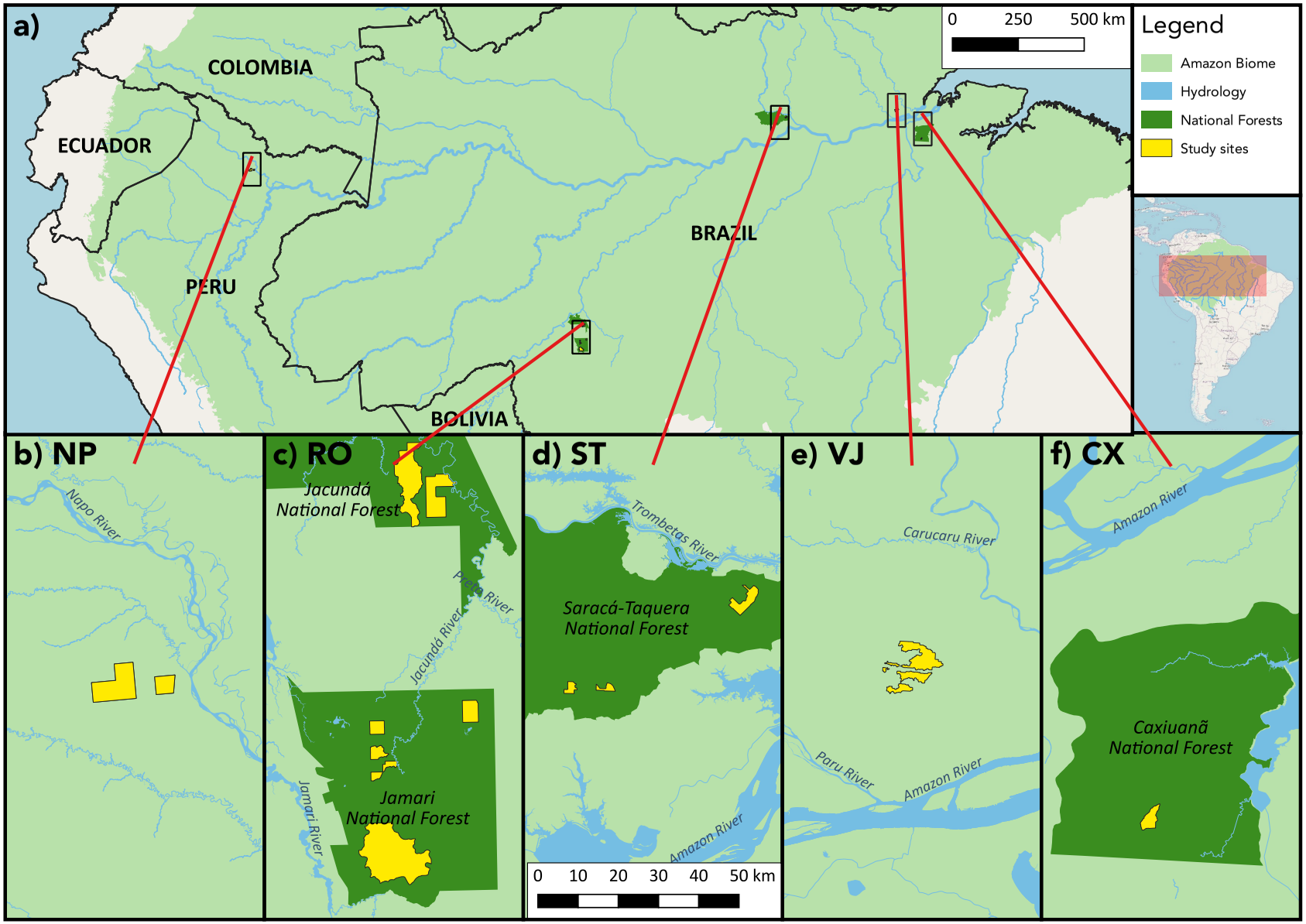

Figure 4.1: Forestry inventory data was obtained from seven companies in the forestry sector spanning the Amazon Basin (a) making up 5 distinct study sites (b-f). All trees $\geq$ 40 cm were were mapped, measured and identified to species level, comprising ~392,000 stems across ~60,000 ha of undisturbed wet tropical lowland forest.

4.2.3 Categorisation of clustering

We assessed the relative roles of functional traits and habitat filtering in determining canopy tree aggregation patterns through the use of spatial point pattern analyses.

We characterised observed spatial patterns into four categories in accordance with their drivers of aggregation, or lack thereof, namely, 'Complete Spatial Randomness' (CSR) (C1), 'Habitat Associations Only' (C2), 'Dispersal Limitation Only' (C3) and 'Habitat and Dispersal Limitation' (C4). We used a three-step approach proposed by Waagepetersen and Guan (2009) and following McFadden et al. (2019), whereby patterns are categorised based on non-random departure from a pair of spatial point pattern null models (Fig. 4.2).

To determine such departure, it is first necessary to quantify the spatial structure of each spatial pattern. Here we implemented the pair correlation function, $g(r)$, which gives the observed number of pairs of points that are r meters apart, standardised for the density of points within the observation window. We restricted analysis up to a maximum radius of 1200 m to account for the variation in observation window size between sites and used the 'translation' correction to control for border effects. We also considered Besag's *L*-function and the *F*-, or empty space, function but ultimately excluded them from the analysis since simulations demonstrated high rates of false positives, even after Benjamini-Hochberg correction.

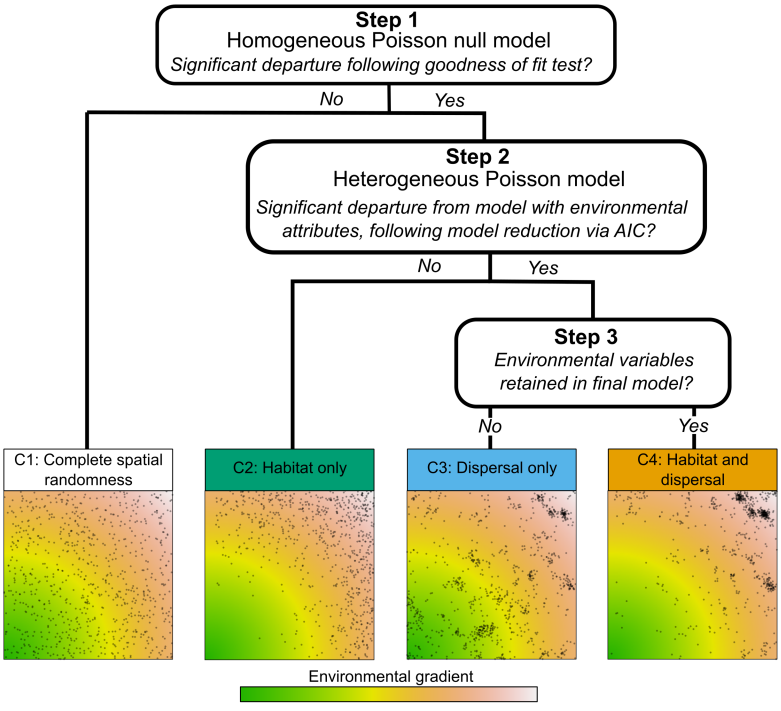

Figure 4.2: Decision tree used to categorise species spatial point patterns

The first step in the categorisation, then, used 999 simulations of the homogeneous Poisson process as a null model and Loosmore's goodness-of-fit test (Cressie, 1992, Diggle, 1986, Loosmore and Ford, 2006) to determine whether the structure of each point pattern differed significantly from CSR. Those patterns exhibiting no departure from CSR were assigned to the 'Complete Spatial Randomness' category (C1). For the second step, for patterns demonstrating non-random spatial structure, we fit the inhomogeneous Poisson model to each pattern with elevation, slope and TWI as environmental covariates. Model reduction via backward AIC selection was used to determine the set of environmental covariates to be included in the null model. We tested for further aggregation beyond that explained by environmental covariates via goodness-of-fit tests with 999 simulations of the inhomogeneous Poisson model. Patterns not exhibiting significant departure were assigned to the 'Habitat Only' category (C2).

Patterns departing from the inhomogeneous Poisson model can be considered as exhibiting a further clustering effect, considered to be mainly a result of dispersal limitation (Lin et al., 2011, Shen et al., 2009a). However it should be noted that further clustering may also arise from missing environmental variables. For those exhibiting significant departure, patterns with no habitat associations were placed into the 'Dispersal Limitation Only' category (C3) and to the 'Habitat and Dispersal Limitation' category (C4) when at least one environmental association was present.

Table 4.1: **Spatial point pattern categories**. Species patterns were categorised according to a decision tree using increasingly complex spatial point pattern models following McFadden et al. (2019), from which, the corresponding habitat association and cluster parameters were estimated.

Category	Spatial point model	Parameters
C1: Complete spatial randomness	Homogeneous Poisson	–
C2: Habitat only	Inhomogenous Poisson	Habitat association coefficients, β_n
C3: Dispersal only	log-Gaussian Cox process	Cluster size (α) and cluster intensity (σ^2)
C4: Habitat and dispersal	log-Gaussian Cox process	β_n, α, σ^2

4.2.4 Parameterisation of habitat association and dispersal limitation

Beyond classification of each observed pattern, we quantified habitat associations and dispersal limitation. No parameters were estimated for patterns in C1 given that

they exhibited no deviance from CSR. We used the inhomogeneous Poisson model to estimate habitat association parameters for patterns in C2, with the reduced set of environmental variables as covariates. To quantify clustering for those patterns placed in C3 and C4, we implemented the log-Gaussian Cox process (LGCP) models to estimate habitat associations (C4 only), cluster size and intensity. Cluster size (α) represents an estimate of the spatial radius over which clustering occurs and cluster intensity (σ^2) represents the density of trees within clusters. Here, aggregation is modelled by the random intensity function:

$log \bigwedge(u) = \mu + H(u)\beta^{\intercal} + D(u)$

where μ is the intercept, β is a vector of habitat association coefficients for the vector of environmental variables, $H(u)$, and $D(u)$ is a general Matérn covariance function (MCF) which describes additional clustering beyond that described by habitat associations. The salient property of the LGCP is that it considers habitat associations and clustering processes concurrently, thereby accounting for the effect of each simultaneously. To optimise model fit, we selected the optimal cluster shape value (v) for the MCF from the set of values 0.1, 0.25, 0.5, 1, 4 and 100. All point pattern analyses were performed using the `spatstat` package (Baddeley et al., 2015).

4.2.5 Functional traits

To determine the drivers of species functional traits on their spatial distributions, we considered six traits related to resource use and dispersal limitation. Adult stature was taken as the maximum DBH observed across all sites, yet we controlled for potential measurement errors by taking the 5th percentile. Values for SLA (excluding rachis and petiole; mm^2 mg^{-1}), leaf nitrogen content (N_{mass}; mg g^{-1}), dispersal mode and dry seed mass (mg) were obtained via the TRY database (Kattge et al., 2011) whilst wood density (mg mm^{-3}) utilised data from both TRY and direct measurements taken from the logging company at VJ. In modelling aggregation for species at VJ, only their site-specific wood density values were used (Table C.2). For dispersal mode, we assigned any missing categories as that of the closest related set of species after confirming consistency of diaspore morphological features (presence of fleshy aril, fruit, wing) using identification keys and herbarium specimens.

Of the 133 species analyses across all sites, the number of missing trait values were high for many traits, specifically dry seed mass, SLA and N_{mass} (Table 4.2). To estimate missing trait values we used phylogenetic imputation for dry seed mass, SLA, N_{mass}, and wood density. This method has proven to give accurate estimates for trait values where phylogenetic signal is strong (Swenson, 2014). Phylogenies were generated with the `V.PhyloMaker` package (Jin and Qian, 2019) which implements

the current largest dated plant phylogeny, derived from a combination of the Smith and Brown (2018) and Zanne et al. (2014) mega-phylogenies. We conducted trait imputation via maximum likelihood estimation and accounted for within species variation by considering multiple observations. We used all available trait data within the genera of species with missing trait values. Entries in the TRY Database often provide data for multiple traits, for example, N_{mass} (mg g^{-1}), nitrogen content per unit area (N_{area}, g m^{-2}) and SLA (mm^2 mg^{-1}) may be recorded for a single leaf observation. Other entries may record only nitrogen content per unit area and/or SLA, yet, contain valuable information regarding N_{mass} given that it can be expressly calculated as $\frac{N_{area} \times SLA}{1000}$. Therefore, to fill data gaps and optimise imputation accuracy, we included inherently related traits as phylogenetic covariates (Table 4.2). Imputation was performed using Phylopars (Bruggeman et al., 2009) which implements cross validation to improve estimates (see Table C.1 for the list of imputed trait values).

Table 4.2: Functional trait data availability for the 133 subject species and those used for phylogenetic imputation. SLA = Specific leaf area excluding rachis and petiole, SLA_{inc} = Specific leaf area excluding rachis and petiole, N_{mass} = Leaf nitrogen content per unit mass, N_{area} = Leaf nitrogen content per unit area

Trait	n missing	n spp used for imputation	n observations used for imputation	Phylogenetic covariates used
Dry seed mass (mg)	88	327	346	Fresh seed mass (mg)
SLA (mm^2 mg^{-1})	56	539	11000	Leaf dry mass (mg) SLA_{inc} (mm^2 mg^{-1})
N_{mass} (mg g^{-1})	34	696	5212	N_{area} (g m^{-2}) SLA (mm^2 mg^{-1})
Wood density (mg mm^{-3})	10	1032	3606	–

4.2.6 Functional drivers and phylogenetic signal of spatial patterns

To determine how spatial patterns of canopy trees may be driven by their functional traits we fit multivariate linear models for each aggregation and habitat association parameter, namely, cluster size, cluster intensity, elevation, slope and Topographic Wetness Index (TWI). For aggregation parameters, we included all traits plus an interaction term between dispersal syndrome and dry seed mass since we expect large, wind dispersed seeds to exhibit stronger dispersal limitation while heavier animal dispersed seeds to be dispersed by larger mammals with a larger home range,

hence, less dispersal limited. For the three habitat association parameters we used all traits but did excluded the interaction term between dispersal mode and dry seed mass since there is no clear ecological interpretation for such an interaction with respect to environmental filtering. The final model was determined via backward stepwise selection via AIC.

Lastly, to identify phylogenetic signal in spatial patterns and to control for any phylogenetic correlation in functional trait values, we fit phylogenetic generalised least squares (PGLS) models to the same set of models with the `caper` package (Orme et al., 2013). Pagel's lamda (δ), which measures the degree of phylogenetic correlation in the response variable, was estimated via maximum likelihood. Again, we used backward stepwise selection via AIC. This method would be inadvisable in some cases since it compares AIC values of models with different lambda values, however for all models, lambda was largely stable throughout model selection and significance did not change.

4.3 Results

4.3.1 Categorising patterns of habitat association and dispersal limitation

Contrary to our prediction, the large majority (82%) of observed spatial point patterns were best described by habitat association and dispersal limitation models (C4) whilst only 1% of patterns (n = 2) exhibited a pattern of CSR (C1) (Fig. 4.3a). The proportion of patterns assigned to each category varied between sites, although C4 was consistently the most prominent at all sites. At RO, all species exhibited both habitat associations and dispersal limitation. Comparatively less species showed patterns consistent with C4 at NP and CX, with comparatively more species exhibiting only habitat associations (C2). Further, NP and CX were the only two sites containing species exhibiting CSR (Fig. 4.3b). (See Table C.3 for full list of pattern categories)

For the 42 species that occurred at multiple sites, category placement was not always consistent between sites. Although 25 species were consistently placed within the same category, the remaining 17 varied from site to site. Almost all category disparities within species were generally 'downgrades' from C4 to C2 or C3 and the proportion of patterns attributed to each category almost exactly matched that of cross-site patterns (Table 4.3 & Fig. 4.3a). This indicates that habitat associations and dispersal limitation are no more similar within species than expected by random.

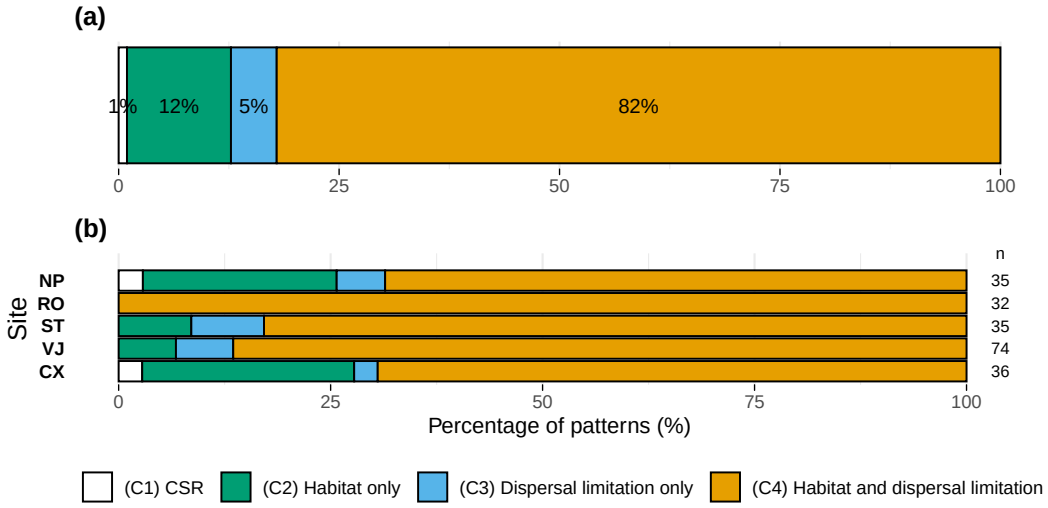

Figure 4.3: Species point patterns were categorised into four spatial aggregation patterns via a decision tree (Table 4.1). Across all sites (a) the large majority of species were best described by models that incorporated both habitat associations and dispersal limitation (category C4). The proportion assigned to each category varied somewhat between sites (b), the most striking of which, being that all species at RO exhibited habitat associations and dispersal limitation.

4.3.2 Habitat associations

Of the patterns that exhibited habitat associations with at least one environmental variable (C2 & C4), 83% were associated with elevation, 58% with slope and 77% with TWI. For all sites, fewer species responded to slope as a driver of aggregation than elevation and TWI. Elevation was the most prominent factor at ST, VJ and CX whilst more species associated with TWI at NP and RO (Fig. 4.4a).

There was some correspondence between environmental associations and the variance of that environmental factor at each site. For example, RO, ST and VJ exhibited the greatest variance in elevation and, equally, had the most amount of species associating with elevation. Likewise, TWI drove the most species aggregation patterns at NP and RO, where the spread of TWI was also greater (Fig. 4.4b). This is consistent with the notion that strong environmental gradients are necessary to influence environmental filtering. However, this observation was not a rule. Variance in slope exhibited almost no observable difference in the proportion of habitat associations and at CX a large proportion of species associated with elevation despite the topography at CX being considerably flatter than other sites.

Despite elevation influencing the majority of aggregation patterns, the strength of associations with TWI and slope were generally stronger. For TWI, more species patterns associated with drier habitats (negative TWI association) than wet (Fig. 4.5).

Table 4.3: The number of species assigned to each aggregation category for species observed at more than one site. The proportion patterns assigned to each category almost exactly matched that of patterns for all species across all sites (Fig. 4.3a). Species with consistent categories are indicated in italics.

Species	C1	C2	C3	C4
Allantoma decandra	0	1	0	1
Apuleia leiocarpa	0	0	0	2
Astronium lecointei	0	0	0	3
Bowdichia nitida	1	0	1	1
Brosimum rubescens	0	1	0	2
Buchenavia parvifolia	0	0	0	2
Carapa guianensis	0	0	0	3
Cariniana micrantha	0	0	0	3
Caryocar glabrum	0	0	0	5
Caryocar villosum	0	0	0	4
Cedrelinga cateniformis	0	0	0	3
Ceiba pentandra	0	0	0	2
Clarisia racemosa	0	2	0	2
Cordia goeldiana	0	1	0	1
Couratari guianensis	0	0	0	4
Dialium guianense	0	0	0	2
Dinizia excelsa	0	0	0	3
Diplotropis racemosa	0	1	0	2
Dipteryx odorata	0	0	0	5
Endopleura uchi	0	2	0	2
Enterolobium schomburgkii	0	0	0	4
Eschweilera coriacea	0	1	0	2
Goupia glabra	0	0	1	3
Handroanthus impetiginosus	0	0	0	2
Handroanthus incanus	0	1	0	1
Handroanthus serratifolius	0	1	0	1
Hymenaea courbaril	0	1	0	2
Hymenolobium excelsum	0	1	0	1
Jacaranda copaia	0	0	0	2
Lecythis pisonis	0	0	0	2
Manilkara bidentata	0	1	0	1
Manilkara huberi	0	0	0	4
Mezilaurus ita-uba	0	0	0	4
Minquartia guianensis	0	0	1	2
Parkia nitida	0	0	0	2
Parkia pendula	0	1	0	2
Peltogyne lecointei	0	0	0	2
Pouteria guianensis	0	0	0	2
Qualea paraensis	0	0	0	3
Simarouba amara	0	1	1	2
Tetragastris panamensis	0	0	0	2
Vouacapoua americana	0	0	0	2
Total	1	16	4	100
Proportion	0.8%	13.2%	3.3%	82.6%

For species that occurred across multiple sites, habitat associations were not consistent; elevational, TWI and slope associations did not always manifest equally

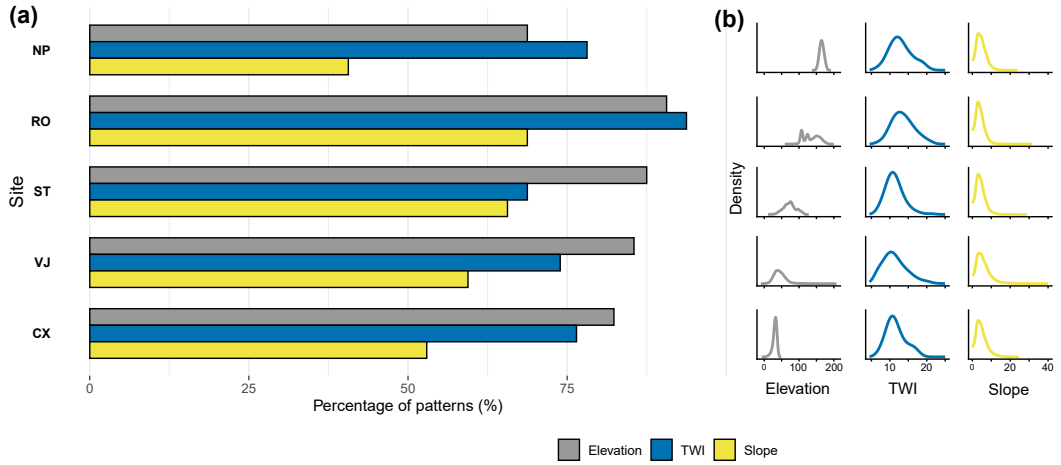

Figure 4.4: For aggregation patterns exhibiting habitat associations (C2 & C4), slope associated with the fewest proportion of species across all sites, with elevation and TWI being the prominent drivers. The proportion of habitat associations varied between sites (a) and there was some correspondence with the environmental heterogeneity (b).

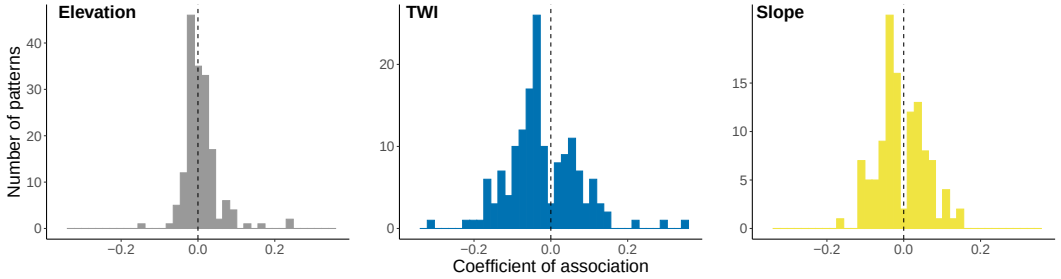

Figure 4.5: Of the species aggregation patterns associating with elevation, TWI or slope (C2 & C4), the strength of association tended to be stronger with TWI and slope than elevation. Note: the apparent bimodal distribution is simply due to patterns in C1 and C3 not represented here.

across sites. For example, *Simarouba amara* was positively correlated with elevation and TWI at RO, VJ and CX but did not exhibit any habitat associations at NP. Further, *Simarouba amara* associated more strongly with TWI at VJ and CX than RO. More interestingly, for many species, the direction of association for environmental factors also varied. For example, while *Cariniana micrantha* consistently associated with drier topography, it associated positively with elevation at RO and CX but negatively at ST (Table C.3).

4.3.3 Dispersal limitation

After accounting for habitat associations, aggregation patterns exhibited a range of dispersal limitation (C2 & C4). Cluster size (α), an estimate of the radius over which

clustering occurs, ranged from 32–1720 m, while cluster intensity (σ^2), describing stem density within clusters ranged from values of 1.0–4.7. This result is inconsistent with a theory of species dispersal equivalence. Further, whilst the range of cluster sizes was generally similar between sites, cluster intensity values varied between sites. At the extremes NP exhibited strong clustering, whereas species at ST exhibited a range of clustering intensity (Fig. 4.6).

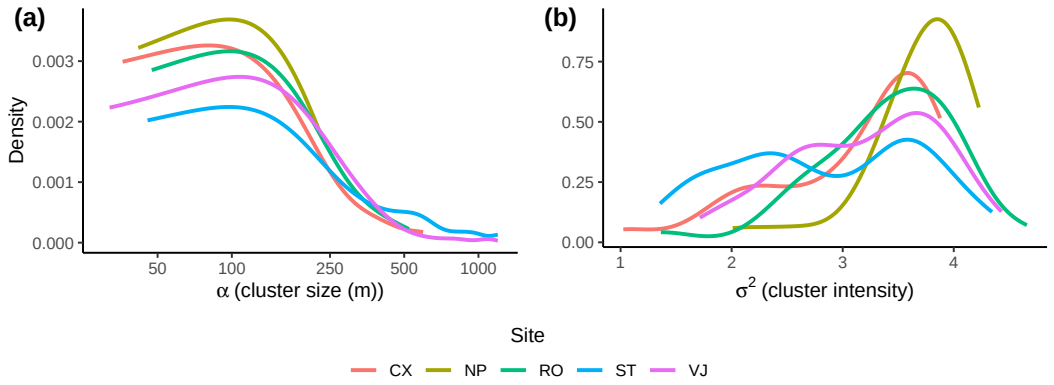

Figure 4.6: Dispersal limitation varied between species at all sites; both cluster size (a) and cluster intensity (b) spanned a range of values. There was little difference in variability of cluster size between sites but the range of cluster intensities varied from site to site. Note: the x axis for α is on the log-scale.

Contrary to our predictions, for species that spanned multiple sites, the degree of dispersal limitation varied. However, variation differed from species to species. For example, dispersal limitation was consistent for *Enterolobium schomburgkii* ($n = 4$) with cluster size ranging between 47.1–69.8 m and cluster intensity between 3.71–4.03. Conversely, cluster size of *Simarouba amara* ($n = 4$) ranged from 92–1720 m and exhibited no dispersal limitation at CX. In general, cluster size exhibited considerably more variation than cluster intensity.

4.3.4 Do species functional traits explain habitat associations and dispersal limitation?

Following backwards stepwise selection of multivariate linear models, only cluster intensity (σ^2), slope and TWI retained any functional traits as explanatory variables. Species with larger seed mass exhibited reduced clustering intensity (Fig. 4.7a) and in line with our predictions, species with low nitrogen content associated more strongly with drier habitats (Fig. 4.7b). Species with higher SLA associated more strongly with sloped topography (Fig. 4.7c). Although each corresponding functional trait was retained in the final model, thereby representing the best model, none were significant and explanatory power was low (Fig. 4.7 & Table C.4).

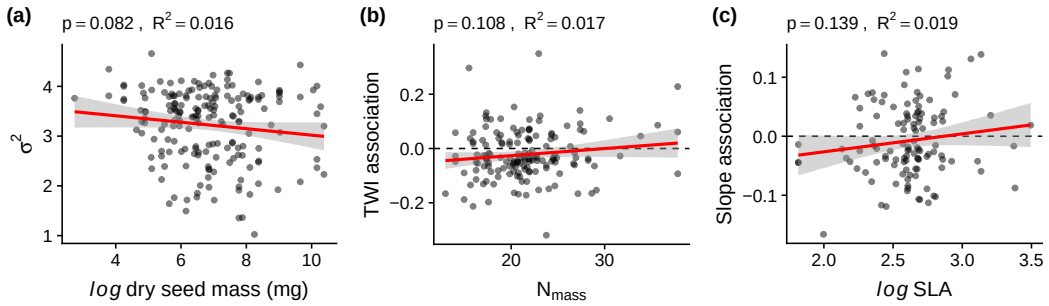

Figure 4.7: Species functional traits predict spatial properties. Dry seed mass is negatively related to dry seed mass (a). Species negatively associated with TWI (i.e. drier habitats) tended to have lower nitrogen content (b). Species positively associated with slope topography tended to have higher specific leaf area (SLA). Red lines represent ordinary least sqaures fits and confidence bands represent the 95% confidence interval. Dry seed mass is measured in mg, SLA in mm^2 mg^{-1}, N_{mass} represents leaf nitrogen content in mg g^{-1} and cluster intensity is unitless.

PGLS models allowed us determine the phylogenetic signal associated with each aggregation parameter and, further, account for species relatedness. The only spatial aggregation parameter explained by functional traits after accounting for phylogenetic signal was cluster intensity which exhibited the same negative relationship with dry seed mass as with the linear model. Interestingly however, effect size was greater (-0.065 v.s. -0.108) and the relationship was statistically significant. Further, dispersal syndrome was a significant predictor, with anemochorous species exhibiting lower clustering intensity than zoochorous species (Fig. 4.8 & Table 4.4).

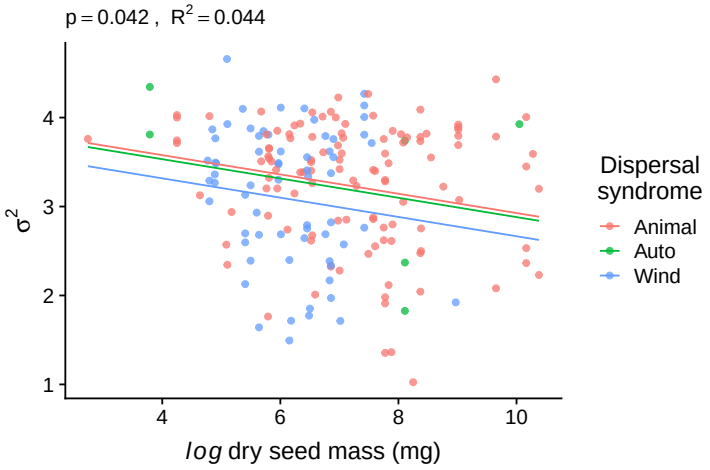

Figure 4.8: After accounting for phylogenetic signal, dry seed mass was more strongly negatively related to cluster intensity and wind-dispersed species tended exhibit less clustering intensity than animal-dispersed species. Lines represent PGLS model fits for each dispersal syndrome.

Table 4.4: PGLS model summary statistics for clustering intensity. Anemochorous and autochorous effect sizes are in comparison to zoochorous species.

	σ^2
Dispersal syndrome:	-0.046^{ns}
Autochorous	(0.315)
Dispersal syndrome:	$-$0.261*
Anemochorous	(0.129)
log(Dry seed mass)	$-$0.108*
	(0.042)
R^2	0.044
F Statistic	2.78* (df = 3; 181)
Pagel's λ	0.104^{ns}

4.4 Discussion

The use of landscape-scale forest inventory data from the forestry sector enabled us to answer key questions regarding the drivers of aggregation of large tropical canopy trees.

4.4.1 Categorising patterns of habitat association and dispersal limitation

The large majority of species were best described by spatial point pattern models that incorporated both habitat associations and dispersal limitation which indicates that both mechanisms play a key role in driving spatial structure of canopy trees. Although the dual roles of habitat association and dispersal limitation has been demonstrated in tropical Asian, Central and South American and African forests (Jalilian et al., 2013, Lin et al., 2011, Réjou-Méchain et al., 2011, Shen et al., 2009b, 2013), such studies were limited to small plots up to 50 ha or across non-contiguous forest. Whether the dual roles scaled to canopy trees, therefore, remained unanswered. McFadden et al. (2019) observed that trees $\geq$ 10 cm DBH were less associated with environmental factors than those < 10 cm DBH. Thus, our finding that 94% of aggregation patterns for trees $\geq$ 40 cm were associated with environmental variables was a surprising and important discovery.

4.4.2 Habitat associations

Under neutral theory we should expect little to no species habitat association (Hubbell, 2001), yet environmental factors drove species aggregation patterns consistently, across multiple sites spanning the Amazon Basin. Further, the number of species associating with individual environmental variables tended to correspond with the degree of environmental heterogeneity at the site, adding credence to the importance

of environmental filtering as a key driver, shaping spatial structure of canopy trees. Although habitat associations were often weak, the large scale of our study design enabled us to detect their influence. Further, we might expect adult canopy trees to exhibit weaker habitat associations. Although Visser et al. (2016) found survival rates of canopy tree seedlings to be greater than small statured species, the inherently longer life cycle of canopy trees means they are more susceptible to stochastic mortality events through time, thus, weakening the observed environmental associations.

Elevation was associated with a large proportion of species, despite exhibiting the weakest associations. One possible explanation for this is that elevational gradients are associated with a wide range of habitat conditions including ambient humidity, precipitation, wind velocity and soil composition gradients (Jucker et al., 2018, Sundqvist et al., 2013). Further, elevation is likely to covary with topographical position, i.e., 'valley v.s. ridge', which is implicated in solar irradiance. Thus, elevational associations may represent different ecological processes for different species depending on their habitat tolerances. The finding that TWI was a strong predictor of spatial aggregation was an unsurprising results, drought tolerance has been demonstrated to shape species distributions (Engelbrecht et al., 2007b) and TWI has been a common driver of species distributions throughout this thesis. Our finding that more species associated with drier habitats in this study could be due the fact that the majority of species considered here were commercially valuable, hardwood species. Slow growing, hardwood species tend to be resource-conservative and hence are more likely to outcompete drought-intolerant species in drier habitats.

4.4.3 Dispersal limitation

Our results find that dispersal limitation, too, is pervasive across all sites and for the large majority of species. This supports recent theory that environmental factors and stochastic dispersal processes superimpose to shape the spatial distributions of species (Bongalov et al., 2019, Chisholm and Pacala, 2010). However, contrary to assertions that dispersal-recruitment processes are stochastic and that species specific dispersal kernels do not contribute to spatial structuring of communities (Bongalov et al., 2019, May et al., 2015), we find species cluster size to exhibit a wide range of scales. Hence, species-specific dispersal limitation is likely to play a key role in shaping canopy tree communities.

Interestingly, variance in cluster intensity (density of stems within clusters) differed between sites. This could arise from differences in communities at each site. Firstly, different species may inherently exhibit different clustering intensities ac-

cording to functional traits. Secondly, the number of species occupying the same niche within the community may vary from site to site which would impact localised species abundance.

4.4.4 Do species functional traits explain habitat associations and dispersal limitation?

Few functional traits explain habitat associations and dispersal limitation in our study. Species with low leaf nitrogen content were found to be associated with drier environments. This is an expected result given that nitrogen is the key nutrient involved in leaf production, low leaf nitrogen content is consistent with a resource-conservative ecological strategy (Westoby et al., 2002), promoting survival under harsh conditions. Low SLA is also a resource conservative trait and was found to be associated with flatter topography. Slope is implicated in controlling soil nutrient gradients (Chadwick and Asner, 2016, Xia et al., 2016) yet how nutrients are distributed is context-dependent. Flat habitats on ridges will have different soil composition to flat habitats in valleys, hence this result is difficult to interpret without soil composition data. Considering Topographic Position Index (TPI), may help to elucidate this relationship.

Species' seed mass was found to predict cluster intensity, with larger-seeded species having lower density within clusters. While cluster intensity can be an indication of dispersal limitation, large-seeded species tend to produce few seeds (Muller-Landau, 2010), resulting in reduced local density, which may also explain this result. Alternatively, larger seeds tend to be dispersed by large vertebrates with large home-ranges (Russo et al., 2007), carrying seeds further. However, contrary to our predictions and previous studies (McFadden et al., 2019, Seidler and Plotkin, 2006), dispersal syndrome was not found to determine cluster size (α).

After accounting for species relatedness via PGLS modelling, we found anemochorous (wind-dispersed species) to exhibit lower cluster density alongside higher seed mass (Fig. 4.8). This is an interesting finding since we would expect anemochrous species to exhibit more limited dispersal than zoochorous species and hence greater density. This observation also contradicts the notion that stronger clustering intensity with larger seed mass is a result of dispersal from large invertebrates. There are several explanations that may account for these observations. Animal dispersed seeds are typically nutrient-rich, which may promote successful recruitment (Muller-Landau, 2010) resulting in greater local stem density. More likely, however, is that the complexities of dispersal are clouded within the rudimentary categorisation of dispersal syndrome used here. Wind dispersed species can suffer from both pre- and post-dispersal seed predation and insect dispersed seeds are unlikely to disperse

far from the parent.

Dispersal syndrome data were taken from the TRY database (Kattge et al., 2011), yet classifications into the 'animal-dispersed' category were often based on single observations. For example *Ormosia coccinea* has a dehiscent seed pod and a diaspore with no aril, typically associated with autochory, yet is designated as zoochorous following a single observation of ingestion by a bird. Further, insect dispersal is not likely occur far from the parent. Taking a morphological approach such as that used by Seidler and Plotkin (2006) may prove more *fruitful*. In addition, because we imputed functional traits based upon a phylogeny that was not fully resolved, this could result in a phylogenetic homogenisation of traits within polytomies.

Lastly, we only had three environmental variables and aggregation patterns could be confused or confounded with dispersal limitation when in fact it is an environmental variable that we did not account for. In particular, we did not measure soil properties, but these have been shown to strongly predict species aggregation patterns McFadden et al. (2019). That said, in our study area, as accross much of the Amazon, there is unlikely to be substantial variation in soils at small spatial scales given the highly weathered nature of lowland tropical soils.

Chapter 5

Discussion

A core issue in community ecology is understanding the processes responsible for driving the composition of species within hyperdiverse tree communities in tropical forests. Here, a single hectare of rainforest can support over 280 tree species (De Oliveira and Mori, 1999, Valencia et al., 1994). Yet despite substantial research efforts, definitive answers to explaining how large numbers of plant species are able to coexist at small spatial scales remain elusive. Tackling this key question requires an understanding of the drivers of hyperdiverse community composition, and in particular teasing apart the roles of deterministic and stochastic processes. While a large number of studies have attempted to disentangle the relative roles of such processes in small forest plots, whether and how these processes scale up to the canopy tree community has previously remained unknown. This thesis sits at this juncture and specifically deals with this issue by focusing on the roles of environmental filtering and dispersal limitation as core, dual drivers of species turnover within tropical forests, in particular demonstrating that stochastic dispersal and environmental filtering can superimpose to dictate spatial community structure.

In Chapter 2, I tackled the question surrounding the relative roles of environmental factors and stochastic dispersal processes in driving β-diversity – the turnover of species with space – and addressed the scale at which environmental factors act to influence community composition. Building upon a recent body of work demonstrating that environmental gradients and stochastic dispersal can act in concert to drive compositional turnover (Adler et al., 2007, Chisholm and Pacala, 2010, Wennekes et al., 2012), I used field data to partition the variance of compositional turnover attributable to environmental variables and geographic distance. My results corroborated recent results from studies implementing high-fidelity hyperspectral imaging across the landscape scale (Bongalov et al., 2019, Draper et al., 2019) and that assert the dual roles of stochastic dispersal and environmental filtering do indeed scale to

the level of the canopy tree community.

I then implemented neutral models using a range of parameters to test whether neutral theory is capable of concurrently explaining the variance attributable to environmental variables and spatially autocorrelated environment. I revealed that neutral simulations were unable to match both the variance attributed to geographic distance only (D) and geographic distance and spatially autocorrelated environment (D + D$\times$E) concurrently within a single forest type. This was a key finding since previous work had only been able to demonstrate that environmental filtering operated at large scales across extreme environmental gradients (Bongalov et al., 2019). Instead, environmental factors can influence community composition at finer scales than previously known for canopy tree communities, indicating that stark forest-type environmental heterogeneity is not a prerequisite for environment to shape community composition.

Whilst the use of high-fidelity hyperspectral imaging offers a promising route forwards in analysing patterns of species distributions, spectral signatures cannot identify individual species. Meanwhile, phylogenetic β-diversity offers insightful inroads into decomposing the drivers of β-diversity (Hardy et al., 2012, Legendre et al., 2009, Liu et al., 2016, Qiao et al., 2015, Saito et al., 2015). In chapter 3, I again tackled the key question of the relative roles of environmental and spatial factors in driving compositional turnover and spatial structuring (Chapter 2), but this time doing so through the lens of phylogenetic β-diversity. I implemented phylogenetic β-diversity (PBD) to analyse the relative roles of environmental and spatial variables through the lens of niche conservatism (Graham and Fine, 2008, Jin et al., 2015). Comparing results against traditionally used taxonomic β-diversity (TBD) metrics demonstrated that environmental factors play a greater role in driving community composition than previously detectable for canopy trees.

I then investigated the scale at which spatial and environmental variables act using two methods, firstly by considering a range of cell sizes and secondly by using partial distance-based redundancy analysis (dbRDA) on fractions of broad-, intermediate- and fine-scaled spatial variables. This revealed two key findings: (1) environmental variables can act alone at scales as low as 1 ha in shaping community composition; but (2) the greatest variation in community composition came from environmental variables acting in concert with spatial factors at broad- and intermediate-scales. These findings both corroborate assertions that environmental variables act more strongly across wider scales (Bongalov et al., 2019, Davidar et al., 2007, Hardy et al., 2012) and strengthen the results of Chapter 2, indicating that environmental variables can operate at fine scales.

Studies working at the local scale on juvenile and sub-adult trees show that envi-

ronmental factors and dispersal limitation explain species aggregation patterns (Lin et al., 2011, McFadden et al., 2019, Réjou-Méchain et al., 2011). In Chapter 4, I furthered this understanding by investigating whether broad-scale variation in canopy (adult) tree patterns of distribution are similarly impacted by environmental variables and dispersal limitation, which is critical given that these are the seed trees from which recruitment occurs. To do so, I took advantage of recent advances in spatial point pattern models (Shen et al., 2009a, 2013, Waagepetersen and Guan, 2009) in combination with a dataset of 392,000 canopy trees spanning 60,000 ha of undisturbed forest across the Amazon Basin. Firstly, I categorised species aggregation patterns in accordance with their environmental associations and dispersal limitation patterns in using a decision tree of increasingly complex spatial point pattern models. This revealed that the large majority of species patterns exhibited both habitat associations and dispersal limitation. This represented a key finding since it was previously unknown whether patterns of spatial aggregation would manifest in the same way for canopy trees as juvenile stems (McFadden et al., 2019). Given that we used environmental variables with a resolution of 12.5 m, this provides further evidence that environmental variables shape spatial structure of community composition.

I then investigated how the strength of environmental associations and clustering parameters varied between sites and species. Cluster size varied considerably, demonstrating that dispersal is not neutral (Lowe and McPeek, 2014) and that dispersal kernels vary between species and sites. Using phylogenetic imputation, I imputed functional traits for the species found across all sites to determine whether environmental associations and/or clustering parameters were determined by species functional traits. Clustering intensity was predicted by both species dispersal syndrome and dry seed mass. This represents a novel finding, demonstrating that functional traits operate to control species aggregation patterns and that these patterns span the entire Amazon Basin.

In combination, therefore, these Chapters yield overarching support for the dual roles of deterministic and stochastic processes in dictating spatial structure of community composition for large tropical canopy trees. This supports work from elsewhere in Latin America (Draper et al., 2019, May et al., 2015) and across the wider tropics (Bongalov et al., 2019, Liu et al., 2016). Further, they demonstrate the power of phylogenetic, functional and spatial point pattern methods for disentangling the key contributors to community assembly dynamics. With more landscape-scale forest inventory datasets emerging from the forestry sector, the prospects for unfurling unanswered questions regarding the key processes governing species distributions of tropical canopy trees are strong. Determining the key processes, especially for canopy trees is of vital importance given that tropical canopy trees are the pri-

mary seed dispersers, competitors and carbons storers within tropical rainforests (Pan et al., 2011, Thomson et al., 2011, Wright, 2002). As tropical forests face increasing threats of land-use change, understanding the underlying mechanisms of community assembly can provide key insights into conservation actions (Socolar et al., 2016).

5.1 Implications for forest management

Selective logging is a key commercial industry within tropical forest nations and is by far the largest-scale degrading force within tropical forests (Edwards et al., 2014a). At least 403 million hectares of tropical forest is committed to selective logging (Blaser et al., 2011) – an area the size of the European Union – with a substantial additional forest area logged illegally (Pacheco et al., 2016); accounting for an estimated 50-90% of tropical timber; (Nellemann and Others, 2012). As such, selective logging is currently responsible for 6% of tropical greenhouse gas emissions (Ellis et al., 2019), a major concern given ongoing climate change.

Selective logging involves the harvesting of commercially viable adult (canopy) trees, which in combination with their extraction along skid trails and roads, damages neighbouring unharvested trees, opens gaps in the forest canopy and simplifies the forest age structure. The resulting penetration of the sunlight to the forest floor and understorey promotes regeneration via growth of the remaining subcanopy trees and understorey saplings (Edwards et al., 2014b). It also can result in impeded succession if climbing vines and bamboos thrive (Putz et al., 2008) and thus greatly reduced long-term productivity (Hawthorne et al., 2012).

The vast majority (99%) of legally mandated selective logging involves 'sustainable forest management (SFM)', which implements regulations designed to retain the economic, social and environmental values of tropical forests over time (Keenan et al., 2015). Specifically, SFM requires regulations on harvest intensity (number of trees cut), minimum felling diameters (cutting only large adult trees), minimum cutting cycle lengths (typically 30 to c.70 years, in Brazil and Malaysia, respectively) and seed-tree retention rates. In turn, the impacts of logging on plant communities appears minimal, given that species richness is similar between logged and primary old-growth (unlogged) forest (Berry et al., 2010). Thus, in theory, selective logging in the tropics will permit harvesting for generations to come.

There are, however, two key reasons for concern. First, many governments have insufficient regulatory conditions and monitoring capacity to enforce prescribed SFM. For example, by 2015, only 37% of low-income countries reported forest inventories that detailed how forests are managed (MacDicken et al., 2015). Second,

recent research from the Amazon suggests that even when SFM is appropriately applied, the intensity of harvest is too high and the return time too short to permit the full recovery of timber stocks to baseline levels (MacDicken et al., 2015). A major area of ongoing forestry research is thus seeking to understand how harvested tree communities are impacted at the large spatial scales relevant to harvest and in turn what that means for forest recovery.

Results and data stemming from this thesis can offer critical insights. The important role of environmental filtering in dictating species distributions at fine scales (Chapter 2 and Chapter 3) may suggest that logging should be performed across entire concessions (akin to land-sharing logging) rather than being concentrated within one area or habitat type (Edwards et al., 2014a). In turn, Chapter 4 identifies habitat associations and variation in dispersal kernels. Of particular concern are those species that have a strong tendency to aggregate, but are also highly dispersal limited. If harvesting such species, it would be vital to ensure that some adult trees are retained within the cluster, via sufficient seed-tree retention, although how such rates should be determined is an area for further research. Currently, in the Amazon, these rules are set at the same level for each tree, but Chapter 4 indicates that species-specific rules are needed with respect to both the number of individuals and how their retention is organised spatially.

Subtractive heterogenisation

Chapter 3 revealed the scales at which environmental variables operate to drive β-diversity. Pivotally, because of the inherently spatial nature of species turnover within tree communities, logging may reorganise this structuring. Of particular concern is the potential for subtractive heterogenisation to occur (Socolar et al., 2016). Via the selective removal of common tree species, logging may increase the rates of species turnover with unknown consequences for ecological processes (e.g. Janzen-Connell effects; (Connell, 1971, Janzen, 1970)), ecosystem functioning (fruit availability) and ecosystem services (carbon stocking, given that logged species tend to have higher wood density).

One potential route in determining whether logging drives substractive heterogenisation is to use spatially explicit records of tree distributions (such as those in Chapters 2-4; Fig. 5.1) in combination with logging records of which stems were cut during harvest (Fig. 5.2). It is thus possible to generate a clearer understanding of how harvesting at realistic intensities per species impacts both diversity metrics and β-diversity patterns.

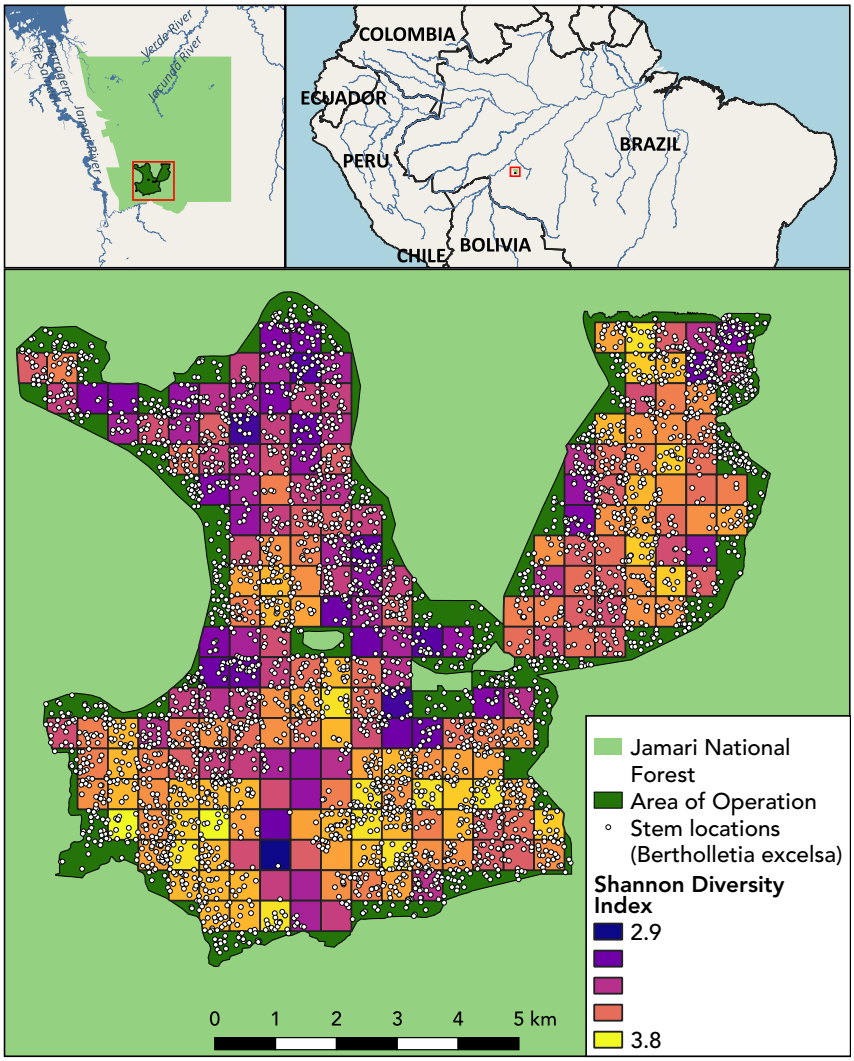

Figure 5.1: Map showing stem locations for *Bertholletia excelsa* and Shannon diversity for cells

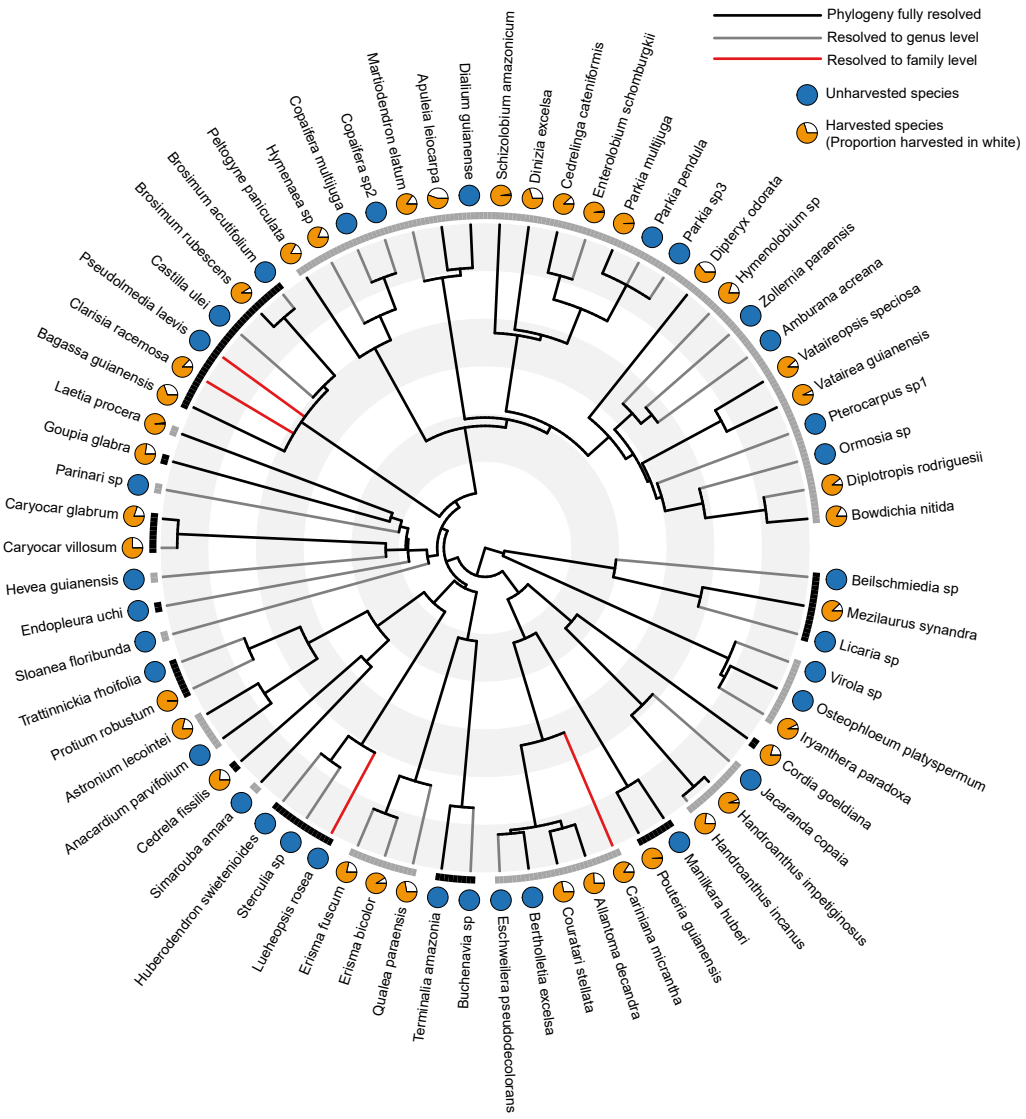

Figure 5.2: Phylogeny of species mapped by AMATA logging concession, Rôndonia, Brazil. Species dots indicate whether a species is harvested or not, and for those harvested, the proportion that were harvested

A preliminary assessment using intensity simulations based upon the spatial point maps and harvest intensities (Fig. 5.3) to generate predicted communities reveals two things. First, as expected, while β_{sor} and β_{sim} increase with pairwise distance between cells, β_{nes} declines. Shared branch lengths between cell pairs increases over distance whilst the nestedness decreases (Baselga, 2012). Assuming functional traits express a phylogenetic signal, this suggests that ecosystem functioning has been altered, likely due to the reduced influence of common, over-harvested species. In turn, changes in functional diversity may represent shifts in key ecosystem services (Tilman et al., 1997).

Second, logged forest has higher turnover of lineages across all separation distances between pairs of cells, suggesting that logging heterogenises phylogenetic community composition across scales (Socolar et al., 2016). This has significant implications for the management of selective logging, suggesting that adoption of harvesting of more species, perhaps via generation of more market opportunities of currently unused species, is important to retain diversity turnover patterns that are similar to primary forest. Forestry services could, for instance, reduce stumpage fees for currently commercially less valuable species and/or increase fees for species that are currently favoured.

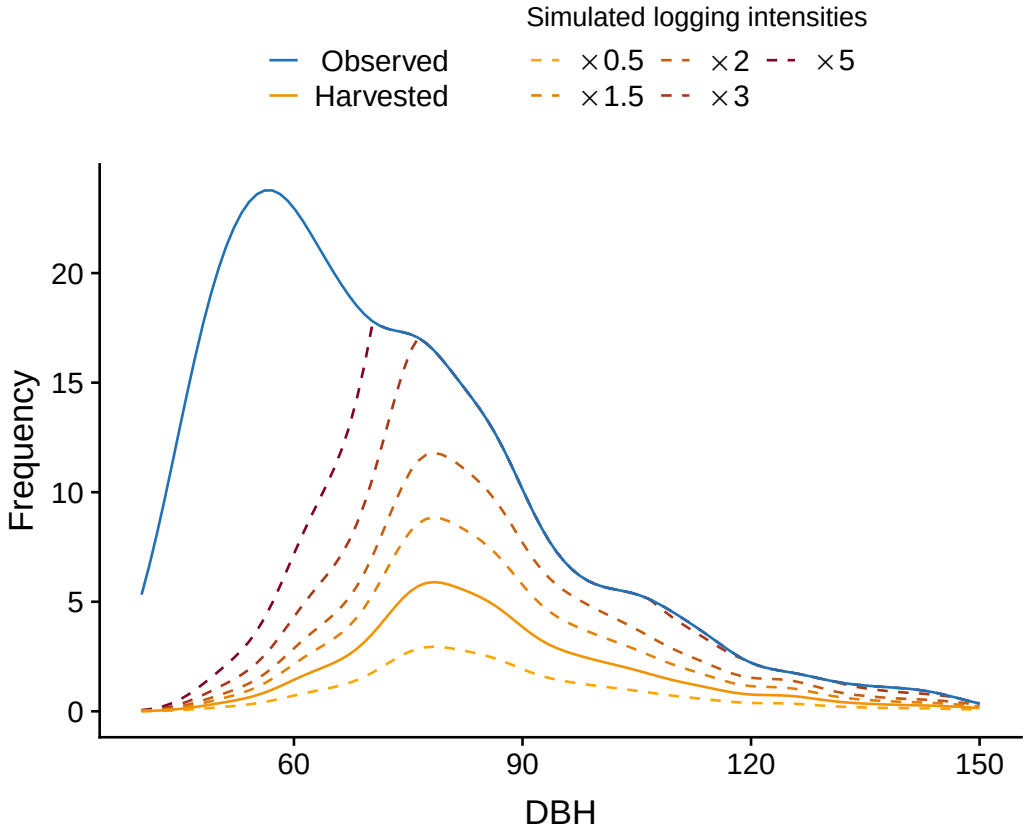

Figure 5.3: Intensity simulations for one species, *Dinizia excelsa*. A range of logging intensities were calculated based on the proportion of stems cut

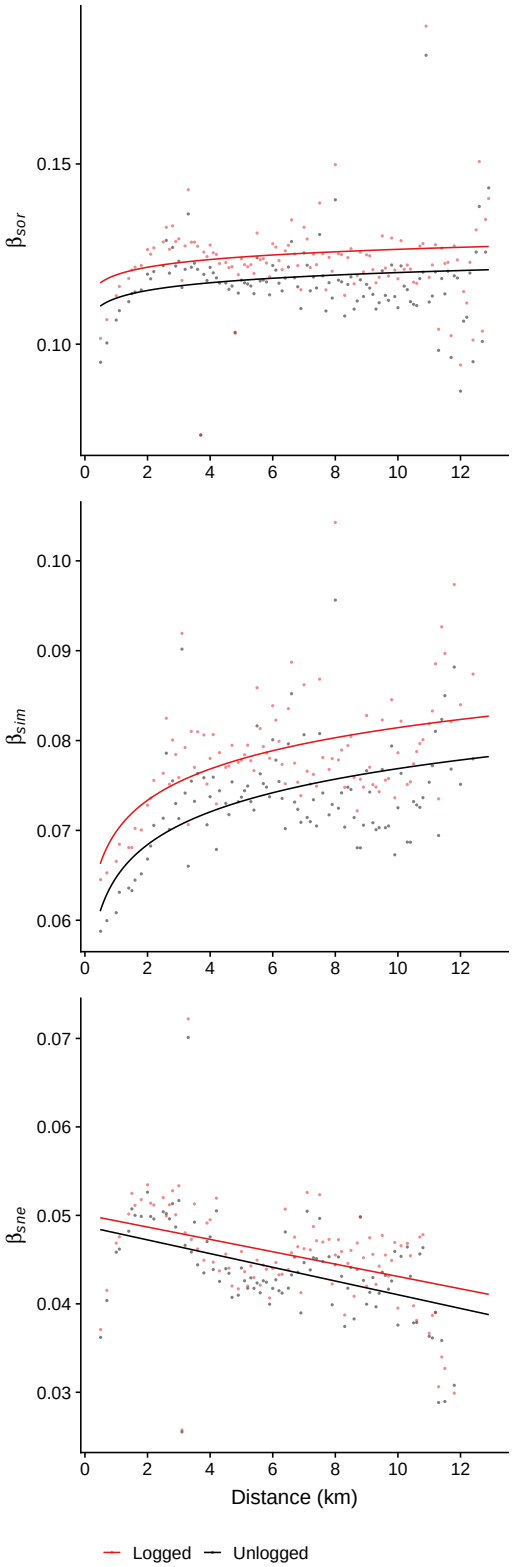

Figure 5.4: The impacts of logging on phylogenetic β-diversity. β_{sor} (a), see Chapter 3, β_{sim} represents phylogenetic diversity attributed to true turnover of lineages (b) and β_{nes} which represents the amount of PBD attributable to nestedness. Distance represents the separation between pairs of plots.

Forest recovery with logging intensity

While many studies have investigated how selective logging impacts forest recovery, the vast majority have done so focusing on broad-scale categories ('conventional' logging or 'reduced-impact' logging) versus patterns in primary forest. What is lacking is a combined assessment of logging impacts at small scales and across life histories. An assessment made at the finer scales at which logging impacts occur would specifically consider the impacts of local intensity (ie number of stems/trees harvested) as well as the spatial arrangement of treefall gaps and skid trails, areas that are edge effected by these impacts, and those that have no (discernable) logging impacts. Similarly, key is understanding survival, growth and recruitment of seedling, sapling, juvenile, and adult life stages.

To this end, I focused upon the AMATA logging concession, Rôndonia, Brazil (page 60; Appendix E) to create a series of 0.5 ha (50 x 100 m) forest plots within primary (x17) and selectively logged (x40) forest (Fig. 5.5).

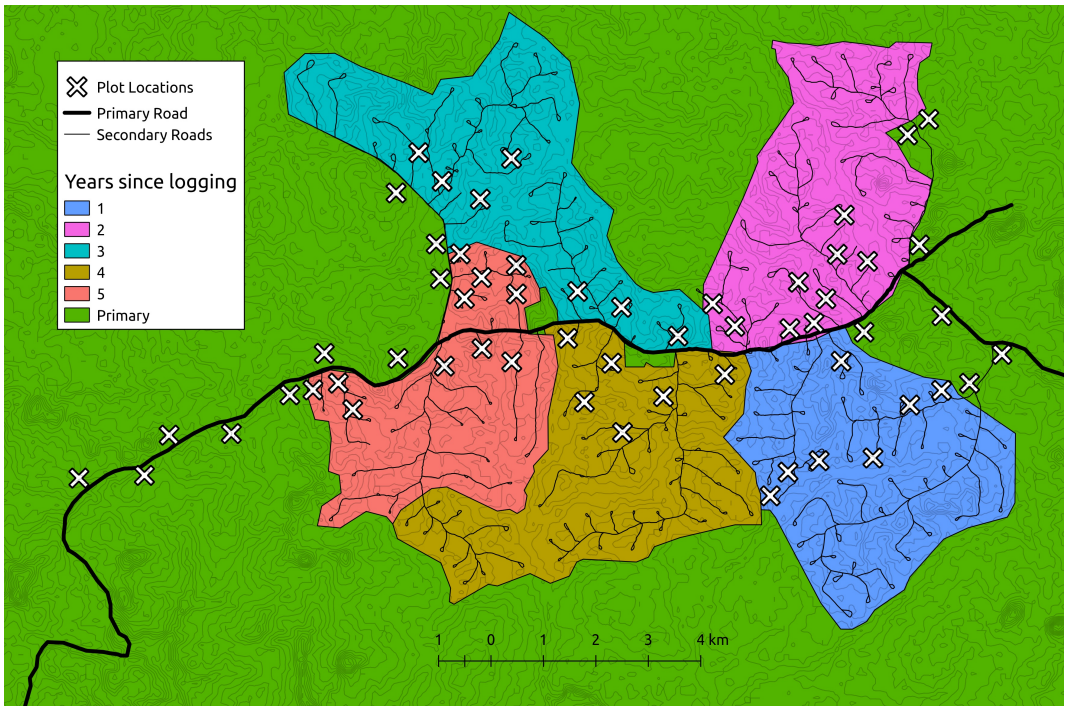

Figure 5.5: Map of sampling locations at AMATA logging concession

We restricted plots to at least 500 m from each other to minimize spatial autocorrelation. Additionally, locations were restricted to 200 m from the main access road, 100 m from secondary roads and 50m from streams to limit plant community edge effects. The logged plots spanned intensities from 1 to 8 stems harvested per hectare, the latter representing extremely high intensities that are far higher than

the legal limit for the Brazilian Amazon (30 m3/ha), and across 1 to 5 years since harvest in 2016 (Fig. 5.6). Local-scale logging intensity metrics were taken from the forest inventory dataset following verification of stump location. Road density metrics were extracted from the forest inventory dataset which includes all primary and secondary roads, mapped with a GPS. Skid trails were mapped by hand within plots.

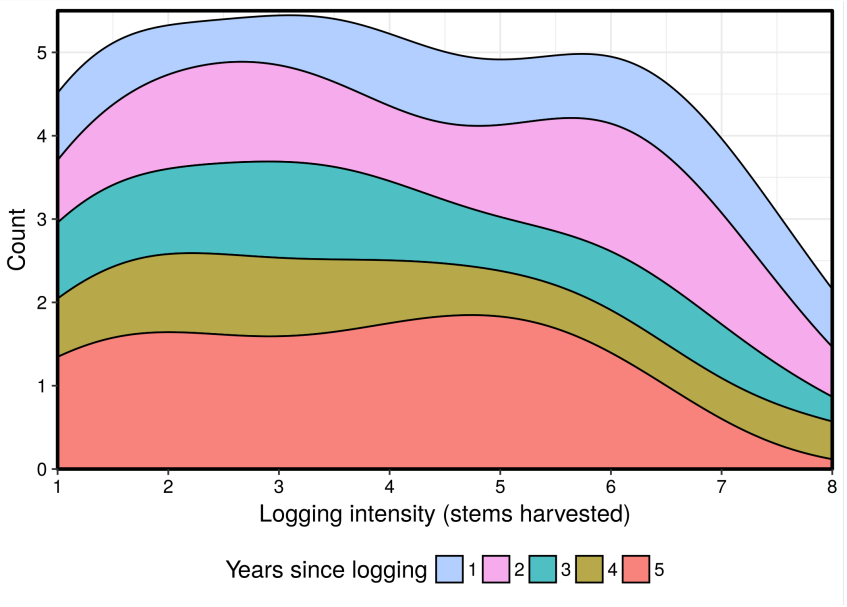

Figure 5.6: Count of sampling plots within logged forests between logging intensities and years since logging in 2016

Within each 0.5 ha plot, I measured, tagged and mapped seedlings (12 m2 in total), saplings (72 m2), juveniles (500 m2), and adults (5000 m2 / 0.5 ha) as per (Fig. 5.7). Sizes of seedlings, saplings, juveniles and adults are in Table 5.1 and abundances of size classes in the 2018 sampling are in Table 5.2. These plots were set up in Apr-Oct 2016, and then re-measured in May-Nov 2017 and Apr-Jul 2018, accounting for 19 months of fieldwork in total.

Table 5.1: Plot dimensions and plant size classes

Life stage	Subplot dimenstions	Number of subplots	Sampling rules
Adult	100×50m	1	DBH $\geq$ 40cm
Juvenile	100×5m	1	DBH $\geq$ 15cm DBH $<$ 40cm
Sapling	8×3m	1	DBH $<$ 1cm Height $\geq$ 50cm
Seedling	4×1m	3	Height $\geq$ 10cm Height $<$ 50cm

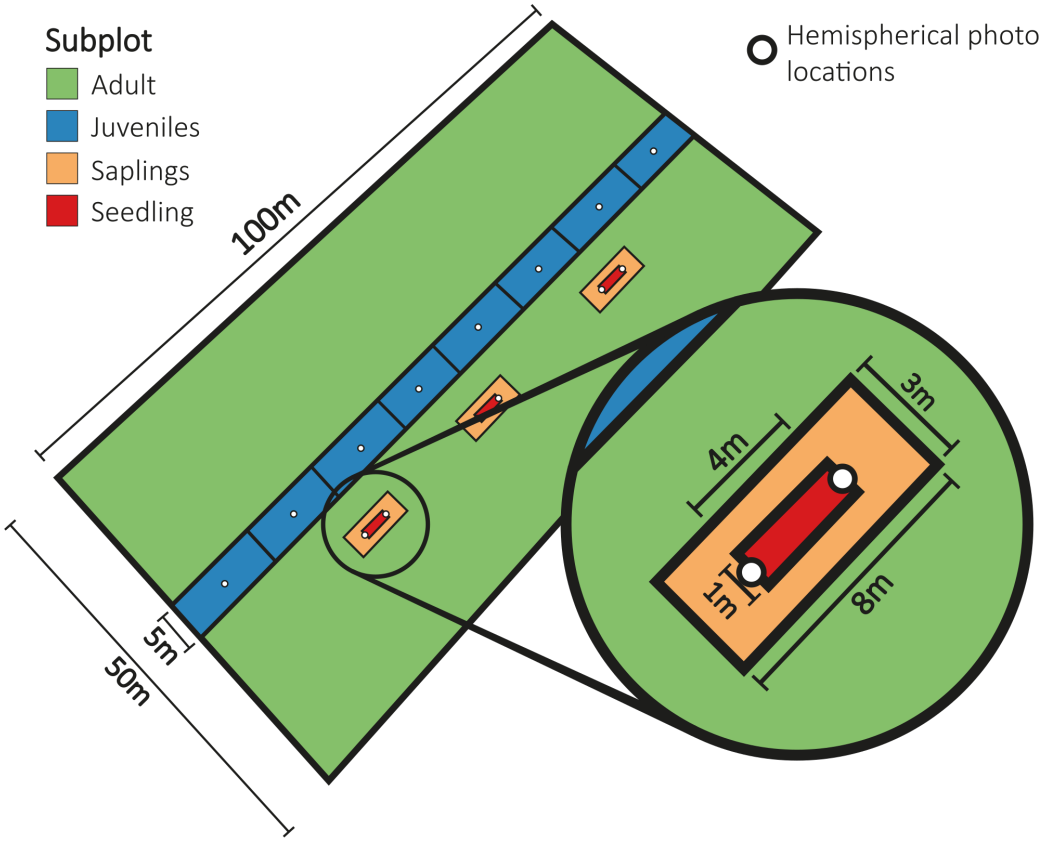

Figure 5.7: Each 100×50 m plot is comprised of a series of subplots representing adult, juvenile, sapling and seedling life stages. Adults are sampled in the full 100×50 m plot (subplot A) and juveniles in a nested 100×5 m belt transect, split into 8 sections (subplot B), that runs down the centre and spans the length of the full plot such that plot-wide logging intensity effects are represented. Three 8×3 m sapling plots (subplots C) are established at 25, 50 and 75 m along the length of the full plot and offset from the juvenile plot by 5 m to prevent damage during sampling of the juvenile plot. A 4×1 m seedling plot (subplots D) is nested centrally within each of the three sapling plots

Species identification was initially made by parabotanist Alex Elias dos Santos. However, as I became better at tree identification towards the end of the 2017 field season it became apparent that the identification of many individuals was egregiously wrong. This revealed that in instances where dos Santos could not identify a plant, he had selected from a short list of ∼50 species rather than registering it as identification unknown. In 2018, In 2018 I collected leaf samples from 4,797 of the individuals in question. These were sent for identification by the lead botanist at INPA (National Institute of Amazonian Research), Paulo Apóstolo Assunção. Unfortunately, the identifications were only concluded and sent to me on 21st July 2019, with c. 1 month of cleaning up still required, and thus precluding their inclusion within the main data-based chapters of this thesis.

Table 5.2: Woody stems sampled for each life stage and their mean abundances in logged and unlogged plots in the 2018 sampling season

Life stage	n	Mean abundance in primary plots	Mean abundance in logged plots
Seedling	8045	118	151
Sapling	7654	115	143
Juvenile	14851	227	275
Adult	7602	137	132

Nevertheless, these data now represent an important repository from which to investigate key questions about logging management impacts on tree recruitment and survival. In particular, important questions include: (1) How do logging skid trails and intensity impact recruitment, survival, and growth; (2) how does the spatial arrangement of congeners affect survival, including Janzen-Connell processes; and (3) how does logging intensity and time since logging impact phylogenetic diversity of seedling, sapling, and juvenile tree communities.

5.2 Conclusions

As we enter the Anthropocene, threats to global biodiversity are growing at an alarming rate. Many predict that we are entering the 6^{th} mass extinction event (Barnosky et al., 2011), in large part driven by land-use change and overharvesting. Improving our understanding of the processes that drive hyperdiversity is the critical foundation upon which predictions of these impacts can be made. In this thesis, I have revealed the relative roles of stochastic and deterministic processes driving community composition and its turnover over space. I have done so focussing on adult canopy trees, which to date have been overlooked at the scales required to fully assess their patterns.

The global importance of tropical timbers and, consequently, the enormous area of tropical forest that has been and that will be selectively logged cannot be understated. The techniques and findings in this thesis highlight potentially fruitful lines for scientific examination of how best to ensure sustainability in wood supply and the recovery towards the spatial patterns and processes of an old-growth tropical forest.

Appendix A

Fine-scale variation in environmental factors shape β-diversity in tropical canopy tree communities

A.1 Supplementary figures

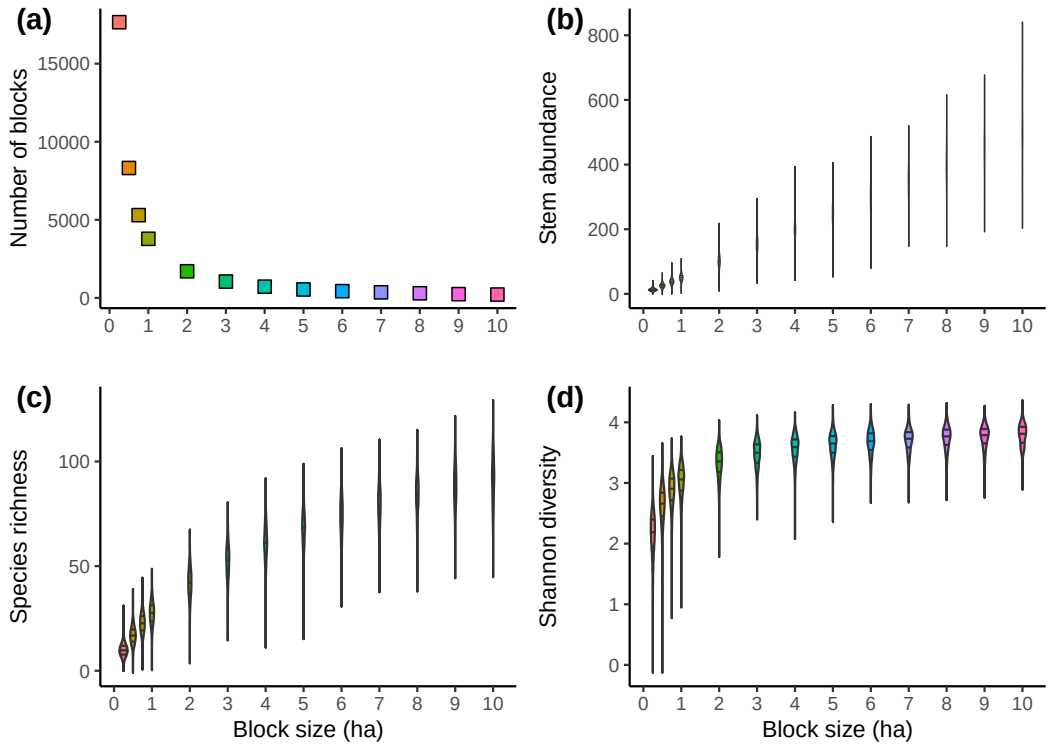

Figure A.1: We overlaid grids of varying resolution over the study site to determine an optimal cell size such that we had sufficient replication (a), variance in stem abundance (b), variance in species richness (c) and stability of alpha diversity (d).

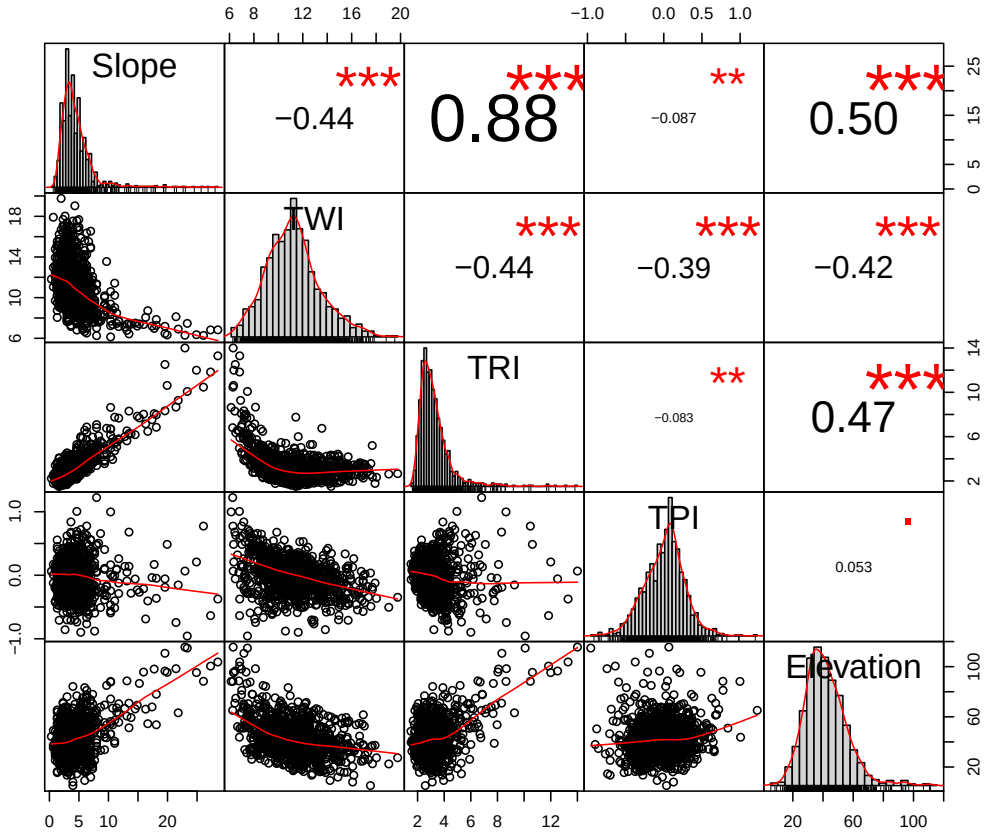

Figure A.2: The spread and autocorrelation of the five environmental variables considered in our analyses.

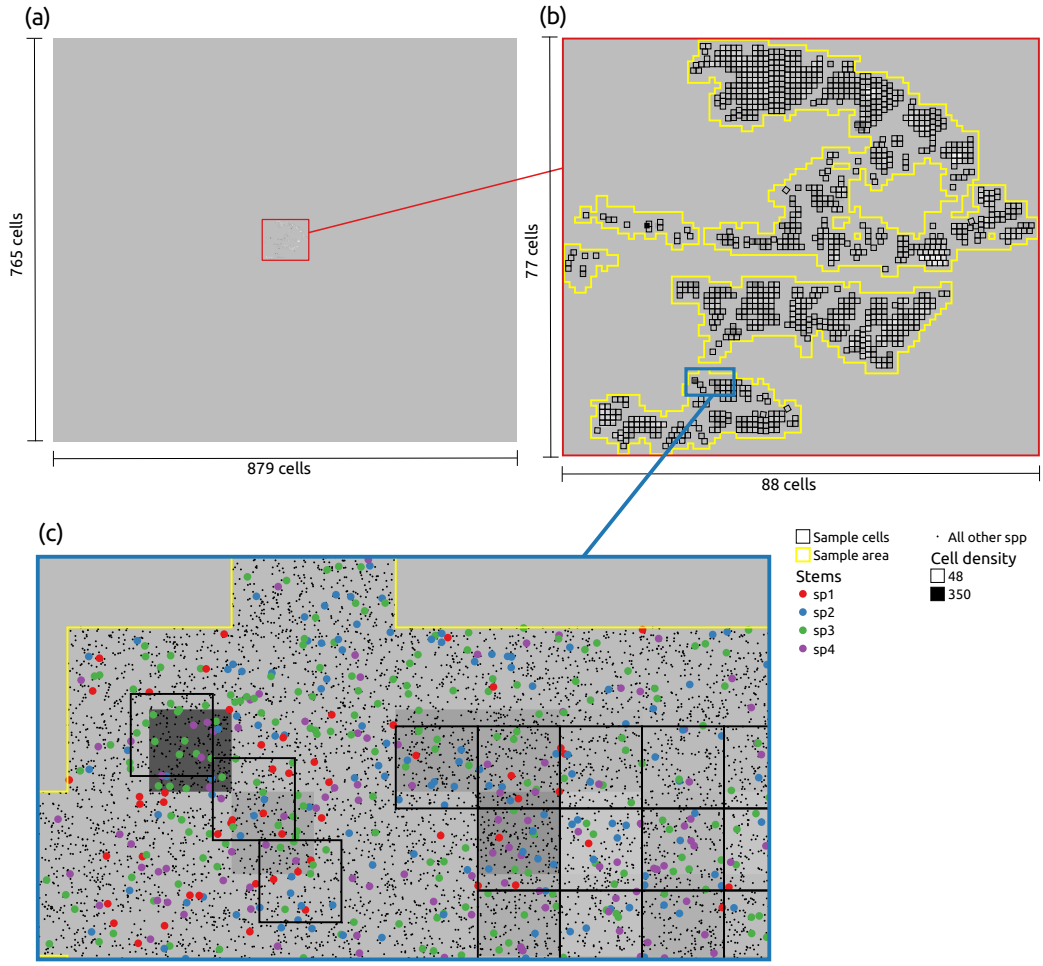

Figure A.3: Neutral simulations were conducted in an arena composed of 672,345 three hectare cells (a), surrounding the study site (b). Stem density (represented here in greyscale) for each cell was assigned as equivalent to that observed at the study site, with all cells falling outside the study area assumed to have the median density of observed cells, following Bongalov et al. (2019) (c). Since the locations of some cells were manually placed and, therefore, offset from the original cell grid, spatially explicit locations were randomly assigned for each simulated individual via the stationary Poisson process. Neutral communities were subsequently assigned to sample cells matching the spatial arrangement of cells used to assess observed communities (c). Stems portrayed in (c) are the result of a matching neutral community. Locations for four species are displayed to illustrate local species distributions under a neutral model

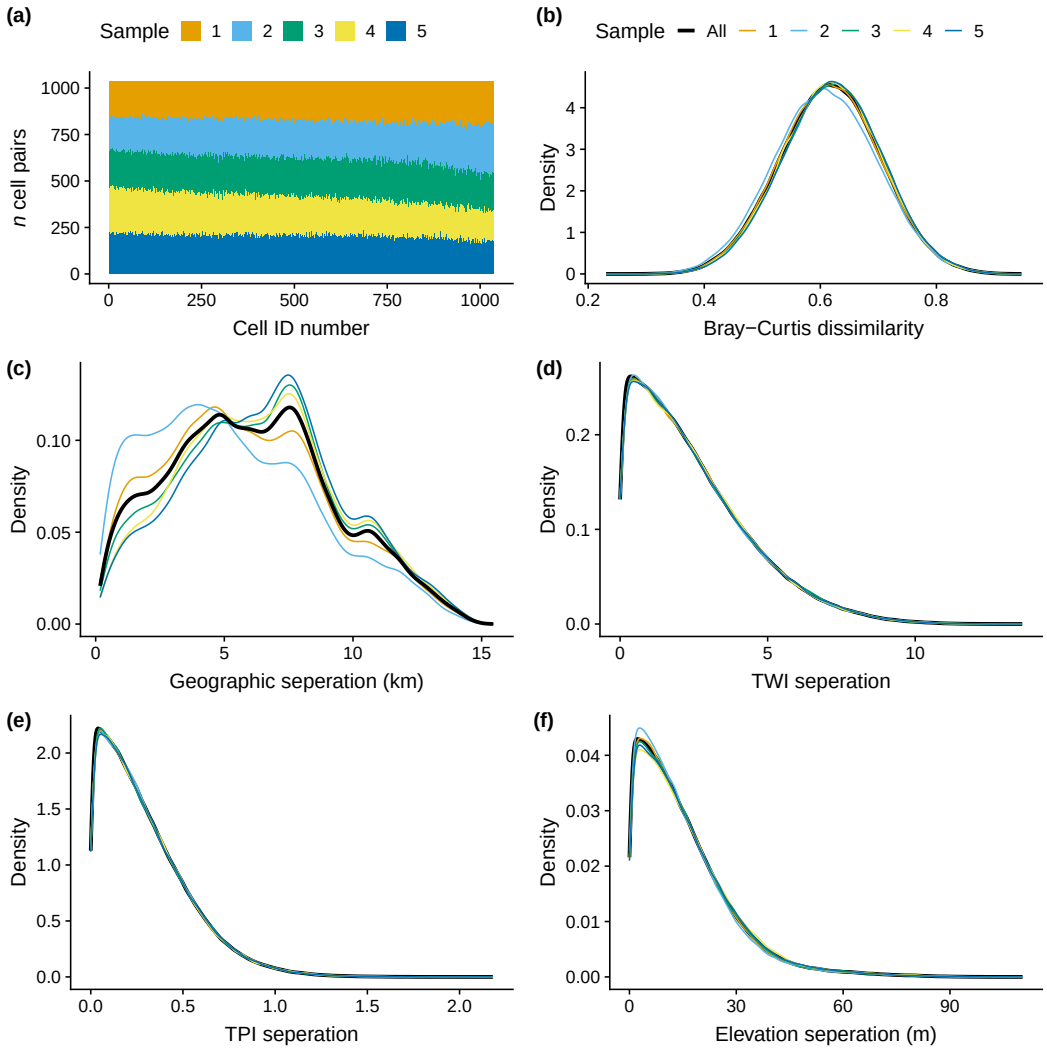

Figure A.4: Observed communities were divided into five samples to determine the underlying variability within observed communities to determine the rejection threshold, σ_i, for simulated communities. Cell representation (a), Bray-Curtis dissimilarity (b), geographic separation (c), TWI separation (d), TPI separation (e) and elevation separation (f) between cell-pair samples are close to evenly distributed

A.2 Species list

Table A.1: List of species observed at Vale do Jari and their corresponding abundances

Family	Genus	Species	Abundance
Anacardiaceae	Anacardium	Anacardium giganteum	984
Anacardiaceae	Anacardium	Anacardium spruceanum	1
Anacardiaceae	Astronium	Astronium graveolens	452
Anacardiaceae	Astronium	Astronium obliquum	675

Continued on next page

Family	Genus	Species	Abundance
Anacardiaceae	Tapirira	Tapirira guianensis	41
Anacardiaceae	Tapirira	Tapirira obtusa	4
Anacardiaceae	Thyrsodium	Thyrsodium guianense	379
Anacardiaceae	Thyrsodium	Thyrsodium spruceanum	31
Annonaceae	Anaxagorea	Anaxagorea dolichocarpa	3
Annonaceae	Duguetia	Duguetia cauliflora	14
Annonaceae	Duguetia	Duguetia surinamensis	3
Annonaceae	Guatteria	Guatteria longicuspis	1
Annonaceae	Guatteria	Guatteria poeppigiana	53
Annonaceae	Onychopetalum	Onychopetalum amazonicum	87
Annonaceae	Rollinia	Rollinia fendleri	1
Annonaceae	Xylopia	Xylopia aromatica	16
Apocynaceae	Aspidosperma	Aspidosperma album	100
Apocynaceae	Aspidosperma	Aspidosperma auriculatum	6
Apocynaceae	Aspidosperma	Aspidosperma carapanauba	14
Apocynaceae	Aspidosperma	Aspidosperma eteanum	429
Apocynaceae	Aspidosperma	Aspidosperma macrocarpon	310
Apocynaceae	Aspidosperma	Aspidosperma megalocarpon	51
Apocynaceae	Aspidosperma	Aspidosperma oblongum	39
Apocynaceae	Aspidosperma	Aspidosperma sandwithianum	25
Apocynaceae	Couma	Couma guianensis	818
Apocynaceae	Geissospermum	Geissospermum sericeum	8
Apocynaceae	Macoubea	Macoubea guianensis	584
Apocynaceae	Malouetia	Malouetia lata	6
Apocynaceae	Parahancornia	Parahancornia fasciculata	88
Apocynaceae	Rauvolfia	Rauvolfia pentaphylla	4
Araliaceae	Schefflera	Schefflera morototoni	332
Arecaceae	Oenocarpus	Oenocarpus bacaba	6
Bignoniaceae	Handroanthus	Handroanthus impetiginosus	7
Bignoniaceae	Handroanthus	Handroanthus serratifolius	141
Bignoniaceae	Jacaranda	Jacaranda copaia	1302
Bignoniaceae	Tabebuia	Tabebuia insignis	35
Bixaceae	Cochlospermum	Cochlospermum orinocense	10
Boraginaceae	Cordia	Cordia americana	1
Boraginaceae	Cordia	Cordia sericicalyx	2
Boraginaceae	Cordia	Cordia sprucei	3
Burseraceae	Protium	Protium apiculatum	1
Burseraceae	Protium	Protium araguense	7
Burseraceae	Protium	Protium decandrum	665
Burseraceae	Protium	Protium giganteum	12
Burseraceae	Protium	Protium guianense	1
Burseraceae	Protium	Protium krukoffii	121
Burseraceae	Protium	Protium pallidum	241
Burseraceae	Protium	Protium paniculatum	4
Burseraceae	Protium	Protium polybotryum	87

Continued on next page

Family	Genus	Species	Abundance
Burseraceae	Protium	Protium sagotianum	49
Burseraceae	Tetragastris	Tetragastris altissima	19
Burseraceae	Tetragastris	Tetragastris panamensis	517
Burseraceae	Trattinnickia	Trattinnickia burserifolia	496
Burseraceae	Trattinnickia	Trattinnickia rhoifolia	766
Calophyllaceae	Caraipa	Caraipa densifolia	3
Cannabaceae	Trema	Trema micrantha	4
Caryocaraceae	Caryocar	Caryocar glabrum	2212
Caryocaraceae	Caryocar	Caryocar microcarpum	7
Caryocaraceae	Caryocar	Caryocar pallidum	9
Caryocaraceae	Caryocar	Caryocar villosum	933
Celastraceae	Cheiloclinium	Cheiloclinium cognatum	23
Celastraceae	Maytenus	Maytenus pittieriana	3
Chrysobalanaceae	Couepia	Couepia guianensis	1
Chrysobalanaceae	Couepia	Couepia robusta	522
Chrysobalanaceae	Hirtella	Hirtella bicornis	320
Chrysobalanaceae	Hirtella	Hirtella eriandra	103
Chrysobalanaceae	Hirtella	Hirtella macrophylla	1
Chrysobalanaceae	Hirtella	Hirtella obidensis	19
Chrysobalanaceae	Hirtella	Hirtella piresii	787
Chrysobalanaceae	Hirtella	Hirtella sprucei	7
Chrysobalanaceae	Licania	Licania egleri	25
Chrysobalanaceae	Licania	Licania heteromorpha	1341
Chrysobalanaceae	Licania	Licania impressa	35
Chrysobalanaceae	Licania	Licania kunthiana	114
Chrysobalanaceae	Licania	Licania laevigata	2
Chrysobalanaceae	Licania	Licania latifolia	481
Chrysobalanaceae	Licania	Licania macrophylla	9
Chrysobalanaceae	Licania	Licania membranacea	10835
Chrysobalanaceae	Licania	Licania micrantha	5467
Chrysobalanaceae	Licania	Licania minutiflora	4
Chrysobalanaceae	Licania	Licania octandra	1241
Chrysobalanaceae	Licania	Licania paraensis	113
Chrysobalanaceae	Licania	Licania silvae	32
Chrysobalanaceae	Parinari	Parinari excelsa	11052
Chrysobalanaceae	Parinari	Parinari montana	664
Clusiaceae	Calophyllum	Calophyllum brasiliense	71
Clusiaceae	Symphonia	Symphonia globulifera	35
Combretaceae	Buchenavia	Buchenavia grandis	36
Combretaceae	Buchenavia	Buchenavia parvifolia	632
Combretaceae	Terminalia	Terminalia amazonia	991
Combretaceae	Terminalia	Terminalia argentea	211
Combretaceae	Terminalia	Terminalia catappa	2
Combretaceae	Terminalia	Terminalia guyanensis	16
Connaraceae	Connarus	Connarus perrottetii	5

Continued on next page

Family	Genus	Species	Abundance
Ebenaceae	Diospyros	Diospyros carbonaria	92
Ebenaceae	Diospyros	Diospyros santaremnensis	21
Ebenaceae	Diospyros	Diospyros velutinosa	25
Elaeocarpaceae	Sloanea	Sloanea grandis	233
Elaeocarpaceae	Sloanea	Sloanea guianensis	270
Elaeocarpaceae	Sloanea	Sloanea obtusifolia	674
Euphorbiaceae	Alchorneopsis	Alchorneopsis floribunda	23
Euphorbiaceae	Conceveiba	Conceveiba guianensis	186
Euphorbiaceae	Glycydendron	Glycydendron amazonicum	1
Euphorbiaceae	Hevea	Hevea brasiliensis	59
Euphorbiaceae	Hevea	Hevea guianensis	85
Euphorbiaceae	Hevea	Hevea spruceana	16
Euphorbiaceae	Mabea	Mabea caudata	1
Euphorbiaceae	Maprounea	Maprounea guianensis	9
Goupiaceae	Goupia	Goupia glabra	13576
Humiriaceae	Endopleura	Endopleura uchi	645
Humiriaceae	Humiria	Humiria balsamifera	345
Humiriaceae	Sacoglottis	Sacoglottis amazonica	53
Humiriaceae	Sacoglottis	Sacoglottis guianensis	1592
Humiriaceae	Vantanea	Vantanea parviflora	4943
Hypericaceae	Vismia	Vismia cayennensis	31
Icacinaceae	Emmotum	Emmotum fagifolium	668
Icacinaceae	Poraqueiba	Poraqueiba guianensis	5
Lacistemataceae	Lacistema	Lacistema aggregatum	8
Lauraceae	Aniba	Aniba canellila	27
Lauraceae	Aniba	Aniba parviflora	4
Lauraceae	Aniba	Aniba puchury-minor	66
Lauraceae	Aniba	Aniba rosaeodora	11
Lauraceae	Dicypellium	Dicypellium caryophyllatum	1
Lauraceae	Licaria	Licaria canella	369
Lauraceae	Mezilaurus	Mezilaurus ita-uba	1059
Lauraceae	Mezilaurus	Mezilaurus lindaviana	4823
Lauraceae	Nectandra	Nectandra cissiflora	148
Lauraceae	Nectandra	Nectandra pichurim	1
Lauraceae	Ocotea	Ocotea aciphylla	45
Lauraceae	Ocotea	Ocotea guianensis	797
Lauraceae	Ocotea	Ocotea schomburgkiana	19
Lauraceae	Ocotea	Ocotea silvae	5
Lauraceae	Ocotea	Ocotea splendens	81
Lauraceae	Ocotea	Ocotea sprucei	11
Lauraceae	Persea	Persea jariensis	1383
Lecythidaceae	Bertholletia	Bertholletia excelsa	8
Lecythidaceae	Corythophora	Corythophora rimosa	427
Lecythidaceae	Couratari	Couratari guianensis	618
Lecythidaceae	Couratari	Couratari oblongifolia	426

Continued on next page

Family	Genus	Species	Abundance
Lecythidaceae	Couroupita	Couroupita guianensis	17
Lecythidaceae	Eschweilera	Eschweilera coriacea	2254
Lecythidaceae	Eschweilera	Eschweilera juruensis	6
Lecythidaceae	Eschweilera	Eschweilera micrantha	108
Lecythidaceae	Eschweilera	Eschweilera obversa	25
Lecythidaceae	Eschweilera	Eschweilera paniculata	1721
Lecythidaceae	Eschweilera	Eschweilera pedicellata	808
Lecythidaceae	Eschweilera	Eschweilera subglandulosa	8
Lecythidaceae	Gustavia	Gustavia hexapetala	1
Lecythidaceae	Lecythis	Lecythis chartacea	57
Lecythidaceae	Lecythis	Lecythis pisonis	1270
Lecythidaceae	Lecythis	Lecythis poiteaui	1980
Leguminosae	Abarema	Abarema curvicarpa	8
Leguminosae	Abarema	Abarema jupunba	315
Leguminosae	Abarema	Abarema piresii	9
Leguminosae	Acacia	Acacia polyphylla	3
Leguminosae	Acosmium	Acosmium nitens	101
Leguminosae	Albizia	Albizia pedicellaris	1890
Leguminosae	Alexa	Alexa grandiflora	38
Leguminosae	Apuleia	Apuleia leiocarpa	7
Leguminosae	Balizia	Balizia elegans	1110
Leguminosae	Batesia	Batesia floribunda	1299
Leguminosae	Bowdichia	Bowdichia nitida	3411
Leguminosae	Campsiandra	Campsiandra implexicaulis	1
Leguminosae	Cedrelinga	Cedrelinga cateniformis	275
Leguminosae	Chamaecrista	Chamaecrista adiantifolia	17
Leguminosae	Chamaecrista	Chamaecrista bahiae	4
Leguminosae	Copaifera	Copaifera martii	136
Leguminosae	Copaifera	Copaifera officinalis	97
Leguminosae	Copaifera	Copaifera reticulata	4
Leguminosae	Crudia	Crudia amazonica	1
Leguminosae	Cynometra	Cynometra spruceana	12
Leguminosae	Dalbergia	Dalbergia spruceana	11
Leguminosae	Dialium	Dialium guianense	965
Leguminosae	Dimorphandra	Dimorphandra macrostachya	19
Leguminosae	Dimorphandra	Dimorphandra multiflora	110
Leguminosae	Dinizia	Dinizia excelsa	8676
Leguminosae	Diplotropis	Diplotropis purpurea	1213
Leguminosae	Diplotropis	Diplotropis racemosa	569
Leguminosae	Dipteryx	Dipteryx magnifica	2295
Leguminosae	Dipteryx	Dipteryx odorata	2343
Leguminosae	Dussia	Dussia discolor	14
Leguminosae	Elizabetha	Elizabetha durissima	1
Leguminosae	Enterolobium	Enterolobium maximum	7
Leguminosae	Enterolobium	Enterolobium schomburgkii	869

Continued on next page

Family	Genus	Species	Abundance
Leguminosae	Hydrochorea	Hydrochorea corymbosa	2
Leguminosae	Hymenaea	Hymenaea courbaril	1347
Leguminosae	Hymenaea	Hymenaea intermedia	80
Leguminosae	Hymenaea	Hymenaea parvifolia	10
Leguminosae	Hymenolobium	Hymenolobium excelsum	690
Leguminosae	Hymenolobium	Hymenolobium flavum	336
Leguminosae	Hymenolobium	Hymenolobium petraeum	498
Leguminosae	Hymenolobium	Hymenolobium sericeum	355
Leguminosae	Inga	Inga alba	233
Leguminosae	Inga	Inga capitata	1
Leguminosae	Inga	Inga gracilifolia	28
Leguminosae	Inga	Inga heterophylla	2075
Leguminosae	Inga	Inga micradenia	3
Leguminosae	Inga	Inga oerstediana	278
Leguminosae	Inga	Inga panurensis	1
Leguminosae	Inga	Inga pezizifera	37
Leguminosae	Inga	Inga rubiginosa	3
Leguminosae	Inga	Inga splendens	141
Leguminosae	Inga	Inga tarapotensis	28
Leguminosae	Macrolobium	Macrolobium brevense	5
Leguminosae	Macrolobium	Macrolobium campestre	5
Leguminosae	Macrolobium	Macrolobium pendulum	47
Leguminosae	Martiodendron	Martiodendron parviflorum	19
Leguminosae	Mora	Mora paraensis	2
Leguminosae	Myrocarpus	Myrocarpus frondosus	2
Leguminosae	Ormosia	Ormosia coccinea	45
Leguminosae	Ormosia	Ormosia coutinhoi	6
Leguminosae	Ormosia	Ormosia flava	68
Leguminosae	Ormosia	Ormosia paraensis	55
Leguminosae	Parkia	Parkia decussata	29
Leguminosae	Parkia	Parkia gigantocarpa	22
Leguminosae	Parkia	Parkia nitida	2179
Leguminosae	Parkia	Parkia pendula	1359
Leguminosae	Parkia	Parkia reticulata	267
Leguminosae	Parkia	Parkia ulei	625
Leguminosae	Peltogyne	Peltogyne paniculata	259
Leguminosae	Peltogyne	Peltogyne paradoxa	115
Leguminosae	Pentaclethra	Pentaclethra macroloba	60
Leguminosae	Piptadenia	Piptadenia gonoacantha	2217
Leguminosae	Pithecellobium	Pithecellobium decandrum	1524
Leguminosae	Platymiscium	Platymiscium ulei	31
Leguminosae	Pterocarpus	Pterocarpus rohrii	188
Leguminosae	Pterocarpus	Pterocarpus santalinoides	19
Leguminosae	Recordoxylon	Recordoxylon stenopetalum	4
Leguminosae	Sclerolobium	Sclerolobium melanocarpum	1678

Continued on next page

Family	Genus	Species	Abundance
Leguminosae	Stryphnodendron	Stryphnodendron paniculatum	11
Leguminosae	Stryphnodendron	Stryphnodendron polystachyum	4
Leguminosae	Stryphnodendron	Stryphnodendron pulcherrimum	181
Leguminosae	Swartzia	Swartzia acuminata	369
Leguminosae	Swartzia	Swartzia grandifolia	11
Leguminosae	Swartzia	Swartzia panacoco	466
Leguminosae	Swartzia	Swartzia polyphylla	3047
Leguminosae	Swartzia	Swartzia racemosa	12
Leguminosae	Swartzia	Swartzia sprucei	6
Leguminosae	Tachigali	Tachigali guianensis	11
Leguminosae	Tachigali	Tachigali melinonii	2177
Leguminosae	Tachigali	Tachigali myrmecophila	9081
Leguminosae	Tachigali	Tachigali paniculata	4954
Leguminosae	Tachigali	Tachigali paraensis	105
Leguminosae	Tachigali	Tachigali tinctoria	1305
Leguminosae	Taralea	Taralea oppositifolia	110
Leguminosae	Vatairea	Vatairea erythrocarpa	753
Leguminosae	Vataireopsis	Vataireopsis speciosa	91
Leguminosae	Vouacapoua	Vouacapoua americana	14962
Leguminosae	Zollernia	Zollernia paraensis	176
Leguminosae	Zygia	Zygia ampla	2
Leguminosae	Zygia	Zygia racemosa	228
Loganiaceae	Antonia	Antonia ovata	284
Malpighiaceae	Byrsonima	Byrsonima aerugo	13
Malpighiaceae	Byrsonima	Byrsonima stipulacea	131
Malvaceae	Apeiba	Apeiba glabra	1081
Malvaceae	Apeiba	Apeiba tibourbou	9
Malvaceae	Guazuma	Guazuma ulmifolia	17
Malvaceae	Luehea	Luehea speciosa	1073
Malvaceae	Lueheopsis	Lueheopsis rosea	569
Malvaceae	Mollia	Mollia speciosa	10
Malvaceae	Pachira	Pachira nervosa	33
Malvaceae	Pseudobombax	Pseudobombax munguba	8
Malvaceae	Quararibea	Quararibea guianensis	2
Malvaceae	Sterculia	Sterculia amazonica	33
Malvaceae	Sterculia	Sterculia frondosa	164
Malvaceae	Sterculia	Sterculia pruriens	4
Malvaceae	Sterculia	Sterculia speciosa	329
Malvaceae	Theobroma	Theobroma subincanum	5
Melastomataceae	Mouriri	Mouriri brachyanthera	3190
Melastomataceae	Mouriri	Mouriri collocarpa	928
Melastomataceae	Mouriri	Mouriri grandiflora	120
Meliaceae	Carapa	Carapa guianensis	419
Meliaceae	Cedrela	Cedrela odorata	8
Meliaceae	Trichilia	Trichilia lecointei	2

Continued on next page

Family	Genus	Species	Abundance
Meliaceae	Trichilia	Trichilia septentrionalis	26
Moraceae	Bagassa	Bagassa guianensis	5
Moraceae	Brosimum	Brosimum acutifolium	5
Moraceae	Brosimum	Brosimum lactescens	25
Moraceae	Brosimum	Brosimum parinarioides	4289
Moraceae	Brosimum	Brosimum rubescens	6
Moraceae	Clarisia	Clarisia racemosa	8
Moraceae	Ficus	Ficus nymphaeifolia	65
Moraceae	Helicostylis	Helicostylis pedunculata	604
Moraceae	Maquira	Maquira sclerophylla	56
Moraceae	Perebea	Perebea guianensis	124
Myristicaceae	Iryanthera	Iryanthera juruensis	7
Myristicaceae	Iryanthera	Iryanthera sagotiana	35
Myristicaceae	Osteophloeum	Osteophloeum platyspermum	49
Myristicaceae	Virola	Virola calophylla	13
Myristicaceae	Virola	Virola flexuosa	24
Myristicaceae	Virola	Virola michelii	150
Myristicaceae	Virola	Virola multicostata	7
Myristicaceae	Virola	Virola sebifera	98
Myristicaceae	Virola	Virola surinamensis	22
Myrtaceae	Myrcia	Myrcia amapensis	3
Myrtaceae	Myrcia	Myrcia splendens	19
Myrtaceae	Myrciaria	Myrciaria floribunda	180
Nyctaginaceae	Guapira	Guapira tomentosa	22
Nyctaginaceae	Neea	Neea constricta	340
Ochnaceae	Ouratea	Ouratea polygyna	4
Ochnaceae	Quiina	Quiina florida	1
Ochnaceae	Touroulia	Touroulia guianensis	5
Olacaceae	Chaunochiton	Chaunochiton kappleri	236
Olacaceae	Douradoa	Douradoa consimilis	197
Olacaceae	Dulacia	Dulacia guianensis	10
Olacaceae	Minquartia	Minquartia guianensis	6228
Olacaceae	Ptychopetalum	Ptychopetalum olacoides	4
Peraceae	Pera	Pera bicolor	90
Peraceae	Pogonophora	Pogonophora schomburgkiana	401
Phyllanthaceae	Amanoa	Amanoa guianensis	151
Polygonaceae	Triplaris	Triplaris weigeltiana	7
Putranjivaceae	Drypetes	Drypetes variabilis	623
Rhabdodendraceae	Rhabdodendron	Rhabdodendron amazonicum	1
Rubiaceae	Capirona	Capirona decorticans	8
Rubiaceae	Chimarrhis	Chimarrhis turbinata	4595
Rubiaceae	Duroia	Duroia macrophylla	4
Rubiaceae	Ferdinandusa	Ferdinandusa elliptica	134
Rubiaceae	Ferdinandusa	Ferdinandusa paraensis	1050
Rubiaceae	Genipa	Genipa americana	3

Continued on next page

Family	Genus	Species	Abundance
Rubiaceae	Psychotria	Psychotria mapourioides	155
Rutaceae	Euxylophora	Euxylophora paraensis	2
Rutaceae	Zanthoxylum	Zanthoxylum culantrillo	17
Rutaceae	Zanthoxylum	Zanthoxylum rhoifolium	4
Salicaceae	Casearia	Casearia arborea	167
Salicaceae	Laetia	Laetia procera	2322
Sapotaceae	Chrysophyllum	Chrysophyllum prieurii	5
Sapotaceae	Manilkara	Manilkara bidentata	13187
Sapotaceae	Manilkara	Manilkara huberi	6447
Sapotaceae	Micropholis	Micropholis acutangula	88
Sapotaceae	Micropholis	Micropholis guyanensis	5
Sapotaceae	Micropholis	Micropholis humboldtiana	778
Sapotaceae	Micropholis	Micropholis mensalis	132
Sapotaceae	Pouteria	Pouteria amazonica	642
Sapotaceae	Pouteria	Pouteria bracteata	158
Sapotaceae	Pouteria	Pouteria caimito	348
Sapotaceae	Pouteria	Pouteria elegans	135
Sapotaceae	Pouteria	Pouteria engleri	175
Sapotaceae	Pouteria	Pouteria franciscana	1
Sapotaceae	Pouteria	Pouteria jariensis	1655
Sapotaceae	Pouteria	Pouteria krukovii	470
Sapotaceae	Pouteria	Pouteria macrocarpa	3318
Sapotaceae	Pouteria	Pouteria oblanceolata	33
Sapotaceae	Pouteria	Pouteria oppositifolia	813
Sapotaceae	Pouteria	Pouteria reticulata	19
Sapotaceae	Pouteria	Pouteria rodriguesiana	1082
Sapotaceae	Pouteria	Pouteria torta	229
Sapotaceae	Sarcaulus	Sarcaulus brasiliensis	29
Simaroubaceae	Simaba	Simaba cedron	1
Simaroubaceae	Simaba	Simaba orinocensis	10
Simaroubaceae	Simarouba	Simarouba amara	480
Siparunaceae	Siparuna	Siparuna decipiens	72
Styracaceae	Styrax	Styrax sieberi	51
Theaceae	Gordonia	Gordonia fruticosa	5
Ulmaceae	Ampelocera	Ampelocera edentula	26
Urticaceae	Cecropia	Cecropia obtusa	1
Urticaceae	Cecropia	Cecropia sciadophylla	1
Urticaceae	Pourouma	Pourouma minor	12
Violaceae	Paypayrola	Paypayrola grandiflora	2
Violaceae	Rinorea	Rinorea guianensis	200
Vochysiaceae	Erisma	Erisma calcaratum	9
Vochysiaceae	Erisma	Erisma uncinatum	938
Vochysiaceae	Qualea	Qualea albiflora	5958
Vochysiaceae	Qualea	Qualea coerulea	199
Vochysiaceae	Qualea	Qualea paraensis	9254

Continued on next page

Family	Genus	Species	Abundance
Vochysiaceae	Qualea	Qualea rosea	3170
Vochysiaceae	Qualea	Qualea wittrockii	1212
Vochysiaceae	Ruizterania	Ruizterania cassiquiarensis	4
Vochysiaceae	Vochysia	Vochysia cayennensis	2
Vochysiaceae	Vochysia	Vochysia divergens	497
Vochysiaceae	Vochysia	Vochysia guianensis	120
Vochysiaceae	Vochysia	Vochysia inundata	7
Vochysiaceae	Vochysia	Vochysia maxima	30
Vochysiaceae	Vochysia	Vochysia obscura	6108
Vochysiaceae	Vochysia	Vochysia splendens	395
Vochysiaceae	Vochysia	Vochysia surinamensis	22
Vochysiaceae	Vochysia	Vochysia tomentosa	3
Vochysiaceae	Vochysia	Vochysia vismiifolia	1071

Appendix B

Phylogenetic beta-diversity informs the factors driving compositional turnover in tropical canopy tree communities

B.1 Supplementary figures

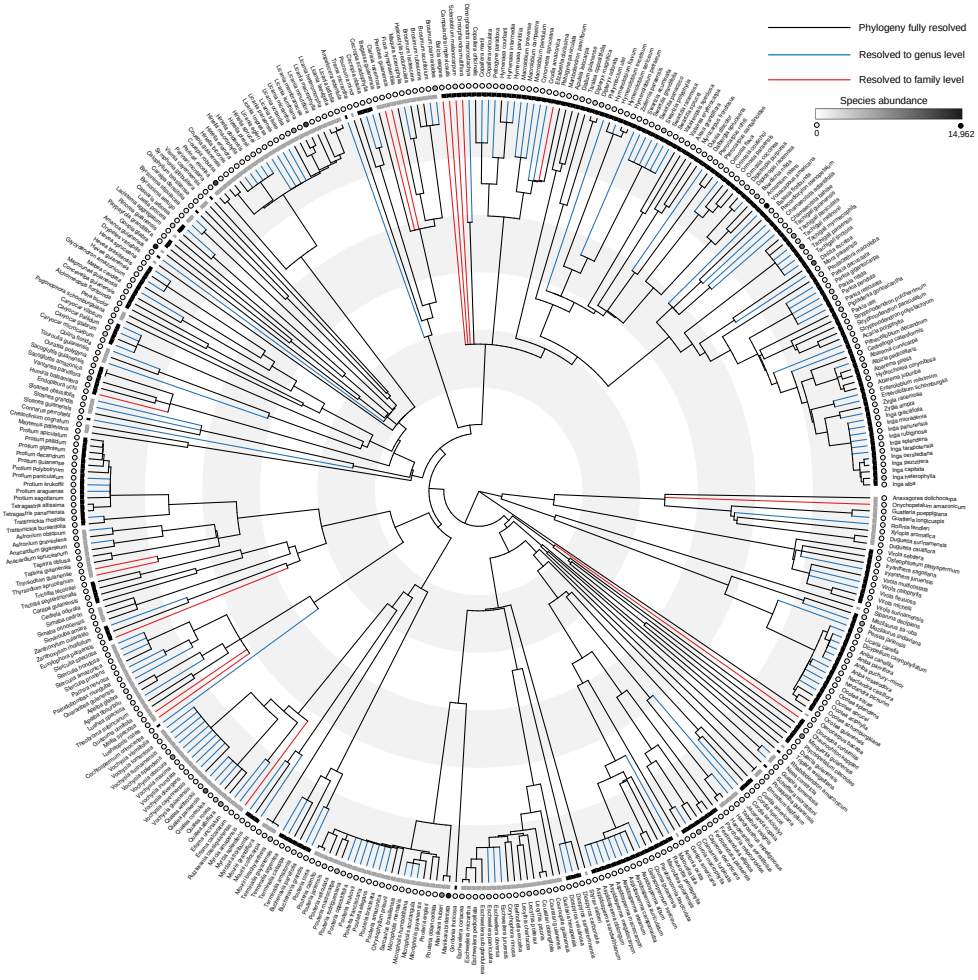

Figure B.1: The phylogenetic tree used to derive metrics of PBD was reconstructed from Zanne et al. (2014) & Smith and Brown (2018) mega-phylogenies. 52% of species were fully resolved to the species level, 44% to the genus level and 4% to the family level. Shading of the points represent species abundance across the study site. Alternating black and grey bars at the tips separate plant families as a visual aid only.

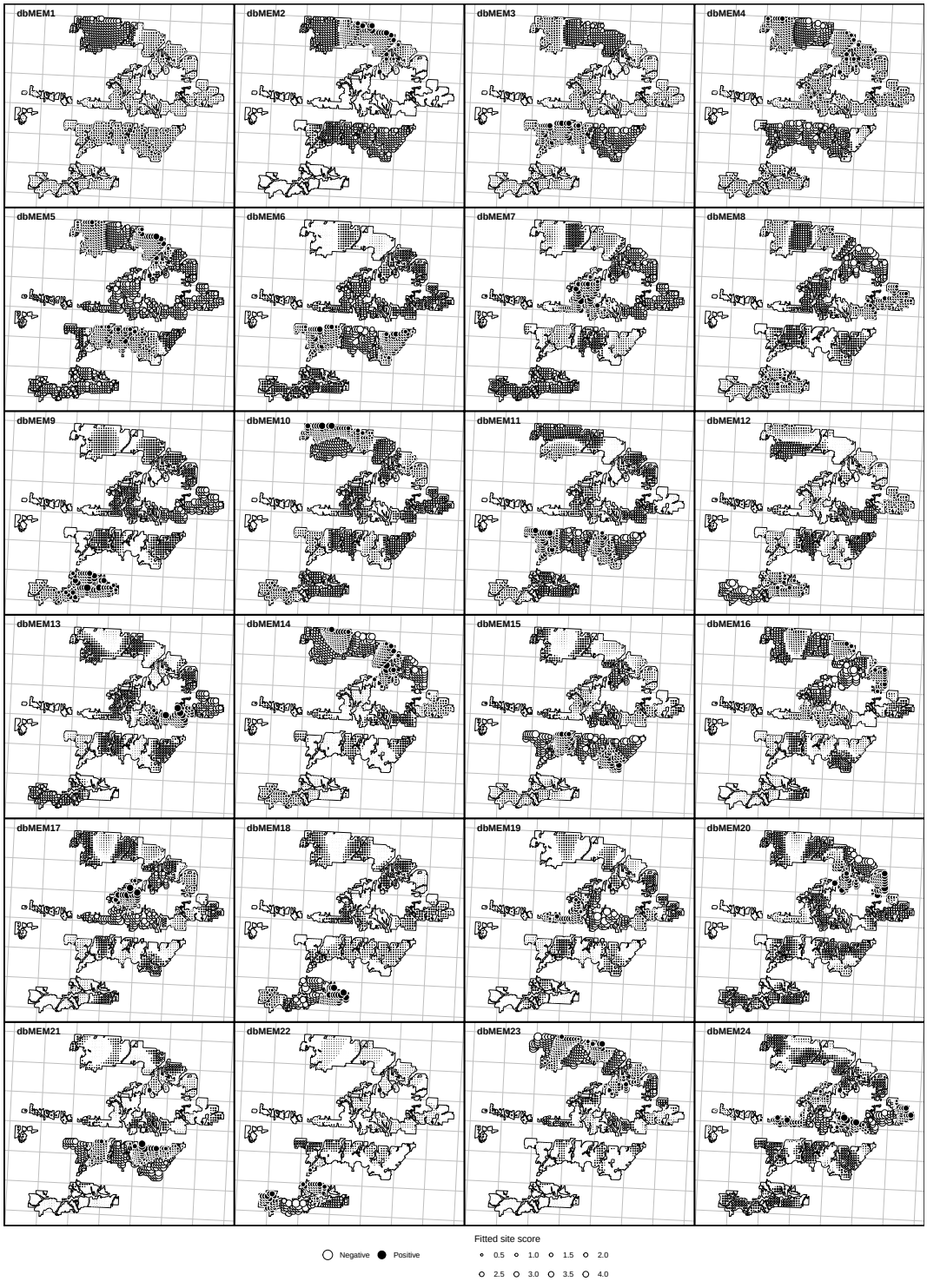

Figure B.2: Map of the 44 distance-based Moran's eigenvector map (dbMEM) variables retained following forward selection for the 3 ha cell size scenario. Points represent the fitted site scores. (*continued on next page*)

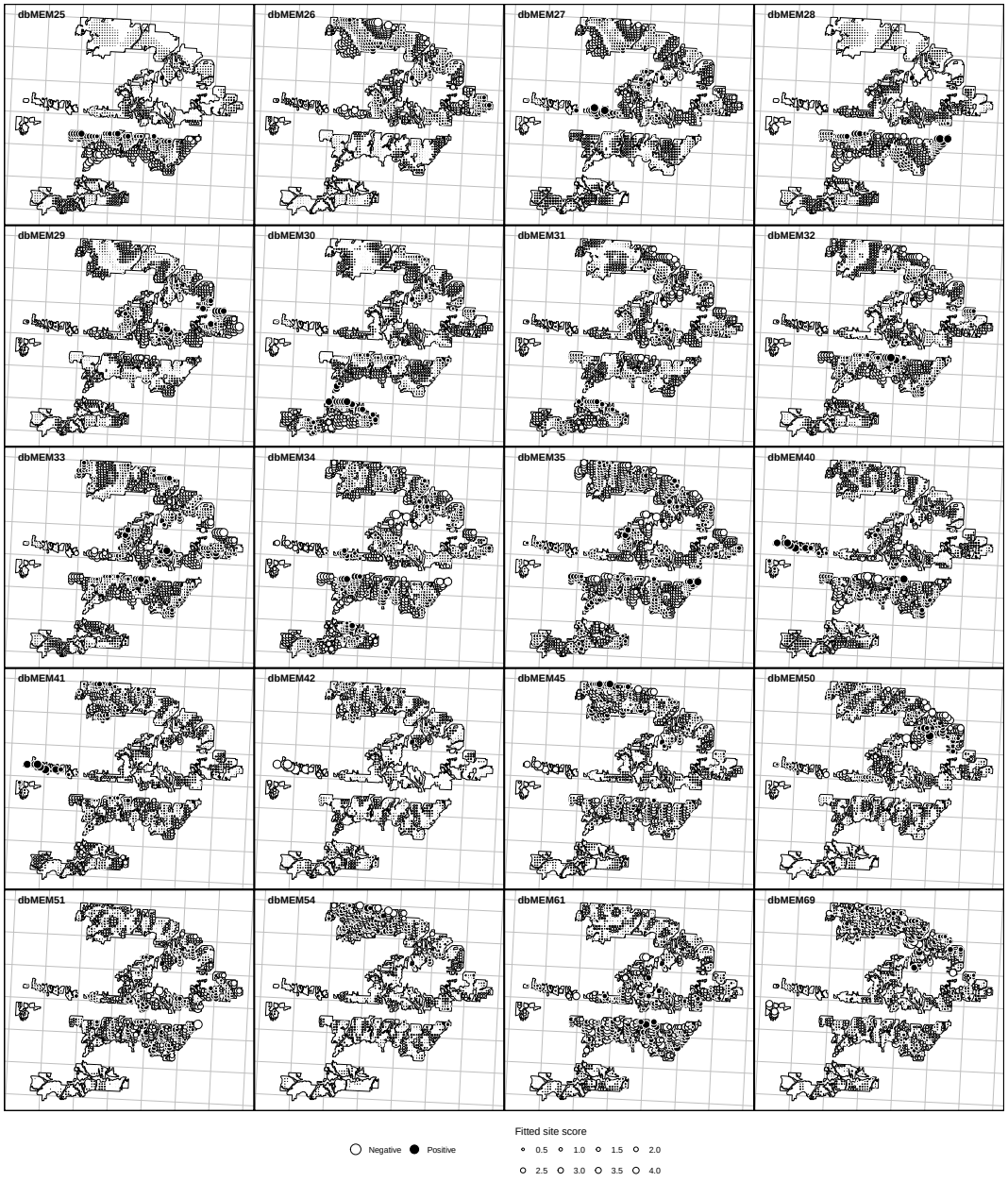

Figure B.2: Maps of the 44 dbMEM variables retained following forward selection for the 3 ha cell size scenario. Points represent the fitted site scores.

B.2 Supplementary tables

Table B.1: The explained variance attributed to spatial (D), spatially autocorrelated environment (D×E) and environmental (E) factors, as R^2_a values, following variance partitioning on dbRDAs. Significance was calculated from 999 permutation tests, note, significance of spatially autocorrelated environment cannot be assessed due to covariance. Significance levels: $p^{***} \leq 0.001$, $p^{**} \leq 0.01$, $p^{*} \leq 0.05$, $p^{ns} > 0.05$

Cell size (ha)	n	All	D	D×E	E
d_{BC}					
1	3785	0.225***	0.180***	0.039	0.0051***
3	1048	0.335***	0.258***	0.067	0.0095***
5	541	0.306***	0.216***	0.068	0.0210***
10	215	0.381***	0.268***	0.088	0.0241***
β_{sor}					
1	3785	0.166***	0.131***	0.030	0.0050***
3	1048	0.223***	0.173***	0.041	0.0090***
5	541	0.202***	0.146***	0.036	0.0188***
10	215	0.263***	0.193***	0.052	0.0177***
D'_{nn}					
1	3785	0.335***	0.252***	0.072	0.0098***
3	1048	0.504***	0.354***	0.129	0.0208***
5	541	0.489***	0.303***	0.145	0.0406***
10	215	0.594***	0.367***	0.185	0.0419***
D'_{pw}					
1	3785	0.026***	0.020***	0.005	0.0006***
3	1048	0.025***	0.018***	0.005	0.0009***
5	541	0.017***	0.010***	0.005	0.0010***
10	215	0.015***	0.009***	0.004	0.0007*

Appendix C

Do functional traits explain aggregation patterns of tropical canopy trees?

C.1 Supplementary figures

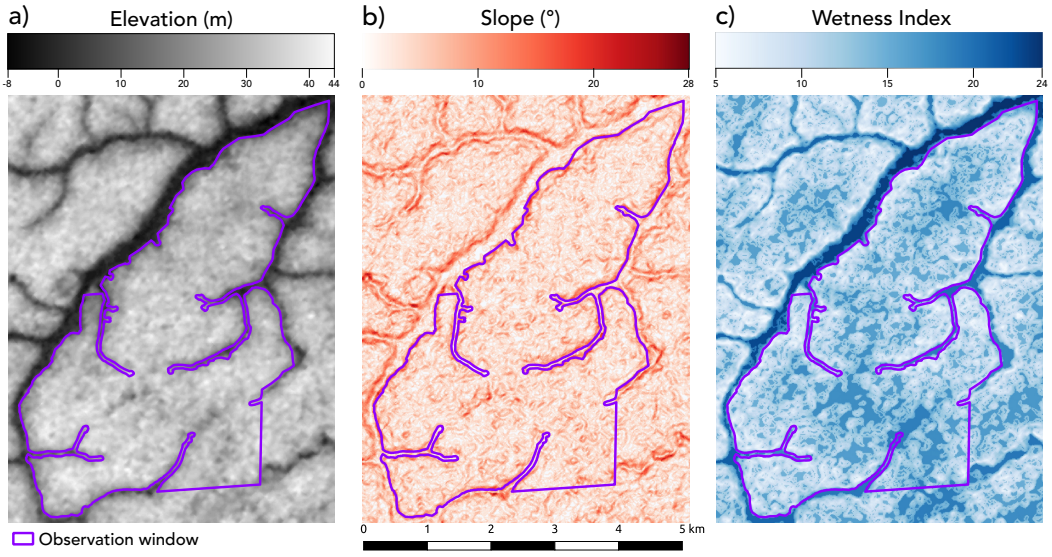

Figure C.1: Elevation (a), slope (b) and TWI (c) were derived from a Digital Elevation Model (DEM) with 12.5 m resolution (JAXA/METI, 2011) in order to determine habitat associations. Environmental variables displayed here are from the Caxiuanã National Forest (CX)

C.2 Supplementary tables

Table C.1: Trait values estimated via phylogenetic imputation. Trait values used in imputation were obtained from the TRY database (Kattge et al., 2011)

Family	Species	max DBH	Dispersal syndrome	N_{mass}	SLA	Dry seed mass	Wood density
Anacardiaceae	Anacardium giganteum	95	Animal	19	15.9	2704	0.456
Anacardiaceae	Anacardium parvifolium	111	Animal	24.3	15.6	2226	0.493
Anacardiaceae	Astronium graveolens	79	Animal	27.5	16.9	103	0.858
Anacardiaceae	Astronium lecointei	113	Wind	22.2	14.5	244	0.797
Anacardiaceae	Astronium obliquum	70	Wind	24.2	15.2	303	0.851
Apocynaceae	Aspidosperma excelsum	145	Wind	22.4	12	484	0.757
Apocynaceae	Aspidosperma spruceanum	104	Wind	16.7	9.3	656	0.757
Apocynaceae	Couma guianensis	64	Animal	17.4	12.3	162	0.477
Apocynaceae	Macoubea guianensis	83	Animal	18.8	17.7	479	0.428
Apocynaceae	Macoubea sprucei	126	Animal	15.9	16.1	479	0.438
Apocynaceae	Parahancornia fasciculata	67	Animal	17.4	11.6	469	0.478
Araliaceae	Schefflera morototoni	64	Animal	18.7	11.3	15	0.444
Bignoniaceae	Handroanthus impetiginosus	150	Wind	26.5	18.2	121	0.832
Bignoniaceae	Handroanthus incanus	123	Wind	31.7	19.4	163	0.902
Bignoniaceae	Handroanthus serratifolius	103	Wind	30.5	21.4	214	0.917
Bignoniaceae	Jacaranda copaia	86	Wind	26.9	15	134	0.368
Boraginaceae	Cordia goeldiana	103	Wind	22.9	23	118	0.492
Burseraceae	Protium decandrum	89	Animal	16.9	10.6	3408	0.529
Burseraceae	Protium pallidum	75	Animal	17.6	12.9	1386	0.523
Burseraceae	Tetragastris panamensis	86	Animal	15.5	11.4	328	0.691
Burseraceae	Trattinnickia rhoifolia	127	Animal	17.7	17.6	375	0.455
Caryocaraceae	Caryocar glabrum	129	Animal	20.8	14.3	8217	0.661
Caryocaraceae	Caryocar villosum	162	Animal	20.7	13.2	25971	0.734
Chrysobalanaceae	Parinari excelsa	88	Animal	18.4	10.4	5173	0.702
Combretaceae	Buchenavia huberi	170	Animal	21.4	18.6	1101	0.766
Combretaceae	Buchenavia parvifolia	159	Animal	22.8	29.4	1101	0.814
Combretaceae	Terminalia amazonia	95	Wind	16.4	15.5	136	0.665
Combretaceae	Terminalia argentea	128	Wind	17.1	14.3	952	0.759
Combretaceae	Terminalia oblonga	113	Wind	24.5	24.7	165	0.676
Euphorbiaceae	Glycydendron amazonicum	91	Animal	29.1	22.4	3828	0.672
Euphorbiaceae	Hevea brasiliensis	77	Auto	27.1	15.1	2630	0.504
Goupiaceae	Goupia glabra	117	Animal	17	13.6	333	0.742
Humiriaceae	Endopleura uchi	92	Animal	15.9	14.8	4369	0.793
Lauraceae	Aniba panurensis	105	Animal	21.7	12.4	1212	0.599
Lauraceae	Beilschmiedia brasiliensis	110	Animal	18.1	14.6	2379	0.59
Lauraceae	Caryodaphnopsis inaequalis	97	Animal	21.6	17.4	3118	0.583
Lauraceae	Licaria canella	68	Animal	22.7	12	1463	0.817
Lauraceae	Mezilaurus ita-uba	118	Animal	20.2	11.6	2379	0.748
Lauraceae	Mezilaurus lindaviana	102	Animal	20.5	15.6	2379	0.706
Lauraceae	Nectandra cissiflora	57	Animal	20.9	13.6	1031	0.581
Lauraceae	Ocotea aciphylla	84	Animal	15.7	11.3	825	0.522
Lauraceae	Ocotea canaliculata	97	Animal	23.4	12.7	949	0.477
Lauraceae	Ocotea guianensis	65	Animal	19.3	11	594	0.5
Lauraceae	Ocotea obovata	86	Animal	21.4	12.7	949	0.533
Lecythidaceae	Allantoma decandra	140	Wind	19	12.2	1894	0.564
Lecythidaceae	Bertholletia excelsa	201	Animal	24.9	11.9	6380	0.643
Lecythidaceae	Cariniana micrantha	201	Wind	20.9	16.6	929	0.585
Lecythidaceae	Couratari guianensis	130	Wind	21.9	13.2	281	0.576
Lecythidaceae	Couratari oblongifolia	100	Wind	23.1	13.5	407	0.57

Continued on next page

Family	Species	max DBH	Dispersal syndrome	N_{mass}	SLA	Dry seed mass	Wood density
Lecythidaceae	Eschweilera coriacea	91	Animal	20.3	10.2	319	0.724
Lecythidaceae	Eschweilera paniculata	73	Animal	21.9	12	2699	0.747
Lecythidaceae	Eschweilera pedicellata	67	Animal	21.6	12.6	1794	0.833
Lecythidaceae	Lecythis lurida	86	Animal	21.8	9.2	2524	0.842
Lecythidaceae	Lecythis pisonis	127	Animal	20.6	14.5	2009	0.834
Lecythidaceae	Lecythis poiteaui	70	Animal	27.4	12.5	2524	0.802
Leguminosae	Abarema jupunba	89	Animal	27.8	14.1	329	0.556
Leguminosae	Acosmium nitens	97	Wind	24	10	128	0.789
Leguminosae	Apuleia leiocarpa	156	Wind	24.7	32.9	607	0.802
Leguminosae	Bowdichia nitida	77	Auto	21.3	8.4	44	0.785
Leguminosae	Cedrelinga cateniformis	207	Wind	37.8	18.1	391	0.485
Leguminosae	Copaifera langsdorffii	115	Animal	22.7	14.5	1072	0.581
Leguminosae	Copaifera martii	89	Animal	23	13.1	1072	0.59
Leguminosae	Copaifera multijuga	91	Animal	26.3	13.1	1072	0.544
Leguminosae	Copaifera officinalis	68	Animal	23	13.1	1072	0.645
Leguminosae	Dialium guianense	67	Animal	26.8	19.1	383	0.854
Leguminosae	Dinizia excelsa	220	Auto	19.8	17.3	3325	0.94
Leguminosae	Diplotropis purpurea	65	Wind	26.7	12.4	330	0.732
Leguminosae	Diplotropis racemosa	89	Wind	27.4	12	406	0.62
Leguminosae	Dipteryx magnifica	95	Animal	19.8	15.1	4796	0.902
Leguminosae	Dipteryx odorata	120	Animal	21.9	14.7	4323	0.931
Leguminosae	Enterolobium schomburgkii	113	Animal	28.2	10.8	70	0.673
Leguminosae	Hymenaea courbaril	125	Animal	18.9	9.6	3234	0.787
Leguminosae	Hymenaea oblongifolia	93	Animal	19.9	13.5	1944	0.739
Leguminosae	Hymenaea parvifolia	100	Animal	17.6	11.5	1945	0.862
Leguminosae	Hymenolobium elatum	163	Wind	24.7	16.4	1672	0.666
Leguminosae	Hymenolobium excelsum	124	Wind	24.3	16.4	1672	0.651
Leguminosae	Hymenolobium flavum	112	Wind	27.8	16.4	1672	0.676
Leguminosae	Hymenolobium petraeum	127	Wind	24.4	16.4	1672	0.663
Leguminosae	Hymenolobium sericeum	91	Wind	24.2	16.4	1672	0.682
Leguminosae	Marmaroxylon racemosum	77	Animal	33.3	17.3	2843	0.836
Leguminosae	Martiodendron elatum	108	Wind	24.5	23.3	717	0.826
Leguminosae	Ormosia coarctata	95	Animal	20.2	12.9	1305	0.589
Leguminosae	Ormosia coccinea	128	Animal	17.6	11.6	660	0.632
Leguminosae	Parkia nitida	100	Animal	21.9	11.3	565	0.373
Leguminosae	Parkia pendula	162	Animal	21.5	17.4	292	0.481
Leguminosae	Parkia ulei	80	Animal	30.4	7.7	470	0.426
Leguminosae	Peltogyne lecointei	88	Wind	16.9	10.5	992	0.736
Leguminosae	Piptadenia gonoacantha	102	Wind	35.7	14.6	270	0.697
Leguminosae	Pseudopiptadenia psilostachya	111	Wind	28.9	9.4	470	0.517
Leguminosae	Pseudopiptadenia suaveolens	118	Wind	30.7	8.9	470	0.629
Leguminosae	Sclerolobium melanocarpum	95	Wind	20.7	11.2	1114	0.621
Leguminosae	Swartzia polyphylla	127	Animal	25.9	14.5	29062	0.724
Leguminosae	Tachigali melinonii	78	Wind	33.1	14.2	951	0.598
Leguminosae	Tachigali myrmecophila	80	Wind	33.9	11.8	951	0.579
Leguminosae	Tachigali paniculata	80	Wind	26.8	12.6	951	0.562
Leguminosae	Vatairea guianensis	115	Auto	18.1	12.5	23139	0.675
Leguminosae	Vatairea paraensis	100	Wind	18.2	12.4	7868	0.691
Leguminosae	Vouacapoua americana	76	Animal	26	14.2	32194	0.767
Malvaceae	Ceiba pentandra	189	Wind	21.2	13.4	133	0.307
Malvaceae	Lueheopsis rosea	67	Wind	17.3	11.1	1182	0.592
Malvaceae	Pterygota alata	105	Wind	22.7	13.2	666	0.547

Continued on next page

Family	Species	max DBH	Dispersal syndrome	N_{mass}	SLA	Dry seed mass	Wood density
Meliaceae	Carapa guianensis	92	Animal	17.3	14.6	15567	0.518
Moraceae	Bagassa guianensis	145	Animal	25.2	18.7	1234	0.714
Moraceae	Brosimum guianense	121	Animal	21.7	15.8	1077	0.815
Moraceae	Brosimum parinarioides	89	Animal	15.6	14.1	1170	0.617
Moraceae	Brosimum rubescens	116	Animal	18.6	13.4	513	0.801
Moraceae	Castilla ulei	98	Animal	24.5	29.2	691	0.412
Moraceae	Clarisia racemosa	93	Animal	23.8	15.7	1946	0.567
Moraceae	Pseudolmedia laevis	83	Animal	19.2	13.8	455	0.584
Myristicaceae	Virola albidiflora	90	Animal	21.2	13.7	1141	0.408
Myristicaceae	Virola elongata	96	Animal	24.3	14.5	347	0.54
Myristicaceae	Virola loretensis	96	Animal	21.2	13.7	1141	0.503
Myristicaceae	Virola sebifera	85	Animal	23.9	13.8	728	0.474
Olacaceae	Minquartia guianensis	95	Animal	20.7	13.4	2324	0.754
Proteaceae	Euplassa pinnata	108	Animal	13	13.5	177	0.534
Rubiaceae	Calycophyllum megistocaulum	119	Wind	28.6	15.6	866	0.691
Rubiaceae	Capirona decorticans	116	Wind	31.9	12.1	866	0.606
Rutaceae	Zanthoxylum juniperinum	86	Animal	22.6	14.6	121	0.486
Salicaceae	Laetia procera	70	Animal	24.7	14.4	164	0.628
Sapotaceae	Manilkara bidentata	92	Animal	15	7.4	835	0.857
Sapotaceae	Manilkara huberi	127	Animal	14	6.1	680	0.842
Sapotaceae	Pouteria caimito	95	Animal	19.5	10.8	3450	0.805
Sapotaceae	Pouteria caimito	95	Animal	19.5	10.8	3450	0.805
Sapotaceae	Pouteria caimito	95	Animal	19.5	10.8	3450	0.805
Sapotaceae	Pouteria caimito	95	Animal	19.5	10.8	3450	0.805
Sapotaceae	Pouteria elegans	64	Animal	17.8	11.7	1785	0.71
Sapotaceae	Pouteria guianensis	94	Animal	17.6	8.7	2648	0.866
Sapotaceae	Sarcaulus brasiliensis	111	Animal	17.8	13.5	8348	0.659
Simaroubaceae	Simarouba amara	92	Animal	17.3	14.8	693	0.392
Vochysiaceae	Qualea albiflora	99	Wind	17.3	11.5	647	0.562
Vochysiaceae	Qualea brevipedicellata	124	Wind	16.4	10.4	635	0.663
Vochysiaceae	Qualea paraensis	95	Wind	17.4	10.6	635	0.634
Vochysiaceae	Vochysia densiflora	102	Wind	16.2	13.6	222	0.378
Vochysiaceae	Vochysia divergens	76	Wind	16.2	13.6	222	0.51
Vochysiaceae	Vochysia obscura	70	Wind	16.2	13.6	222	0.467
Vochysiaceae	Vochysia vismiifolia	76	Wind	16.2	13.6	222	0.467

Table C.2: Wood density values specific to species at the Vale do Jari site (VJ), obtained from the concessionaire

Family	Species	Wood density
Anacardiaceae	Anacardium giganteum	0.465
Anacardiaceae	Astronium obliquum	0.844
Apocynaceae	Couma guianensis	0.499
Apocynaceae	Macoubea guianensis	0.427
Apocynaceae	Parahancornia fasciculata	0.488
Bignoniaceae	Handroanthus impetiginosus	0.614
Boraginaceae	Cordia goeldiana	0.33
Burseraceae	Protium pallidum	0.463
Burseraceae	Tetragastris panamensis	0.773
Burseraceae	Trattinnickia rhoifolia	0.453
Caryocaraceae	Caryocar glabrum	0.597

Continued on next page

Family	Species	Wood density
Caryocaraceae	Caryocar villosum	0.642
Chrysobalanaceae	Parinari excelsa	0.71
Euphorbiaceae	Glycydendron amazonicum	0.686
Goupiaceae	Goupia glabra	0.713
Lauraceae	Licaria canella	0.679
Lauraceae	Mezilaurus ita-uba	0.823
Lauraceae	Mezilaurus lindaviana	0.733
Lauraceae	Nectandra cissiflora	0.488
Lauraceae	Ocotea aciphylla	0.643
Lauraceae	Ocotea guianensis	0.467
Lecythidaceae	Bertholletia excelsa	0.635
Lecythidaceae	Couratari guianensis	0.781
Lecythidaceae	Couratari oblongifolia	0.752
Lecythidaceae	Lecythis lurida	0.833
Lecythidaceae	Lecythis pisonis	0.809
Lecythidaceae	Lecythis poiteaui	0.81
Leguminosae	Acosmium nitens	0.819
Leguminosae	Apuleia leiocarpa	0.678
Leguminosae	Bowdichia nitida	0.567
Leguminosae	Cedrelinga cateniformis	0.521
Leguminosae	Copaifera martii	0.573
Leguminosae	Copaifera officinalis	0.744
Leguminosae	Dialium guianense	0.921
Leguminosae	Dinizia excelsa	0.774
Leguminosae	Diplotropis purpurea	0.573
Leguminosae	Diplotropis racemosa	0.465
Leguminosae	Dipteryx magnifica	0.917
Leguminosae	Dipteryx odorata	0.974
Leguminosae	Enterolobium schomburgkii	0.622
Leguminosae	Hymenaea courbaril	0.78
Leguminosae	Hymenaea parvifolia	0.769
Leguminosae	Hymenolobium excelsum	0.627
Leguminosae	Hymenolobium flavum	0.661
Leguminosae	Hymenolobium petraeum	0.7
Leguminosae	Hymenolobium sericeum	0.759
Leguminosae	Marmaroxylon racemosum	0.772
Leguminosae	Ormosia coccinea	0.783
Leguminosae	Parkia nitida	0.324
Leguminosae	Parkia pendula	0.572
Leguminosae	Parkia ulei	0.33
Leguminosae	Peltogyne lecointei	0.619
Leguminosae	Pseudopiptadenia psilostachya	0.416
Leguminosae	Tachigali myrmecophila	0.484
Leguminosae	Vouacapoua americana	0.757
Malvaceae	Lueheopsis rosea	0.602
Malvaceae	Pterygota alata	0.747
Meliaceae	Carapa guianensis	0.576
Moraceae	Brosimum guianense	0.911
Moraceae	Brosimum parinarioides	0.685
Moraceae	Brosimum rubescens	0.636
Moraceae	Clarisia racemosa	0.707
Myristicaceae	Virola sebifera	0.675
Olacaceae	Minquartia guianensis	0.895

Continued on next page

Family	Species	Wood density
Rubiaceae	Capirona decorticans	0.819
Salicaceae	Laetia procera	0.657
Sapotaceae	Manilkara huberi	0.562
Sapotaceae	Pouteria caimito	0.709
Sapotaceae	Pouteria caimito	0.709
Sapotaceae	Pouteria caimito	0.686
Sapotaceae	Pouteria caimito	0.686
Sapotaceae	Pouteria elegans	0.874
Vochysiaceae	Qualea albiflora	0.399
Vochysiaceae	Qualea paraensis	0.448

Table C.3: **Species habitat associations and dispersal limitation parameters per species and site:** Species aggregation patterns were categorised describing their habitat associations and dispersal limitation via a decision tree, implementing a series of increasingly complex spatial point pattern models (Table 4.1). Subsequently, parameters describing elevational, TWI and slope associations and dispersal limitation as cluster size (α) and cluster intensity (σ^2) were extracted.

Species	Site	Category	Elevation	TWI	Slope	α	σ^2
Abarema jupunba	VJ	C3	–	–	–	123.9	3.57
Acosmium nitens	VJ	C4	-0.015	-0.149	-0.061	322.1	3.87
Allantoma decandra	NP	C2	0.138	–	0.050	–	–
Allantoma decandra	RO	C4	-0.019	0.017	–	66.8	3.71
Anacardium giganteum	VJ	C4	–	0.021	0.062	49.3	3.85
Anacardium parvifolium	CX	C2	-0.018	-0.047	-0.034	–	–
Aniba panurensis	NP	C4	–	-0.122	-0.04	109.6	3.93
Apuleia leiocarpa	NP	C4	-0.062	-0.138	–	109.3	4.10
Apuleia leiocarpa	RO	C4	0.024	-0.024	0.019	521.9	2.64
Aspidosperma excelsum	ST	C4	-0.005	-0.028	–	541.8	1.72
Aspidosperma spruceanum	ST	C4	-0.009	–	0.066	1226.3	1.77
Astronium graveolens	VJ	C4	-0.012	–	–	161.9	3.13
Astronium lecointei	RO	C4	0.018	-0.007	-0.019	60.5	3.24
Astronium lecointei	ST	C4	0.006	-0.043	-0.056	178.6	2.39
Astronium lecointei	CX	C4	0.041	–	–	56.1	3.88
Astronium obliquum	VJ	C4	-0.01	–	–	59.8	3.85
Bagassa guianensis	RO	C4	-0.017	-0.092	–	181.0	2.85
Beilschmiedia brasiliensis	NP	C4	-0.014	-0.132	-0.038	103.6	3.30
Bertholletia excelsa	RO	C4	0.012	-0.034	-0.025	63.0	3.22
Bowdichia nitida	ST	C3	–	–	–	153.9	4.34
Bowdichia nitida	VJ	C4	-0.009	-0.028	-0.022	52.5	3.81
Bowdichia nitida	CX	C1	–	–	–	–	–
Brosimum guianense	NP	C4	0.035	-0.069	–	109.9	4.23
Brosimum parinarioides	VJ	C4	-0.008	0.037	0.020	59.3	3.77
Brosimum rubescens	NP	C2	0.069	-0.082	-0.057	–	–
Brosimum rubescens	RO	C4	-0.033	-0.104	-0.041	101.8	3.91
Brosimum rubescens	ST	C4	-0.021	–	–	107.5	3.15
Buchenavia huberi	RO	C4	0.015	-0.038	-0.042	198.8	3.42
Buchenavia parvifolia	ST	C4	-0.013	-0.034	-0.088	147.7	2.28
Buchenavia parvifolia	VJ	C4	-0.011	-0.045	–	89.2	3.53
Calycophyllum megistocaulum	ST	C4	–	-0.165	-0.089	97.3	2.69
Capirona decorticans	CX	C3	–	–	–	56.1	3.79

Continued on next page

Species	Site	Category	Elevation	TWI	Slope	α	σ^2
Carapa guianensis	NP	C4	–	-0.121	–	72.1	3.79
Carapa guianensis	VJ	C4	0.010	0.132	0.114	202.5	4.43
Carapa guianensis	CX	C4	0.162	0.109	0.042	358.9	2.08
Cariniana micrantha	RO	C4	0.002	-0.032	-0.015	47.3	3.62
Cariniana micrantha	ST	C4	-0.035	-0.054	-0.103	457.0	2.17
Cariniana micrantha	CX	C4	0.043	-0.104	–	110.9	2.39
Caryocar glabrum	NP	C4	–	-0.168	-0.055	121.9	3.92
Caryocar glabrum	RO	C4	-0.004	0.049	0.009	77.8	3.89
Caryocar glabrum	ST	C4	-0.02	–	–	76.2	3.87
Caryocar glabrum	VJ	C4	-0.005	-0.02	0.034	52.1	3.69
Caryocar glabrum	CX	C4	–	-0.09	-0.067	59.4	3.80
Caryocar villosum	RO	C4	-0.012	0.021	0.011	81.5	4.01
Caryocar villosum	ST	C4	0.006	-0.044	–	172.2	2.36
Caryocar villosum	VJ	C4	0.009	–	0.022	234.7	2.53
Caryocar villosum	CX	C4	-0.022	-0.051	–	92.7	3.45
Caryodaphnopsis inaequalis	NP	C4	–	-0.172	–	58.8	3.81
Castilla ulei	RO	C4	–	-0.041	-0.017	75.9	3.26
Cedrelinga cateniformis	NP	C4	0.071	-0.093	–	72.1	3.49
Cedrelinga cateniformis	RO	C4	0.012	0.061	–	195.2	3.47
Cedrelinga cateniformis	VJ	C4	–	0.228	0.102	380.1	3.30
Ceiba pentandra	NP	C4	0.076	0.068	–	225.2	3.36
Ceiba pentandra	CX	C4	0.077	–	0.109	165.7	3.27
Clarisia racemosa	NP	C2	-0.143	-0.32	-0.113	–	–
Clarisia racemosa	RO	C4	-0.003	0.008	-0.031	70.5	2.86
Clarisia racemosa	ST	C4	-0.026	-0.072	–	969.6	2.88
Clarisia racemosa	CX	C2	-0.063	-0.062	–	–	–
Copaifera langsdorffii	CX	C2	0.044	0.047	–	–	–
Copaifera martii	VJ	C4	0.037	–	-0.064	125.4	3.69
Copaifera multijuga	RO	C4	-0.015	0.007	-0.013	60.4	2.84
Copaifera officinalis	VJ	C2	0.034	0.102	–	–	–
Cordia goeldiana	RO	C4	-0.019	-0.153	-0.059	80.1	3.52
Cordia goeldiana	CX	C2	0.232	0.350	0.139	–	–
Couma guianensis	VJ	C4	-0.01	-0.042	-0.049	222.9	2.57
Couratari guianensis	RO	C4	0.003	-0.04	-0.037	53.2	3.79
Couratari guianensis	ST	C4	–	-0.087	–	281.5	1.64
Couratari guianensis	VJ	C4	0.007	0.106	0.087	194.7	2.68
Couratari guianensis	CX	C4	0.098	0.029	–	41.5	3.62
Couratari oblongifolia	VJ	C4	0.022	0.120	0.034	229.0	2.69
Dialium guianense	NP	C4	–	-0.061	–	78.1	3.85
Dialium guianense	VJ	C4	-0.016	–	0.071	77.0	3.20
Dinizia excelsa	RO	C4	0.022	0.025	0.034	151.6	2.37
Dinizia excelsa	VJ	C4	–	-0.065	-0.033	364.4	1.83
Dinizia excelsa	CX	C4	0.033	-0.094	–	61.8	3.74
Diplotropis purpurea	VJ	C4	-0.012	-0.056	–	60.0	3.81
Diplotropis racemosa	ST	C4	–	0.091	–	94.4	3.62
Diplotropis racemosa	VJ	C4	–	0.069	–	95.1	4.11
Diplotropis racemosa	CX	C2	–	–	–	–	–
Dipteryx magnifica	VJ	C4	0.007	0.015	0.013	79.7	3.82
Dipteryx odorata	NP	C4	–	-0.085	-0.04	121.5	3.74
Dipteryx odorata	RO	C4	0.003	-0.037	-0.022	108.2	4.09
Dipteryx odorata	ST	C4	0.004	0.070	0.051	63.0	2.48
Dipteryx odorata	VJ	C4	0.005	0.034	0.024	56.5	3.78

Continued on next page

Species	Site	Category	Elevation	TWI	Slope	α	σ^2
Dipteryx odorata	CX	C4	-0.021	-0.047	-0.107	369.6	2.04
Endopleura uchi	RO	C4	0.026	0.025	0.030	308.8	2.50
Endopleura uchi	ST	C2	0.008	0.018	-0.025	–	–
Endopleura uchi	VJ	C4	0.020	0.059	–	303.1	2.75
Endopleura uchi	CX	C2	-0.06	-0.213	-0.107	–	–
Enterolobium schomburgkii	RO	C4	-0.013	-0.044	-0.021	67.3	4.00
Enterolobium schomburgkii	ST	C4	-0.007	-0.037	-0.044	69.8	4.03
Enterolobium schomburgkii	VJ	C4	-0.005	–	0.034	47.1	3.74
Enterolobium schomburgkii	CX	C4	0.024	–	–	60.8	3.71
Eschweilera coriacea	NP	C2	0.044	-0.048	–	–	–
Eschweilera coriacea	VJ	C4	0.019	0.153	0.072	1090.4	3.81
Eschweilera coriacea	CX	C4	-0.013	-0.163	–	91.7	3.20
Eschweilera paniculata	VJ	C4	0.028	0.073	–	1504.7	2.80
Eschweilera pedicellata	VJ	C4	0.014	–	–	473.2	2.47
Euplassa pinnata	CX	C4	-0.034	-0.166	–	132.2	2.94
Glycydendron amazonicum	CX	C4	0.027	-0.154	-0.042	242.4	1.02
Goupia glabra	RO	C4	0.002	–	–	107.9	3.32
Goupia glabra	ST	C3	–	–	–	61.1	3.54
Goupia glabra	VJ	C4	-0.016	-0.027	-0.018	56.0	3.66
Goupia glabra	CX	C4	-0.031	-0.131	-0.073	64.7	3.65
Handroanthus impetiginosus	RO	C4	-0.005	–	–	137.4	3.29
Handroanthus impetiginosus	ST	C4	0.015	–	0.112	561.8	3.06
Handroanthus incanus	NP	C2	-0.066	–	–	–	–
Handroanthus incanus	RO	C4	0.037	-0.028	–	389.7	4.66
Handroanthus serratifolius	ST	C4	0.033	0.110	0.131	317.6	4.10
Handroanthus serratifolius	VJ	C2	0.020	–	–	–	–
Hevea brasiliensis	NP	C2	-0.036	-0.167	–	–	–
Hymenaea courbaril	ST	C4	-0.007	-0.034	-0.025	45.5	3.72
Hymenaea courbaril	VJ	C4	0.015	0.050	0.017	72.6	3.05
Hymenaea courbaril	CX	C2	0.084	0.110	0.048	–	–
Hymenaea oblongifolia	NP	C4	–	-0.034	0.055	89.0	4.02
Hymenaea parvifolia	ST	C4	-0.015	-0.017	-0.034	49.4	3.41
Hymenolobium elatum	CX	C4	-0.039	-0.051	-0.101	79.2	3.81
Hymenolobium excelsum	ST	C2	-0.011	–	-0.026	–	–
Hymenolobium excelsum	VJ	C4	–	0.051	0.023	78.1	4.01
Hymenolobium flavum	VJ	C4	0.008	0.063	0.031	109.1	2.76
Hymenolobium petraeum	VJ	C3	–	–	–	151.7	4.27
Hymenolobium sericeum	VJ	C4	–	0.035	–	105.1	4.14
Jacaranda copaia	ST	C4	-0.009	–	–	82.8	3.77
Jacaranda copaia	VJ	C4	-0.018	-0.034	0.038	68.5	3.49
Laetia procera	VJ	C4	–	0.042	0.060	167.9	2.34
Lecythis lurida	CX	C4	0.052	0.037	–	52.4	3.49
Lecythis pisonis	ST	C4	0.006	–	0.040	64.7	3.40
Lecythis pisonis	VJ	C4	-0.008	0.060	0.075	129.3	2.55
Lecythis poiteaui	VJ	C4	0.031	0.140	–	593.4	2.12
Licaria canella	VJ	C4	-0.015	–	–	231.8	3.23
Lueheopsis rosea	VJ	C4	-0.01	–	–	181.8	2.57
Macoubea guianensis	VJ	C4	-0.007	–	–	107.5	3.77
Macoubea sprucei	NP	C1	–	–	–	–	–
Manilkara bidentata	NP	C2	–	-0.09	–	–	–
Manilkara bidentata	ST	C4	-0.007	-0.188	-0.166	1594.6	3.61
Manilkara huberi	RO	C4	0.011	-0.048	–	132.3	3.40

Continued on next page

Species	Site	Category	Elevation	TWI	Slope	α	σ^2
Manilkara huberi	ST	C4	0.013	-0.028	-0.045	49.6	3.52
Manilkara huberi	VJ	C4	0.025	0.058	-0.014	90.7	2.62
Manilkara huberi	CX	C4	–	–	-0.045	36.1	3.50
Marmaroxylon racemosum	CX	C2	–	–	-0.053	–	–
Martiodendron elatum	RO	C4	–	-0.035	–	82.2	3.98
Mezilaurus ita-uba	RO	C4	0.024	0.076	–	227.3	3.28
Mezilaurus ita-uba	ST	C4	-0.008	-0.084	-0.119	802.5	1.35
Mezilaurus ita-uba	VJ	C4	-0.012	-0.053	–	259.7	1.98
Mezilaurus ita-uba	CX	C4	–	-0.059	–	43.2	3.60
Mezilaurus lindaviana	VJ	C4	-0.022	-0.067	–	151.3	1.91
Minquartia guianensis	RO	C4	0.005	-0.102	-0.033	64.3	3.76
Minquartia guianensis	ST	C3	–	–	–	130.3	2.76
Minquartia guianensis	VJ	C4	-0.008	–	0.038	48.9	2.62
Nectandra cissiflora	VJ	C3	–	–	–	124.0	4000
Ocotea aciphylla	NP	C4	-0.054	-0.134	–	157.8	4.01
Ocotea canaliculata	ST	C4	-0.01	-0.045	–	276.9	2.32
Ocotea guianensis	VJ	C4	-0.012	–	–	193.4	3.39
Ocotea obovata	NP	C4	–	-0.065	–	78.7	4.07
Ormosia coarctata	ST	C2	–	–	–	–	–
Ormosia coccinea	NP	C2	0.024	-0.053	–	–	–
Parahancornia fasciculata	VJ	C2	0.013	–	–	–	–
Parinari excelsa	VJ	C4	0.012	0.059	–	92.7	3.55
Parkia nitida	NP	C4	0.085	0.067	0.058	95.2	3.38
Parkia nitida	VJ	C4	-0.009	-0.019	–	80.7	3.93
Parkia pendula	RO	C4	-0.004	-0.077	-0.039	77.2	4.07
Parkia pendula	ST	C4	-0.005	-0.044	–	70.8	3.51
Parkia pendula	VJ	C2	-0.012	-0.017	0.025	–	–
Parkia ulei	VJ	C3	–	–	–	64.2	3.81
Peltogyne lecointei	RO	C4	0.028	0.030	-0.008	55.6	3.76
Peltogyne lecointei	CX	C4	-0.041	–	0.074	70.4	3.56
Piptadenia gonoacantha	VJ	C4	0.020	0.086	–	67.8	2.93
Pouteria caimito	NP	C4	0.068	-0.049	–	47.6	3.78
Pouteria elegans	VJ	C4	0.024	0.107	–	138.5	4.27
Pouteria guianensis	RO	C4	0.013	-0.065	-0.037	358.5	1.36
Pouteria guianensis	CX	C4	-0.042	-0.198	–	113.8	2.61
Protium decandrum	VJ	C2	-0.025	–	0.062	–	–
Protium pallidum	VJ	C4	0.019	–	–	337.7	3.29
Pseudolmedia laevis	RO	C4	–	-0.073	-0.066	140.4	2.74
Pseudopiptadenia psilostachya	ST	C4	0.007	-0.065	-0.055	69.7	2.40
Pseudopiptadenia suaveolens	ST	C4	0.030	–	-0.043	374.3	1.49
Pterygota alata	ST	C4	-0.036	-0.03	-0.043	1484.2	1.85
Qualea albiflora	VJ	C4	–	-0.026	-0.038	77.3	3.34
Qualea brevipedicellata	CX	C4	-0.044	-0.055	-0.077	120.7	3.41
Qualea paraensis	NP	C4	0.042	–	–	57.5	3.55
Qualea paraensis	VJ	C4	-0.016	-0.038	-0.016	31.9	2.75
Qualea paraensis	CX	C4	-0.035	-0.039	–	87.4	2.79
Sarcaulus brasiliensis	CX	C4	–	-0.085	-0.093	55.2	3.07
Schefflera morototoni	VJ	C4	0.012	0.037	–	87.6	3.76
Sclerolobium melanocarpum	VJ	C4	0.011	-0.049	-0.117	1538.6	1.71
Simarouba amara	NP	C3	–	–	–	92.0	4.06
Simarouba amara	RO	C4	0.005	0.013	–	103.6	3.78
Simarouba amara	VJ	C4	0.023	0.120	0.068	1720.6	2.68

Continued on next page

Species	Site	Category	Elevation	TWI	Slope	α	σ^2
Simarouba amara	CX	C2	0.027	0.081	–	–	–
Swartzia polyphylla	VJ	C3	–	–	–	47.9	3.59
Tachigali melinonii	VJ	C4	0.005	–	-0.029	80.2	2.82
Tachigali myrmecophila	VJ	C4	0.015	0.046	–	47.7	2.34
Tachigali paniculata	VJ	C4	-0.009	-0.016	0.021	122.8	1.97
Terminalia amazonia	VJ	C4	–	-0.023	–	66.3	3.49
Terminalia argentea	VJ	C4	-0.02	-0.066	–	134.1	3.37
Terminalia oblonga	NP	C4	0.056	–	0.036	88.6	3.93
Tetragastris panamensis	VJ	C4	–	–	0.070	342.5	2.90
Tetragastris panamensis	CX	C4	0.244	0.297	0.140	596.8	1.76
Trattinnickia rhoifolia	VJ	C4	-0.021	-0.023	0.041	74.6	3.41
Vatairea guianensis	NP	C4	0.038	–	–	89.2	3.93
Vatairea paraensis	ST	C4	-0.014	–	-0.081	604.0	1.92
Virola albidiflora	NP	C3	–	–	–	103.4	3.82
Virola elongata	NP	C4	-0.045	0.056	–	41.7	3.51
Virola loretensis	NP	C4	-0.025	-0.121	-0.022	65.7	3.60
Virola sebifera	NP	C4	-0.017	–	–	209.1	2.01
Vochysia densiflora	NP	C4	0.087	–	0.029	105.7	2.60
Vochysia divergens	VJ	C4	-0.016	-0.08	-0.084	801.0	2.13
Vochysia obscura	VJ	C4	-0.047	-0.114	-0.088	229.8	3.13
Vochysia vismiifolia	VJ	C4	-0.017	-0.05	-0.024	197.7	2.70
Vouacapoua americana	VJ	C4	0.031	0.084	-0.008	310.5	3.20
Vouacapoua americana	CX	C4	0.077	–	0.014	90.3	2.23
Zanthoxylum juniperinum	NP	C4	–	-0.085	-0.037	147.6	4.02

Table C.4: **Results from multivariate linear models spatial parameters predicted by species functional traits:** Following backwards stepwise selection via AIC, only models for cluster intensity (σ^2), Slope and TWI retained functional traits. Although retained, neither log(Dry seed mass), log(SLA) or N_{mass} were significant for (σ^2), slope and TWI, respectively. The numbers in parenthesis below the effect size represent the standard error.

	σ^2	Slope	TWI
log(Dry seed mass)	−0.065		
	(0.037)		
log(SLA)		0.030	
		(0.020)	
N_{mass}			0.003
			(0.002)
Observations	185	115	154
R^2	0.016	0.019	0.017
Adjusted R^2	0.011	0.011	0.010
Residual Std. Error	0.727 (df = 183)	0.061 (df = 113)	0.092 (df = 152)
F Statistic	3.041* (df = 1; 183)	2.220 (df = 1; 113)	2.618 (df = 1; 152)

Appendix D

Subtractive heterogenisation

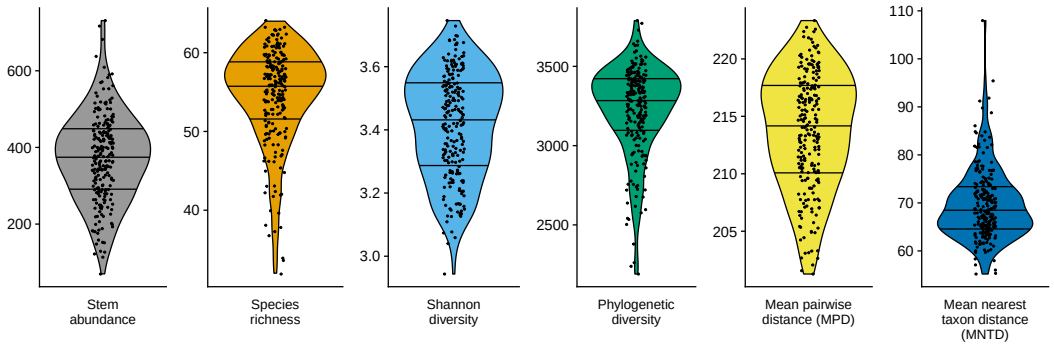

Figure D.1: Distribution of various taxonomic and phylogenetic diversity indices in Jamari National Forest

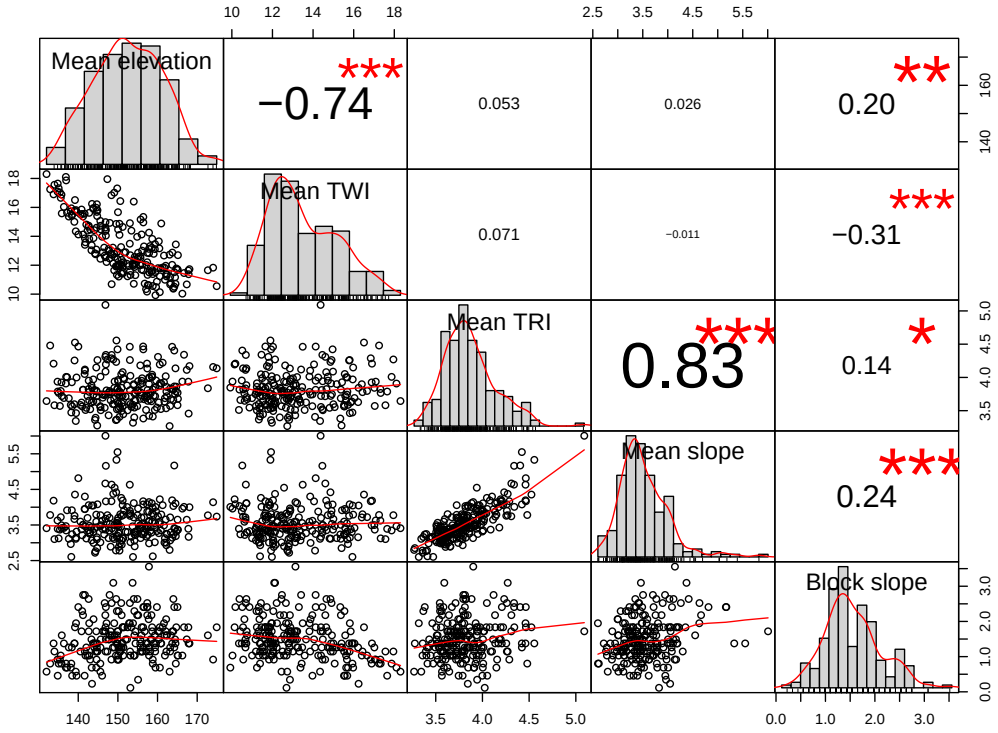

Figure D.2: Correlation of environmental variables at in Jamari National Forest

Appendix E

Forest recovery with logging intensity

E.1 Study site

The study site is based in Jamari National Forest, Rondonia, Brazil, (9°22'S, 62°58'W). Precipitation is seasonal with distinct wet and dry seasons and a mean annual rainfall of 2315 mm and the dominant soil type is alluvial ferrasol. The area comprises 220,000 ha of wet lowland tropical forest containing three Forest Management Units (FMU) which were offered to auction by the Brazilian government in 2009 for sustainable harvesting. Our study is located within the 96,000 ha making up FMUIII and is divided into Annual Production Units (APU) which are logged during each dry season (Fig. 5.5). Selective logging commenced here in 2011 with and average of 1.6 trees harvested per hectare extracted. A forest inventory is conducted in each APU in the year preceding logging activities whereby all commercial and protected species are identified, GPS mapped and their height and DBH recorded. Extraction rate varies spatially across the landscape due to natural differences in the abundance of commercially desirable species which affords the opportunity to study the impacts of logging intensity using explicitly derived disturbance metrics.

Acronyms

β_{sor} Phylosor. 40, 41, 45–49, 52, 54

d_{BC} Bray-Curtis dissimilarity index. 15, 40, 45–48, 52, 54

APU Annual Production Unit. 63

CSR Complete Spatial Randomness. 65–67, 69

DBH diameter at breast height. 2, 14, 38, 63, 67, 75, 112–114

dbMEM distance-based Moran's eigenvector map. vii–ix, 39–41, 45, 48, 50–52, 57, 58, 108, 109

dbRDA distance-based redundancy analysis. vii, viii, x, 41, 44–49, 51, 52, 80, 110

DEM Digital Elevation Model. 16, 30, 39, 111

GDM Generalised Dissimilarity Modelling. x, 18, 19, 21, 22, 24–26, 28

IBAMA Brazilian Institute of Environment and Renewable Natural Resources. 14, 37

LGCP log-Gaussian Cox process. 67

m.a.s.l meters above sea level. 7, 16, 62

MCF Matérn covariance function. 67

MNTD mean nearest taxon distance. 41

MPD mean pairwise distance. 42

mRD mean relative deviation. vii, 21–23

PBD phylogenetic β-diversity. v, vii–ix, 9, 10, 35–37, 39–48, 51, 53–55, 57–59, 80, 87, 107

PCNM principle coordinates of neighbourhood matrix. 39

PDF Probability Density Function. 19, 20

PGLS phylogenetic generalised least squares. viii, x, 69, 74, 75, 77

SLA specific leaf area. viii, x, 62, 67, 68, 73, 74, 77

TBD taxonomic β-diversity. v, viii, 9, 10, 35–37, 39, 40, 44–47, 51, 53–55, 57, 58, 80

TPI Topographic Position Index. 15, 16, 24, 25, 31, 39, 48, 57, 77, 96

TRI Terrain Ruggedness Index. 15, 16, 25, 39, 48, 56

TWI Topographic Wetness Index. viii, 15, 16, 24, 25, 30, 39, 48, 56, 57, 68, 70–74, 76, 96, 111, 116–120

VIF variance inflation factor. 39

Bibliography

Adler, P. B., HilleRisLambers, J., and Levine, J. M. A niche for neutrality. *Ecology Letters*, 10(2):95–104, 2007.

Alvarez-Buylla, E. R. Density dependence and patch dynamics in tropical rain forests: matrix models and applications to a tree species. *The American Naturalist*, 143(1): 155–191, 1994.

Anderse, K. M., Turner, B. L., and Dalling, J. W. Seedling performance trade-Offs influencing habitat filtering along a soil nutrient gradient in a tropical forest. *Ecology*, 95(12):3399–3413, 2014.

Anderson, M. J. Permutational Multivariate Analysis of Variance (PERMANOVA). *Wiley StatsRef: Statistics Reference Online*, pages 1–15, 2017.

Anderson, M. J., Crist, T. O., Chase, J. M., Vellend, M., Inouye, B. D., Freestone, A. L., Sanders, N. J., Cornell, H. V., Comita, L. S., Davies, K. F., Harrison, S. P., Kraft, N. J. B., Stegen, J. C., and Swenson, N. G. Navigating the multiple meanings of β diversity: a roadmap for the practicing ecologist. *Ecology Letters*, 14(1):19–28, 2011.

Anderson-Teixeira, K. J., Davies, S. J., Bennett, A. C., Gonzalez-Akre, E. B., Muller-Landau, H. C., Joseph Wright, S., Abu Salim, K., Almeyda Zambrano, A. M., Alonso, A., Baltzer, J. L., and Others. CTFS-Forest GEO: a worldwide network monitoring forests in an era of global change. *Global change biology*, 21(2):528–549, 2015.

Asefa, M., Brown, C., Cao, M., Zhang, G., Ci, X., Sha, L., Li, J., Lin, L., and Yang, J. Contrasting effects of space and environment on functional and phylogenetic dissimilarity in a tropical forest. *Journal of Plant Ecology*, 12(2):314–326, 2019.

Azevedo-Ramos, C., Silva, J. N. M., and Merry, F. The evolution of Brazilian forest concessions. *Elementa: Science of the Anthropocene*, 3(0):000048, 2015.

Baddeley, A., Rubak, E., and Turner, R. *Spatial point patterns: methodology and applications with R*. Chapman and Hall/CRC, 2015.

Baldeck, C. A., Harms, K. E., Yavitt, J. B., John, R., Turner, B. L., Valencia, R., Navarrete, H., Bunyavejchewin, S., Kiratiprayoon, S., Yaacob, A., Supardi, M. N., Davies, S. J., Hubbell, S. P., Chuyong, G. B., Kenfack, D., Thomas, D. W., and Dalling, J. W. Habitat filtering across tree life stages in tropical forest communities. *Proceedings of the Royal Society B: Biological Sciences*, 280(1766), 2013.

Baldeck, C. A., Kembel, S. W., Harms, K. E., Yavitt, J. B., John, R., Turner, B. L., Madawala, S., Gunatilleke, N., Gunatilleke, S., Bunyavejchewin, S., Kiratiprayoon, S., Yaacob, A., Supardi, M. N. N., Valencia, R., Navarrete, H., Davies, S. J., Chuyong, G. B., Kenfack, D., Thomas, D. W., and Dalling, J. W. Phylogenetic turnover along local environmental gradients in tropical forest communities. *Oecologia*, 182(2):547–557, 2016.

Baltzer, J. L., Thomas, S. C., Nilus, R., and Burslem, D. F. Edaphic specialization in tropical trees: Physiological correlates and responses to reciprocal transplantation. *Ecology*, 86(11):3063–3077, 2005.

Barnosky, A. D., Matzke, N., Tomiya, S., Wogan, G. O., Swartz, B., Quental, T. B., Marshall, C., McGuire, J. L., Lindsey, E. L., Maguire, K. C., Mersey, B., and Ferrer, E. A. Has the Earth's sixth mass extinction already arrived? *Nature*, 471(7336):51–57, 2011.

Baselga, A. The relationship between species replacement, dissimilarity derived from nestedness, and nestedness. *Global Ecology and Biogeography*, 21(12): 1223–1232, 2012.

Berry, N. J., Phillips, O. L., Lewis, S. L., Hill, J. K., Edwards, D. P., Tawatao, N. B., Ahmad, N., Magintan, D., Khen, C. V., Maryati, M., Ong, R. C., and Hamer, K. C. The high value of logged tropical forests: lessons from northern Borneo. *Biodiversity and Conservation*, 19(4):985–997, 2010.

Beven, K. J. and Kirkby, M. J. A physically based, variable contributing area model of basin hydrology / Un modèle à base physique de zone d'appel variable de l'hydrologie du bassin versant. *Hydrological Sciences Bulletin*, 24(1):43–69, 1979.

Blanchet, F. G., Legendre, P., and Borcard, D. Forward selection of explanatory variables. *Ecology*, 89(9):2623–2632, 2008.

Blaser, J., Sarre, A., Poore, D., and Johnson, S. E. Status of Tropical Forest Management. Technical report, ITTO Technical Series, 2011.

Böhner, J. and Selige, T. Spatial prediction of soil attributes using terrain analysis and climate regionalisation. *SAGA - Analysis and Modelling Applications*, 115:13–27, 2006.

Bongalov, B., Burslem, D. F. R. P., Jucker, T., Thompson, S. E. D., Rosindell, J., Swinfield, T., Nilus, R., Clewley, D., Phillips, O. L., and Coomes, D. A. Reconciling the contribution of environmental and stochastic structuring of tropical forest diversity through the lens of imaging spectroscopy. *Ecology Letters*, page ele.13357, 2019.

Borcard, D. and Legendre, P. All-scale spatial analysis of ecological data by means of principal coordinates of neighbour matrices. *Ecological Modelling*, 153(1-2):51–68, 2002.

Borcard, D., Gillet, F., and Legendre, P. *Numerical ecology with R*. Springer, 2018.

Brown, P. E. Model-based geostatistics the easy way. *Journal of Statistical Software*, 63(12):1–24, 2015.

Bruggeman, J., Heringa, J., and Brandt, B. W. PhyloPars: Estimation of missing parameter values using phylogeny. *Nucleic Acids Research*, 37(SUPPL. 2):W179–84, 2009.

Cáceres, M. D., Legendre, P., Valencia, R., Cao, M., Chang, L. W., Chuyong, G., Condit, R., Hao, Z., Hsieh, C. F., Hubbell, S., Kenfack, D., Ma, K., Mi, X., Supardi Noor, M. N., Kassim, A. R., Ren, H., Su, S. H., Sun, I. F., Thomas, D., Ye, W., and He, F. The variation of tree beta diversity across a global network of forest plots. *Global Ecology and Biogeography*, 21(12):1191–1202, 2012.

Chadwick, K. D. and Asner, G. P. Tropical soil nutrient distributions determined by biotic and hillslope processes. *Biogeochemistry*, 127(2-3):273–289, 2016.

Chang, L. W., Zelený, D., Li, C. F., Chiu, S. T., and Hsieh, C. F. Better environmental data may reverse conclusions about niche- and dispersal-based processes in community assembly. *Ecology*, 94(10):2145–2151, 2013.

Chisholm, R. A. and Pacala, S. W. Niche and neutral models predict asymptotically equivalent species abundance distributions in high-diversity ecological communities. *Proceedings of the National Academy of Sciences*, 107(36):15821–15825, 2010.

Chisholm, R. A., Condit, R., Rahman, K. A., Baker, P. J., Bunyavejchewin, S., Chen, Y. Y., Chuyong, G., Dattaraja, H. S., Davies, S., Ewango, C. E., Gunatilleke, C. V., Nimal Gunatilleke, I. A., Hubbell, S., Kenfack, D., Kiratiprayoon, S., Lin, Y., Makana, J. R., Pongpattananurak, N., Pulla, S., Punchi-Manage, R., Sukumar, R., Su, S. H., Sun, I. F., Suresh, H. S., Tan, S., Thomas, D., and Yap, S. Temporal variability of forest communities: Empirical estimates of population change in 4000 tree species. *Ecology Letters*, 17(7):855–865, 2014.

Clark, D. B., Clark, D. A., and Read, J. M. Edaphic variation and the mesoscale distribution of tree species in a neotropical rain forest. *Journal of Ecology*, 86(1):101–112, 1998.

Clark, D. B., Palmer, M. W., and Clark, D. A. Edaphic factors and the landscape-scale distributions of tropical rain forest trees. *Ecology*, 80(8):2662–2675, 1999a.

Clark, J. S., Silman, M., Kern, R., Macklin, E., and Hillerislambers, J. Seed dispersal near and far: Patterns across temperate and tropical forests. *Ecology*, 80(5): 1475–1494, 1999b.

Comita, L. S., Queenborough, S. A., Murphy, S. J., Eck, J. L., Xu, K., Krishnadas, M., Beckman, N., and Zhu, Y. Testing predictions of the Janzen-Connell hypothesis: A meta-analysis of experimental evidence for distance- and density-dependent seed and seedling survival. *Journal of Ecology*, 102(4):845–856, 2014.

Condit, R., Ashton, P. S., Baker, P., Bunyavejchewin, S., Gunatilleke, S., Gunatilleke, N., Hubbell, S. P., Foster, R. B., Itoh, A., LaFrankie, J. V., Lee, H. S., Losos, E., Manokaran, N., Sukumar, R., and Yamakura, T. Spatial patterns in the distribution of tropical tree species. *Science (New York, N.Y.)*, 288(5470):1414–8, 2000b.

Condit, R., Ashton, P. S., Baker, P., Bunyavejchewin, S., Gunatilleke, S., Gunatilleke, N., Hubbell, S. P., Foster, R. B., Itoh, A., LaFrankie, J. V., Lee, H. S., Losos, E., Manokaran, N., Sukumar, R., and Yamakura, T. Spatial Patterns in the Distribution of Tropical Tree Species. *Science*, 288(5470):1414–1418, 2000a.

Condit, R., Hubbell, S. P., and Foster, R. B. Density dependence in two understory tree species in a neotropical forest. *Ecology*, 75(3):671–680, 1994.

Condit, R., Pitman, N., Leigh, E. G., Chave, J., Terborgh, J., Foster, R. B., Núñez, P., Aguilar, S., Valencia, R., Villa, G., Muller-Landau, H. C., Losos, E., and Hubbell, S. P. Beta-diversity in tropical forest trees. *Science (New York, N.Y.)*, 295(5555):666–9, 2002.

Connell, J. H. On the role of natural enemies in preventing competitive exclusion in some marine animals and in rain forest trees. *Dynamics of populations*, 298:312, 1971.

Conrad, O., Bechtel, B., Bock, M., Dietrich, H., Fischer, E., Gerlitz, L., Wehberg, J., Wichmann, V., and Böhner, J. System for automated geoscientific analyses (SAGA) v. 2.1. 4. *Geoscientific Model Development*, 8(7):1991–2007, 2015.

Cornwell, W. K. and Ackerly, D. D. Community assembly and shifts in plant trait distributions across an environmental gradient in coastal California. *Ecological Monographs*, 79(1):109–126, 2009.

Cressie, N. Statistics for spatial data. *Terra Nova*, 4(5):613–617, 1992.

Davidar, P., Rajagopal, B., Mohandass, D., Puyravaud, J. P., Condit, R., Wright, S. J., and Leigh, E. G. The effect of climatic gradients, topographic variation and species traits on the beta diversity of rain forest trees. *Global Ecology and Biogeography*, 16(4):510–518, 2007.

De Oliveira, A. A. and Mori, S. A. A central Amazonian terra firme forest. I. High tree species richness on poor soils. *Biodiversity and Conservation*, 8(9):1219–1244, 1999.

Diggle, P. J. Displaced amacrine cells in the retina of a rabbit: analysis of a bivariate spatial point pattern. *Journal of neuroscience methods*, 18(1-2):115–125, 1986.

Dijkshoorn, K., Huting, J., and Tempel, P. Update of the 1: 5 million Soil and Terrain Database for Latin America and the Caribbean (SOTERLAC). *ISRIC Rep*, 1(1):25, 2005.

Draper, F. C., Baraloto, C., Brodrick, P. G., Phillips, O. L., Martinez, R. V., Honorio Coronado, E. N., Baker, T. R., Zárate Gómez, R., Amasifuen Guerra, C. A., Flores, M., Garcia Villacorta, R., V. A. Fine, P., Freitas, L., Monteagudo-Mendoza, A., J. W Brienen, R., and Asner, G. P. Imaging spectroscopy predicts variable distance decay across contrasting Amazonian tree communities. *Journal of Ecology*, 107(2):696–710, 2019.

Dray, S., Legendre, P., and Peres-Neto, P. R. Spatial modelling: a comprehensive framework for principal coordinate analysis of neighbour matrices (PCNM). *Ecological Modelling*, 196(3-4):483–493, 2006.

Dray, S., Bauman, D., Blanchet, G., Borcard, D., Clappe, S., Guenard, G., Jombart, T., Larocque, G., Legendre, P., Madi, N., and Wagner, H. H. *adespatial: Multivariate Multiscale Spatial Analysis*, 2019.

Duque, Á., Phillips, J. F., Von Hildebrand, P., Posada, C. A., Prieto, A., Rudas, A., Suescún, M., and Stevenson, P. Distance decay of tree species similarity in protected areas on terra firme forests in Colombian Amazonia. *Biotropica*, 41(5):599–607, 2009.

Duque, A., Muller-Landau, H. C., Valencia, R., Cardenas, D., Davies, S., de Oliveira, A., Pérez, Á. J., Romero-Saltos, H., and Vicentini, A. Insights into regional patterns

of Amazonian forest structure, diversity, and dominance from three large terra-firme forest dynamics plots. *Biodiversity and Conservation*, 26(3):669–686, 2017.

Dyer, J. M. Assessing topographic patterns in moisture use and stress using a water balance approach. *Landscape Ecology*, 24(3):391–403, 2009.

Edwards, D. P., Gilroy, J. J., Woodcock, P., Edwards, F. A., Larsen, T. H., Andrews, D. J., Derhé, M. A., Docherty, T. D., Hsu, W. W., Mitchell, S. L., Ota, T., Williams, L. J., Laurance, W. F., Hamer, K. C., and Wilcove, D. S. Land-sharing versus land-sparing logging: Reconciling timber extraction with biodiversity conservation. *Global Change Biology*, 20(1):183–191, 2014a.

Edwards, D. P., Tobias, J. A., Sheil, D., Meijaard, E., and Laurance, W. F. Maintaining ecosystem function and services in logged tropical forests. *Trends in Ecology & Evolution*, 29(9):511–520, 2014b.

Edwards, D. P., Socolar, J. B., Mills, S. C., Burivalova, Z., Koh, L. P., and Wilcove, D. S. Conservation of tropical forests in the Anthropocene. *Current Biology*, In press, 2019.

Ellis, P. W., Gopalakrishna, T., Goodman, R. C., Putz, F. E., Roopsind, A., Umunay, P. M., Zalman, J., Ellis, E. A., Mo, K., Gregoire, T. G., and Griscom, B. W. Reduced-impact logging for climate change mitigation (RIL-C) can halve selective logging emissions from tropical forests. *Forest Ecology and Management*, 438(February):255–266, 2019.

Engelbrecht, B., Comita, L., Condit, R., Kursar, T., Tyree, M., Turner, B., and Hubbell, S. Drought sensitivity shapes species distribution patterns in tropical forests. *Nature*, 447(3):80–83, 2007a.

Engelbrecht, B. M. J., Comita, L. S., Condit, R., Kursar, T. A., Tyree, M. T., Turner, B. L., and Hubbell, S. P. Drought sensitivity shapes species distribution patterns in tropical forests. *Nature*, 447(7140):80–82, 2007b.

Ferreira, G. *Modelagem ambiental de espécies de árvores no vale do Jari, Monte Dourado, Pará usando dados de inventário florestal*. Thesis, Instituto de Pesquisas Jardim Botânico do Rio de Janeiro, 2009.

Ferrier, S., Manion, G., Elith, J., and Richardson, K. Using generalized dissimilarity modelling to analyse and predict patterns of beta diversity in regional biodiversity assessment. *Diversity and Distributions*, 13(3):252–264, 2007.

Fischer, G., Nachtergaele, F., Prieler, S., Van Velthuizen, H. T., Verelst, L., and Wiberg, D. Global agro-ecological zones assessment for agriculture (GAEZ 2008). *IIASA, Laxenburg, Austria and FAO, Rome, Italy*, 10, 2008.

Gause, G. F. *The struggle for existence*. Williams and Wilkins, 1934.

Gilbert, G. S., Foster, R. B., and Hubbell, S. P. Density and distance-to-adult effects of a canker disease of trees in a moist tropical forest. *Oecologia*, 98(1):100–108, 1994.

Graham, C. H. and Fine, P. V. A. Phylogenetic beta diversity: Linking ecological and evolutionary processes across space in time. *Ecology Letters*, 11(12):1265–1277, 2008.

Grubb, P. J. The Maintenance of Species-richness in Plant Communities: the Importance of the Regeneration Niche. *Biological Reviews*, 52(1):107–145, 1977.

Guisan, A., Weiss, S. B., and Weiss, A. D. GLM versus CCA spatial modeling of plant species distribution. *Plant Ecology*, 143(1):107–122, 1999.

Hammond, D. S., Brown, V. K., and Others. Disturbance, phenology and life-history characteristics: factors influencing distance/density-dependent attack on tropical seeds and seedlings. *Disturbance, phenology and life-history characteristics: factors influencing distance/density-dependent attack on tropical seeds and seedlings.*, pages 51–78, 1998.

Harborne, J. B. Biochemical interactions between higher plants. *Introduction to ecological biochemistry" Academic Press, London*, 1993.

Hardin, G. The Competitive Exclusion Principle. *Science*, 131(3409):1292–1297, 1960.

Hardy, O. J., Couteron, P., Munoz, F., Ramesh, B. R., and Pélissier, R. Phylogenetic turnover in tropical tree communities: Impact of environmental filtering, biogeography and mesoclimatic niche conservatism. *Global Ecology and Biogeography*, 21(10):1007–1016, 2012.

Harms, K. E., Condit, R., Hubbell, S. P., and Foster, R. B. Habitat associations of trees and shrubs in a 50-ha neotropical forest plot. *Journal of Ecology*, 89(6):947–959, 2001a.

Harms, K. E., Condit, R., Hubbell, S. P., and Foster, R. B. Habitat associations of trees and shrubs in a 50-ha neotropical forest plot. *Journal of Ecology*, 89(6):947–959, 2001b.

Hart, S. P., Usinowicz, J., and Levine, J. M. The spatial scales of species coexistence. *Nature Ecology & Evolution*, 1(8):1066–1073, 2017.

Hawthorne, W. D., Sheil, D., Agyeman, V. K., Abu Juam, M., and Marshall, C. A. Logging scars in Ghanaian high forest: Towards improved models for sustainable production. *Forest Ecology and Management*, 271:27–36, 2012.

Hijmans, R. J., Cameron, S. E., Parra, J. L., Jones, P. G., and Jarvis, A. Very high resolution interpolated climate surfaces for global land areas. *International Journal of Climatology*, 25(15):1965–1978, 2005.

Hubbell, S. P. *The unified neutral theory of biodiversity and biogeography*. Princeton University Press, 2001.

Hubbell, S. P. Neutral theory in community ecology and the hypothesis of functional equivalence, 2005. URL http://doi.wiley.com/10.1111/j.0269-8463.2005.00965.x.

Hubbell, S. P., Condit, R., and Foster, R. B. Barro Colorado forest census plot data, 2005.

Jalilian, A., Guan, Y., and Waagepetersen, R. Decomposition of Variance for Spatial Cox Processes. *Scandinavian journal of statistics, theory and applications*, 40(1): 119–137, 2013.

Janzen, D. H. Herbivores and the Number of Tree Species in Tropical Forests. *The American Naturalist*, 104(940):501–528, 1970.

JAXA/METI. ALOS PALSAR L1.5, 2011.

Jin, L. S., Cadotte, M. W., and Fortin, M.-J. Phylogenetic turnover patterns consistent with niche conservatism in montane plant species. *Journal of Ecology*, 103(3): 742–749, 2015.

Jin, Y. and Qian, H. V.PhyloMaker: an R package that can generate very large phylogenies for vascular plants. *Ecography*, page ecog.04434, 2019.

John, R., Dalling, J. W., Harms, K. E., Yavitt, J. B., Stallard, R. F., Mirabello, M., Hubbell, S. P., Valencia, R., Navarrete, H., Vallejo, M., and Foster, R. B. Soil nutrients influence spatial distributions of tropical tree species. *Proceedings of the National Academy of Sciences of the United States of America*, 104(3):864–9, 2007a.

John, R., Dalling, J. W., Harms, K. E., Yavitt, J. B., Stallard, R. F., Mirabello, M., Hubbell, S. P., Valencia, R., Navarrete, H., Vallejo, M., and Others. Soil nutrients influence spatial distributions of tropical tree species. *Proceedings of the National Academy of Sciences*, 104(3):864–869, 2007b.

Jucker, T., Bongalov, B., Burslem, D. F., Nilus, R., Dalponte, M., Lewis, S. L., Phillips, O. L., Qie, L., and Coomes, D. A. Topography shapes the structure, composition and function of tropical forest landscapes, 2018. URL https://onlinelibrary.wiley.com/doi/pdf/10.1111/ele.12964.

Kahn, F. The distribution of palms as a function of local topography in Amazonian terra-firme forests. *Cellular and Molecular Life Sciences*, 43(3):251–259, 1987.

Kattge, J., Díaz, S., Lavorel, S., Prentice, I. C., Leadley, P., Bönisch, G., Garnier, E., Westoby, M., Reich, P. B., Wright, I. J., Cornelissen, J. H., Violle, C., Harrison, S. P., Van Bodegom, P. M., Reichstein, M., Enquist, B. J., Soudzilovskaia, N. A., Ackerly, D. D., Anand, M., Atkin, O., Bahn, M., Baker, T. R., Baldocchi, D., Bekker, R., Blanco, C. C., Blonder, B., Bond, W. J., Bradstock, R., Bunker, D. E., Casanoves, F., Cavender-Bares, J., Chambers, J. Q., Chapin, F. S., Chave, J., Coomes, D., Cornwell, W. K., Craine, J. M., Dobrin, B. H., Duarte, L., Durka, W., Elser, J., Esser, G., Estiarte, M., Fagan, W. F., Fang, J., Fernández-Méndez, F., Fidelis, A., Finegan, B., Flores, O., Ford, H., Frank, D., Freschet, G. T., Fyllas, N. M., Gallagher, R. V., Green, W. A., Gutierrez, A. G., Hickler, T., Higgins, S. I., Hodgson, J. G., Jalili, A., Jansen, S., Joly, C. A., Kerkhoff, A. J., Kirkup, D., Kitajima, K., Kleyer, M., Klotz, S., Knops, J. M., Kramer, K., Kühn, I., Kurokawa, H., Laughlin, D., Lee, T. D., Leishman, M., Lens, F., Lenz, T., Lewis, S. L., Lloyd, J., Llusià, J., Louault, F., Ma, S., Mahecha, M. D., Manning, P., Massad, T., Medlyn, B. E., Messier, J., Moles, A. T., Müller, S. C., Nadrowski, K., Naeem, S., Niinemets, Ü., Nöllert, S., Nüske, A., Ogaya, R., Oleksyn, J., Onipchenko, V. G., Onoda, Y., Ordoñez, J., Overbeck, G., Ozinga, W. A., Patiño, S., Paula, S., Pausas, J. G., Peñuelas, J., Phillips, O. L., Pillar, V., Poorter, H., Poorter, L., Poschlod, P., Prinzing, A., Proulx, R., Rammig, A., Reinsch, S., Reu, B., Sack, L., Salgado-Negret, B., Sardans, J., Shiodera, S., Shipley, B., Siefert, A., Sosinski, E., Soussana, J. F., Swaine, E., Swenson, N., Thompson, K., Thornton, P., Waldram, M., Weiher, E., White, M., White, S., Wright, S. J., Yguel, B., Zaehle, S., Zanne, A. E., and Wirth, C. TRY - a global database of plant traits. *Global Change Biology*, 17(9):2905–2935, 2011.

Keenan, R. J., Reams, G. A., Achard, F., de Freitas, J. V., Grainger, A., and Lindquist, E. Dynamics of global forest area: Results from the FAO Global Forest Resources Assessment 2015. *Forest Ecology and Management*, 352:9–20, 2015.

Kier, G., Mutke, J., Dinerstein, E., Ricketts, T. H., Küper, W., Kreft, H., and Barthlott, W. Global patterns of plant diversity and floristic knowledge. *Journal of Biogeography*, 32(7):1107–1116, 2005.

Kraft, N. J. B., Valencia, R., and Ackerly, D. D. Functional Traits and Niche-Based Tree Community Assembly in an Amazonian Forest. *Science*, 322(5684):580–582, 2008.

Legendre, P. and Anderson, M. J. Distance-based redundancy analysis: testing multispecies responses in multifactorial ecological experiments. *Ecological monographs*, 69(1):1–24, 1999.

Legendre, P. and Legendre, L. F. J. *Numerical ecology*, volume 24. Elsevier, 2012.

Legendre, P., Mi, X., Ren, H., Ma, K., Yu, M., Sun, I.-F., and He, F. Partitioning beta diversity in a subtropical broad-leaved forest of China. *Ecology*, 90(3):663–674, 2009.

Li, D., Trotta, L., Marx, H. E., Allen, J. M., Sun, M., Soltis, D. E., Soltis, P. S., Guralnick, R. P., and Baiser, B. For common community phylogenetic analyses, go ahead and use synthesis phylogenies. *Ecology*, 2019.

Liang, J., Crowther, T. W., Picard, N., Wiser, S., Zhou, M., Alberti, G., Schulze, E.-D., McGuire, A. D., Bozzato, F., Pretzsch, H., De-Miguel, S., Paquette, A., Hérault, B., Scherer-Lorenzen, M., Barrett, C. B., Glick, H. B., Hengeveld, G. M., Nabuurs, G.-J., Pfautsch, S., Viana, H., Vibrans, A. C., Ammer, C., Schall, P., Verbyla, D., Tchebakova, N., Fischer, M., Watson, J. V., Chen, H. Y. H., Lei, X., Schelhaas, M.-J., Lu, H., Gianelle, D., Parfenova, E. I., Salas, C., Lee, E., Lee, B., Kim, H. S., Bruelheide, H., Coomes, D. A., Piotto, D., Sunderland, T., Schmid, B., Gourlet-Fleury, S., Sonké, B., Tavani, R., Zhu, J., Brandl, S., Vayreda, J., Kitahara, F., Searle, E. B., Neldner, V. J., Ngugi, M. R., Baraloto, C., Frizzera, L., Bałazy, R., Oleksyn, J., Zawiła-Niedz wiecki, T., Bouriaud, O., Bussotti, F., Finér, L., Jaroszewicz, B., Jucker, T., Valladares, F., Jagodzinski, A. M., Peri, P. L., Gonmadje, C., Marthy, W., O'Brien, T., Martin, E. H., Marshall, A. R., Rovero, F., Bitariho, R., Niklaus, P. A., Alvarez-Loayza, P., Chamuya, N., Valencia, R., Mortier, F., Wortel, V., Engone-Obiang, N. L., Ferreira, L. V., Odeke, D. E., Vasquez, R. M., Lewis, S. L., and Reich, P. B. Positive biodiversity-productivity relationship predominant in global forests. *Science (New York, N.Y.)*, 354(6309):aaf8957, 2016.

Lieberman, M., Lieberman, D., Hartshorn, G. S., and Peralta, R. Small-scale altitudinal variation in lowland wet tropical forest vegetation. *The journal of ecology*, pages 505–516, 1985.

Lin, Y.-C., Chang, L.-W., Yang, K.-C., Wang, H.-H., and Sun, I.-F. Point patterns of tree distribution determined by habitat heterogeneity and dispersal limitation. *Oecologia*, 165:175–184, 2011.

Liu, J., Yunhong, T., and Slik, J. W. Topography related habitat associations of tree species traits, composition and diversity in a Chinese tropical forest. *Forest Ecology and Management*, 330:75–81, 2014.

Liu, J., Qian, H., Jin, Y., Wu, C., Chen, J., Yu, S., Wei, X., Jin, X., Liu, J., and Yu, M. Disentangling the drivers of taxonomic and phylogenetic beta diversities in disturbed and undisturbed subtropical forests. *Scientific Reports*, 6(1):35926, 2016.

Loosmore, N. B. and Ford, E. D. STATISTICAL INFERENCE USING THE G OR K POINT PATTERN SPATIAL STATISTICS. *Ecology*, 87(8):1925–1931, 2006.

Losos, J. B. Phylogenetic niche conservatism, phylogenetic signal and the relationship between phylogenetic relatedness and ecological similarity among species. *Ecology Letters*, 11(10):995–1003, 2008.

Lowe, W. H. and McPeek, M. A. Is dispersal neutral? *Trends in ecology & evolution*, 29(8):444–50, 2014.

MacDicken, K. G., Sola, P., Hall, J. E., Sabogal, C., Tadoum, M., and de Wasseige, C. Global progress toward sustainable forest management. *Forest Ecology and Management*, 352:47–56, 2015.

Manion, G., Lisk, M., Ferrier, S., Nieto-Lugilde, D., Mokany, K., and Fitzpatrick, M. C. *gdm: Generalized Dissimilarity Modeling*, 2018.

Mantel, N. The detection of disease clustering and a generalized regression approach. *Cancer research*, 27(2 Part 1):209–220, 1967.

Martinez-Ramos, M. J. SARUKHÁ N, AND D. PIN ERO. 1988. The demography of tropical trees in the context of forest gap dynamics: the case of Astrocaryum mexicanum at Los Tuxtlas tropical rain forest. *Plant population ecology*, pages 293–313.

Marvin, D. C., Asner, G. P., Knapp, D. E., Anderson, C. B., Martin, R. E., Sinca, F., and Tupayachi, R. Amazonian landscapes and the bias in field studies of forest structure and biomass. *Proceedings of the National Academy of Sciences of the United States of America*, 111(48):E5224–32, 2014.

May, F., Huth, A., and Wiegand, T. Moving beyond abundance distributions: Neutral theory and spatial patterns in a tropical forest. *Proceedings of the Royal Society B: Biological Sciences*, 282(1802):1–8, 2015.

Mayfield, M. M. and Levine, J. M. Opposing effects of competitive exclusion on the phylogenetic structure of communities. *Ecology Letters*, 13(9):1085–1093, 2010.

McFadden, I. R., Bartlett, M. K., Wiegand, T., Turner, B. L., Sack, L., Valencia, R., and Kraft, N. J. Disentangling the functional trait correlates of spatial aggregation in tropical forest trees. *Ecology*, 100(3), 2019.

McKane, R. B., Johnson, L. C., Shaver, G. R., Nadelhoffer, K. J., Rastetter, E. B., Fry, B., Giblin, A. E., Kielland, K., Kwlatkowski, B. L., Laundre, J. A., and Murray, G. Resource-based niches provide a basis for plant species diversity and dominance in arctic tundra. *Nature*, 415(6867):68–71, 2002.

Moore, I. D., Gessler, P. E., Nielsen, G. A., and Peterson, G. A. Soil attribute prediction using terrain analysis. *Soil Science Society of America Journal*, 57(2):443–452, 1993.

Muller-Landau, H. C. The tolerance-fecundity trade-off and the maintenance of diversity in seed size. *Proceedings of the National Academy of Sciences of the United States of America*, 107(9):4242–4247, 2010.

Munoz, F. Distance-based eigenvector maps (DBEM) to analyse metapopulation structure with irregular sampling. *Ecological Modelling*, 220(20):2683–2689, 2009.

Myers, J. A., Chase, J. M., Jiménez, I., Jørgensen, P. M., Araujo-Murakami, A., Paniagua-Zambrana, N., and Seidel, R. Beta-diversity in temperate and tropical forests reflects dissimilar mechanisms of community assembly. *Ecology Letters*, 16(2): 151–157, 2013.

Naimi, B. usdm: uncertainty analysis for species distribution models. R package version 1.1-15. *R Documentation http://www. rdocu-mentation. org/packages/usdm*, 2015.

Nellemann, C. and Others. Green carbon, black trade: illegal logging, tax fraud and laundering in the world's tropical forests. *Green carbon, black trade: illegal logging, tax fraud and laundering in the world's tropical forests.*, 2012.

Ness, J. H., Rollinson, E. J., and Whitney, K. D. Phylogenetic distance can predict susceptibility to attack by natural enemies. *Oikos*, 120(9):1327–1334, 2011.

Orme, D., Freckleton, R., Thomas, G., and Petzoldt, T. The caper package: comparative analysis of phylogenetics and evolution in R. *R package version*, 5(2):1–36, 2013.

Pacheco, P., Cerutti, P. O., Edwards, D. P., Lescuyer, G., Mejía, E., Navarro, G., Obidzinski, K., Pokorny, B., and Sist, P. Multiple and Intertwined Impacts of Illegal Forest Activities. Technical report, IURFO, 2016.

Paine, C. E., Norden, N., Chave, J., Forget, P. M., Fortunel, C., Dexter, K. G., and Baraloto, C. Phylogenetic density dependence and environmental filtering predict seedling mortality in a tropical forest. *Ecology Letters*, 15(1):34–41, 2012.

Palmer, M. W. Variation in Species Richness : Towards a Unification of Hypotheses. *Folia Geobotanica & Phytotaxonomica*, 29(4):511–530, 1994.

Pan, Y., Birdsey, R. A., Fang, J., Houghton, R., Kauppi, P. E., Kurz, W. A., Phillips, O. L., Shvidenko, A., Lewis, S. L., Canadell, J. G., Ciais, P., Jackson, R. B., Pacala, S. W., McGuire, A. D., Piao, S., Rautiainen, A., Sitch, S., and Hayes, D. A Large and Persistent Carbon Sink in the World's Forests. *Science*, 333(6045):988–993, 2011.

Pashirzad, M., Ejtehadi, H., Vaezi, J., and Shefferson, R. P. Spatial scale- dependent phylogenetic signal in species distributions along geographic and elevation gradients in a mountainous rangeland. (January):10364–10373, 2018.

Peacock, J., Baker, T. R., Lewis, S. L., Lopez-Gonzalez, G., and Phillips, O. L. The RAINFOR database: monitoring forest biomass and dynamics. *Journal of Vegetation Science*, 18(4):535–542, 2007.

Phillips, O. L., Baker, T. R., Arroyo, L., Higuchi, N., Killeen, T. J., Laurance, W. F., Lewis, S. L., Lloyd, J., Malhi, Y., Monteagudo, A., Neill, D. A., Núñez Vargas, P., Silva, J. N. M., Terborgh, J., Vásquez Martínez, R., Alexiades, M., Almeida, S., Brown, S., Chave, J., Comiskey, J. A., Czimczik, C. I., Di Fiore, A., Erwin, T., Kuebler, C., Laurance, S. G., Nascimento, H. E. M., Olivier, J., Palacios, W., Patiño, S., Pitman, N. C. A., Quesada, C. A., Saldias, M., Torres Lezama, A., and Vinceti, B. Pattern and process in Amazon tree turnover, 1976–2001. *Philosophical Transactions of the Royal Society of London. Series B: Biological Sciences*, 359(1443):381–407, 2004.

Pinto, S. M. and MacDougall, A. S. Dispersal Limitation and Environmental Structure Interact to Restrict the Occupation of Optimal Habitat. *The American Naturalist*, 175(6):675–686, 2010.

Poorter, L. and Markesteijn, L. Seedling Traits Determine Drought Tolerance of Tropical Tree Species. *Biotropica*, 40(3):321–331, 2008.

Pos, E., Guevara Andino, J. E., Sabatier, D., Molino, J.-F., Pitman, N., Mogollón, H., Neill, D., Cerón, C., Rivas, G., Di Fiore, A., Thomas, R., Tirado, M., Young, K. R., Wang, O., Sierra, R., García-Villacorta, R., Zagt, R., Palacios, W., Aulestia, M., and ter Steege, H. Are all species necessary to reveal ecologically important patterns? *Ecology and Evolution*, 4(24):4626–4636, 2014.

Purves, D. W. and Turnbull, L. A. Different but equal: The implausible assumption at the heart of neutral theory. *Journal of Animal Ecology*, 79(6):1215–1225, 2010.

Putz, F. E., Sist, P., Fredericksen, T., and Dykstra, D. Reduced-impact logging: Challenges and opportunities. *Forest Ecology and Management*, 256(7):1427–1433, 2008.

Qian, H. and Jin, Y. An updated megaphylogeny of plants, a tool for generating plant phylogenies and an analysis of phylogenetic community structure. *Journal of Plant Ecology*, 9(2):233–239, 2016.

Qiao, X., Li, Q., Jiang, Q., Lu, J., Franklin, S., Tang, Z., Wang, Q., Zhang, J., Lu, Z., Bao, D., Guo, Y., Liu, H., Xu, Y., and Jiang, M. Beta diversity determinants in Badagongshan, a subtropical forest in central China. *Scientific Reports*, 5(1):17043, 2015.

R Core Team. *R: A Language and Environment for Statistical Computing*. R Foundation for Statistical Computing, Vienna, Austria, 2019.

Ramsay, J. O. and Others. Monotone regression splines in action. *Statistical science*, 3(4):425–441, 1988.

Réjou-Méchain, M., Flores, O., Bourland, N., Doucet, J.-L., Fétéké, R. F., Pasquier, A., and Hardy, O. J. Spatial aggregation of tropical trees at multiple spatial scales. *Journal of Ecology*, 99(6):1373–1381, 2011.

Ricotta, C. and Burrascano, S. Testing for differences in beta diversity with asymmetric dissimilarities. *Ecological Indicators*, 9(4):719–724, 2009.

Rosindell, J. and Cornell, S. J. Species–area curves, neutral models, and long-distance dispersal. *Ecology*, 90(7):1743–1750, 2009.

Rosindell, J., Wong, Y., and Etienne, R. S. A coalescence approach to spatial neutral ecology. *Ecological Informatics*, 3(3):259–271, 2008.

Rosindell, J., Hubbell, S. P., and Etienne, R. S. The Unified Neutral Theory of Biodiversity and Biogeography at Age Ten. *Trends in Ecology & Evolution*, 26(7):340–348, 2011.

Russo, S. E., Porrs, M. D., and TAN, S. 23 Determinants of Tree Species Distributions: Comparing the Roles of Dispersal, Seed Size and Soil Specialization in a Bornean Rainforest. *SEED DISPERSAL*, page 499, 2007.

Russo, S. E., Brown, P., Tan, S., and Davies, S. J. Interspecific demographic trade-offs and soil-related habitat associations of tree species along resource gradients. *Journal of Ecology*, 96(1):192–203, 2008.

Sairam, R. K. and Tyagi, A. Physiology and Molecular Biology of Stress Tolerance in Plants. *Current Science*, 86(3):407–421, 2004.

Saito, V. S., Soininen, J., Fonseca-Gessner, A. A., and Siqueira, T. Dispersal traits drive the phylogenetic distance decay of similarity in Neotropical stream metacommunities. *Journal of Biogeography*, 42(11):2101–2111, 2015.

Seidler, T. G. and Plotkin, J. B. Seed dispersal and spatial pattern in tropical trees. *PLoS Biology*, 4(11):2132–2137, 2006.

Shen, G., Yu, M., Hu, X.-S., Mi, X., Ren, H., Sun, I.-F., and Ma, K. Species–area relationships explained by the joint effects of dispersal limitation and habitat heterogeneity, 2009a. URL http://doi.wiley.com/10.1890/08-1646.1https://esajournals.onlinelibrary.wiley.com/doi/pdf/10.1890/08-1646.1.

Shen, G., Yu, M., Hu, X.-S., Mi, X., Ren, H., Sun, I.-F., and Ma, K. Species-area relationships explained by the joint effects of dispersal limitation and habitat heterogeneity. Technical Report 11, 2009b.

Shen, G., He, F., Waagepetersen, R., Sun, I.-F., Hao, Z., Chen, Z.-S., and Yu, M. Quantifying effects of habitat heterogeneity and other clustering processes on spatial distributions of tree species. *Ecology*, 94(11):2436–2443, 2013.

Silva Matos, D. M., Freckleton, R. P., and Watkinson, A. R. The role of density dependence in the population dynamics of a tropical palm. *Ecology*, 80(8):2635–2650, 1999.

Silvertown, J. Plant coexistence and the niche. *Trends in Ecology & Evolution*, 19(11):605–611, 2004.

Silvertown, J., Dodd, M. E., Gowing, D. J., and Mountford, J. O. Hydrologically defined niches reveal a basis for species richness in plant communities. *Nature*, 400(6739):61–63, 1999.

Smith, S. A. and Brown, J. W. Constructing a broadly inclusive seed plant phylogeny. *American Journal of Botany*, 105(3):302–314, 2018.

Socolar, J. B., Gilroy, J. J., Kunin, W. E., and Edwards, D. P. How Should Beta-Diversity Inform Biodiversity Conservation?, 2016. URL https://www.sciencedirect.com/science/article/pii/S016953471500289X.

Srivastava, D. S., Cadotte, M. W., Macdonald, A. A. M., Marushia, R. G., and Mirotchnick, N. Phylogenetic diversity and the functioning of ecosystems. *Ecology Letters*, 15(7):637–648, 2012.

Sturges, H. A. The Choice of a Class Interval. *Journal of the American Statistical Association*, 21(153):65–66, 2012.

Sundqvist, M. K., Sanders, N. J., and Wardle, D. A. Community and Ecosystem Responses to Elevational Gradients: Processes, Mechanisms, and Insights for Global Change. *Annual Review of Ecology, Evolution, and Systematics*, 44(1):261–280, 2013.

Svenning, J. Microhabitat specialization in a species rich palm community in Amazonian Ecuador. *Journal of Ecology*, 87(1):55–65, 1999.

Swenson, N. G. Phylogenetic Beta Diversity Metrics, Trait Evolution and Inferring the Functional Beta Diversity of Communities. *PLoS ONE*, 6(6):e21264, 2011.

Swenson, N. G. Phylogenetic imputation of plant functional trait databases. *Ecography*, 37(2):105–110, 2014.

ter Steege, H. ATDN & RAINFOR (2010) Contribution of current and historical processes to patterns of tree diversity and composition of the Amazon. *Amazonia, landscape and species evolution: A look into the past (ed. by C. Hoorn, H. Vonhof and F. Wesselingh)*, pages 349–359.

ter Steege, H., Pitman, N. C. A., Phillips, O. L., Chave, J., Sabatier, D., Duque, A., Molino, J.-F., Prévost, M.-F., Spichiger, R., Castellanos, H., von Hildebrand, P., and Vásquez, R. Continental-scale patterns of canopy tree composition and function across Amazonia. *Nature*, 443(7110):444–447, 2006.

Ter Steege, H., Pitman, N. C., Sabatier, D., Baraloto, C., Salomão, R. P., Guevara, J. E., Phillips, O. L., Castilho, C. V., Magnusson, W. E., Molino, J. F., Monteagudo, A., Vargas, P. N., Montero, J. C., Feldpausch, T. R., Coronado, E. N., Killeen, T. J., Mostacedo, B., Vasquez, R., Assis, R. L., Terborgh, J., Wittmann, F., Andrade, A., Laurance, W. F., Laurance, S. G., Marimon, B. S., Marimon, B. H., Vieira, I. C. G., Amaral, I. L., Brienen, R., Castellanos, H., López, D. C., Duivenvoorden, J. F., Mogollón, H. F., Matos, F. D. D. A., Dávila, N., García-Villacorta, R., Diaz, P. R. S., Costa, F., Emilio, T., Levis, C., Schietti, J., Souza, P., Alonso, A., Dallmeier, F., Montoya, A. J. D., Piedade, M. T. F., Araujo-Murakami, A., Arroyo, L., Gribel, R., Fine, P. V., Peres, C. A., Toledo, M., Aymard C., G. A., Baker, T. R., Cerón, C., Engel, J., Henkel, T. W., Maas, P., Petronelli, P., Stropp, J., Zartman, C. E., Daly, D., Neill, D., Silveira, M., Paredes, M. R., Chave, J., Lima Filho, D. D. A., Jørgensen, P. M., Fuentes, A., Schöngart, J., Valverde, F. C., Di Fiore, A., Jimenez, E. M., Mora, M. C. P., Phillips, J. F., Rivas, G., Van Andel, T. R., Von Hildebrand, P., Hoffman, B., Zent, E. L., Malhi, Y., Prieto, A., Rudas, A., Ruschell, A. R., Silva, N., Vos, V., Zent, S., Oliveira, A. A., Schutz, A. C., Gonzales, T., Nascimento, M. T.,

Ramirez-Angulo, H., Sierra, R., Tirado, M., Medina, M. N. U., Van Der Heijden, G., Vela, C. I., Torre, E. V., Vriesendorp, C., Wang, O., Young, K. R., Baider, C., Balslev, H., Ferreira, C., Mesones, I., Torres-Lezama, A., Giraldo, L. E. U., Zagt, R., Alexiades, M. N., Hernandez, L., Huamantupa-Chuquimaco, I., Milliken, W., Cuenca, W. P., Pauletto, D., Sandoval, E. V., Gamarra, L. V., Dexter, K. G., Feeley, K., Lopez-Gonzalez, G., and Silman, M. R. Hyperdominance in the Amazonian tree flora. *Science*, 342(6156), 2013.

Thomson, F. J., Moles, A. T., Auld, T. D., and Kingsford, R. T. Seed dispersal distance is more strongly correlated with plant height than with seed mass. *Journal of Ecology*, 99(6):1299–1307, 2011.

Tiessen, H., Chacon, P., and Cuevas, E. Phosphorus and nitrogen status in soils and vegetation along a toposequence of dystrophic rainforests on the upper Rio Negro. *Oecologia*, 99(1-2):145–150, 1994.

Tilman, D., Knops, J., Wedin, D., Reich, P., Ritchie, M., and Siemann, E. The influence of functional diversity and composition on ecosystem processes. *Science*, 277(Table 2):1300–1302, 1997.

TPL. The Plant List, 2013. URL http://www.theplantlist.org.

Tucker, C. M., Cadotte, M. W., Carvalho, S. B., Davies, T. J., Ferrier, S., Fritz, S. A., Grenyer, R., Helmus, M. R., Jin, L. S., Mooers, A. O., Pavoine, S., Purschke, O., Redding, D. W., Rosauer, D. F., Winter, M., and Mazel, F. A guide to phylogenetic metrics for conservation, community ecology and macroecology. *Biological Reviews*, 92 (2):698–715, 2017.

Tuomisto, H. and Ruokolainen, K. Distribution of Pteridophyta and Melastomataceae along an edaphic gradient in an Amazonian rain forest. *Journal of vegetation Science*, 5(1):25–34, 1994.

Tuomisto, H., Ruokolainen, K., and Yli-Halla, M. Dispersal, environment, and floristic variation of Western Amazonian forests. *Science*, 299(5604):241–244, 2003.

Valencia, R., Balslev, H., and Paz-Y-Miño-C, G. High tree alpha-diversity in Amazonian Ecuador. *Biodiversity and Conservation*, 3(1):21–28, 1994.

Valencia, R., Foster, R. B., Villa, G., Condit, R., Svenning, J. C., Hernández, C., Romoleroux, K., Losos, E., Magård, E., and Balslev, H. Tree species distributions and local habitat variation in the Amazon: Large forest plot in eastern Ecuador. *Journal of Ecology*, 92(2):214–229, 2004.

Valladares, F. and Niinemets, Ü. Shade Tolerance, a Key Plant Feature of Complex Nature and Consequences. *Annual Review of Ecology, Evolution, and Systematics*, 39(1):237–257, 2008.

Visser, M. D., Bruijning, M., Wright, S. J., Muller-Landau, H. C., Jongejans, E., Comita, L. S., and de Kroon, H. Functional traits as predictors of vital rates across the life cycle of tropical trees. *Functional Ecology*, 30(2):168–180, 2016.

Volkov, I., Banavar, J. R., Hubbell, S. P., and Maritan, A. Neutral theory and relative species abundance in ecology. *Nature*, 424(6952):1035–1037, 2003.

Waagepetersen, R. and Guan, Y. Two-step estimation for inhomogeneous spatial point processes. *Journal of the Royal Statistical Society: Series B (Statistical Methodology)*, 71(3):685–702, 2009.

Wang, B. C. and Smith, T. B. Closing the seed dispersal loop. *Trends in Ecology & Evolution*, 17(8):379–386, 2002.

Wang, X., Wiegand, T., Swenson, N. G., Wolf, A. T., Howe, R. W., Hao, Z., Lin, F., Ye, J., and Yuan, Z. Mechanisms underlying local functional and phylogenetic beta diversity in two temperate forests. *Ecology*, 96(4):1062–1073, 2015.

Webb, C. O. and Donoghue, M. J. Phylomatic: tree assembly for applied phylogenetics. *Molecular Ecology Notes*, 5(1):181–183, 2005.

Webb, C. O. and Peart, D. R. High seed dispersal rates in faunally intact tropical rain forest: Theoretical and conservation implications. *Ecology Letters*, 4(5):491–499, 2001.

Webb, C. O., Ackerly, D. D., McPeek, M. A., and Donoghue, M. J. Phylogenies and community ecology. *Annual Review of Ecology and Systematics*, 33:475–505, 2002.

Wennekes, P. L., Rosindell, J., and Etienne, R. S. The Neutral—Niche Debate: A Philosophical Perspective. *Acta Biotheoretica*, 60(3):257–271, 2012.

Werner, F. A. and Homeier, J. Is tropical montane forest heterogeneity promoted by a resource-driven feedback cycle? Evidence from nutrient relations, herbivory and litter decomposition along a topographical gradient. *Functional Ecology*, 29 (3):430–440, 2015.

Westoby, M., Falster, D. S., Moles, A. T., Vesk, P. A., and Wright, I. J. Plant ecological strategies: Some leading dimensions of variation between species. *Annual Review of Ecology and Systematics*, 33:125–159, 2002.

Whittaker, R. H. Vegetation of the Siskiyou Mountains, Oregon and California. *Ecological Monographs*, 30(3):279–338, 1960.

Whittaker, R. H. Gradient analysis of vegetation. *Biological reviews of the Cambridge Philosophical Society*, 42(2):207–264, 1967.

Wilson, J. B., Peet, R. K., Dengler, J., and Pärtel, M. Plant species richness: the world records. *Journal of Vegetation Science*, 23(4):796–802, 2012.

Wright, S. J. Plant diversity in tropical forests: A review of mechanisms of species coexistence. *Oecologia*, 130(1):1–14, 2002.

Xia, S.-W., Chen, J., Schaefer, D., and Goodale, U. M. Effect of topography and litterfall input on fine-scale patch consistency of soil chemical properties in a tropical rainforest. *Plant and Soil*, 404(1-2):385–398, 2016.

Yang, J., Swenson, N. G., Zhang, G., Ci, X., Cao, M., Sha, L., Li, J., Ferry Slik, J. W., and Lin, L. Local-scale Partitioning of Functional and Phylogenetic Beta Diversity in a Tropical Tree Assemblage. *Scientific Reports*, 5(1):12731, 2015.

Yordanov, I., Velikova, V., and Tsonev, T. Plant responses to drought, acclimation, and stress tolerance. *Photosynthetica*, 38(2):171–186, 2000.

Zanne, A. E., Tank, D. C., Cornwell, W. K., Eastman, J. M., Smith, S. A., FitzJohn, R. G., McGlinn, D. J., O'Meara, B. C., Moles, A. T., Reich, P. B., Royer, D. L., Soltis, D. E., Stevens, P. F., Westoby, M., Wright, I. J., Aarssen, L., Bertin, R. I., Calaminus, A., Govaerts, R., Hemmings, F., Leishman, M. R., Oleksyn, J., Soltis, P. S., Swenson, N. G., Warman, L., and Beaulieu, J. M. Three keys to the radiation of angiosperms into freezing environments. *Nature*, 506(7486):89–92, 2014.

Zhang, J. L., Swenson, N. G., Chen, S. B., Liu, X. J., Li, Z. S., Huang, J. H., Mi, X. C., and Ma, K. P. Phylogenetic beta diversity in tropical forests: Implications for the roles of geographical and environmental distance. *Journal of Systematics and Evolution*, 51(1):71–85, 2013.